Universität Rostock

Traditio et Innovatio

Green natural zeolite catalyst-preparation, characterization and acid catalytic performance

Dissertation

zur

Erlangung des akademischen Grades

doctor rerum naturalium (Dr. rer. nat.)

der Mathematisch-Naturwissenschaftlichen Fakultät

der Universität Rostock

vorgelegt von Riaz Muhammad, geb. am 03.01.1982 in Charsadda, Pakistan

Rostock, 27.04.2018

https://doi.org/10.18453/rosdok_id00002519

Die vorliegende Arbeit wurde in der Zeit von May 2015 bis October 2017 am Institut für Chemie der Universität Rostock am Lehrstuhl für Anorganische Chemie in der Arbeitsgruppe von Prof. Dr. Axel Schulz angefertigt

Datum der Einreichung: 27.04.2018

Datum der Verteidigung: 10.07.2018

1. Gutachter: Prof. Dr. Axel Schulz, Institut für Chemie, Universität Rostock

2. Gutachter: Prof. Dr. Christian Jäger, BAM, Berlin

3. Gutachter: Prof. Dr. Raja Al Otaibi, KACST, Saudi Arabia

4. Gutachter: Dr. Hendrik Kosslick, Leibniz Institut für Katalyse, Rostock

ERKLÄRUNG

Ich versichere hiermit an Eides statt, dass ich die vorliegende Arbeit selbstständig angefertigt und ohne fremde Hilfe verfasst habe. Dazu habe ich keine außer den von mir angegebenen Hilfsmitteln und Quellen verwendet und die den benutzten Werken inhaltlich und wörtlich entnommenen Stellen habe ich als solche kenntlich gemacht.

Rostock, 27.04.2018

…….
Riaz Muhammad

Acknowledgements

I express my sincere and greatest gratitude to my supervisor Prof. Dr. Axel Schulz who provided me the opportunity to join his research group. I am thankful for his constant encouragement and unlimited cooperation during the research work and thanks to him for all he did for me. I would also like to express my deepest and sincere gratitude to my supervisor Dr. Hendrik Kosslick for continuous support during my PhD study and related research, for his patience, motivation, sympathetic attitude, encouragement, guidance and support which enabled me to complete my experimental work and developed an understanding of this thesis. I am thankful to Prof. Dr. Christian Jäger for solid state NMR characterization of my samples at BAM, Berlin. He always encouraged me to work hard and to come up with task accomplishment. Thanks to him for all he did for me. Dr. Dirk Michalik for NMR measurements, Dr. Christine Fischer (LIKAT) for GC analysis, Dr. Marcus Frank and Dr. Armin Springer (EMZ) for SEM measurements.

I would also like to say special thanks to Dr. Ronald Wustrack, Dr. Jonas Bresien and Dr. Jörg Harloff for their support, help and fruitful discussion. Many thanks to Sören Arlt for TG-DSC analysis and for help with organizational and formal matter regarding submission of my thesis. Also I am thankful to all colleagues in AK Schulz group for their encouragement, friendship and support during my work. Special thanks to my best friend Faiz M. Khan for their company and inspiration during my PhD studies and stay at Rostock and many thanks to Dr. Farooq Ibad. I give best regards to all my friends and colleagues who encouraged me throughout my PhD studies. Last but not the least; I am heartily thankful to my family: my parents, my wife, my son and my daughter for their spiritual support, prayers and encouragement during my PhD studies and in every movement of my life.

Summary

Natural microporous clinoptilolite zeolite-CLIN was acidified via ammonium ion exchange (0.5 M NH_4NO_3, 80°C, 1 h) followed by calcination (300-600°C) and HCl treatment (0.1-2M, 80°C, 1h) under soft conditions, i.e. low temperature, acid concentration, short treatment time, and moderate post thermal treatment. The influence of the modification type and treatment conditions on the structure, morphology, acidity and texture was studied by XRD, SEM, FTIR, ICP-AES, TG/DSC, ammonia-TPD, ^{1}H, ^{27}Al and ^{29}SI MAS NMR and N_2-ads-des. The catalytic activity was investigated in the acid catalyzed acetalization of benzaldehyde with butandiol-1, 3. The ions exchange experiments show that a part of the cations of clinoptilolite readily exchange with ammonium ions and as well as by acid treatment. High temperature calcination (600-800°C) of NH_4-CLIN, treatment with concentrated acid and calcination of acid treated CLIN at 400-500°C has a more severe impact on the clinoptilolite structure. It causes a loss of material (*ca.* 24%), of crystallinity, and partial amorphization. For NH_4-CLIN calcined at 450°C, highest values of porosity, acidity and catalytic activity in the acetalization reaction were observed. Maximum decomposition of NH_4^+ ions occurs at 450°C, and is responsible for the markedly improved acidity and activity. A relative decrease in porosity, acidity and activity was observed after calcination beyond 450°C. Only some local framework changes could be seen by XRD pattern and FTIR spectra after calcination at 600°C. This decrease can be correlated to the transition of framework tetra-coordinated aluminium $Al^{[IV]}$ to penta-coordinated aluminium $Al^{[V]}$. For NH_4-CLIN calcined at 600°C, a dramatic and markedly decrease in acidity and activity is observed due to maximum conversion of framework aluminium to penta-coordinated $Al^{[V]}$. A model was proposed. After calcination at 700°C and 800°C, the structure collapsed as shown by XRD pattern and FTIR spectra. For HCl-treated H-CLIN catalysts the porosity, acidity and activity were increased with growing acid treatment concentration. But only small increase in porosity was observed. But high mass loss of *ca.* 24 % compared to calcined NH_4-CLIN was observed. The porosity, acidity, and catalytic activity of acid treated CLIN were decreased after calcination at 400°C, 450°C and 500°C respectively. The stability of acid sites was lower due to dehydroxylation. These findings show that the catalytic activity of H-CLIN catalysts depends on both, the acidity, i.e. the number of BS, and the (micro) porosity determining the accessibility of BS and mass transfer to and from the catalyst. A synthesis-structure-porosity-acidity-activity relationship was found with H-CLIN catalysts. Obtained H-CLIN catalysts were potential and active acid catalysts.

Zusammenfassung

Natürlicher mikroporöser Zeolith Klinoptilolith wurde sauer modifiziert durch Austausch der enthaltenen Kationen mit Ammonium-Ionen (0.5 M NH_4NO_3, 80°C, 1 h) und anschließender thermischer Zersetzung als auch mittels direkten Austausches mit Protonen via HCl-Behandlung (0.1-2 M, 80°C, 1h). Dies erfolgte unter milden Bedingungen, d.h. niedriger Temperatur und Säure- oder Salzkonzentration, kurzer Behandlungszeit und moderater thermischer Behandlung. Der Einfluss der Art der Modifizierung und der Behandlungsbedingungen auf die Struktur, Morphologie, Textur und Azidität wurde mittels XRD, SEM, FTIR, ICP-AES, TG/DSC, Ammoniak-TPD ^{1}H-, ^{27}Al- uns ^{29}Si MAS NMR untersucht. Die katalytische Aktivität wurde mittels der säure-katalysierten Azetalisierung von Benzaldehyd mit Butandiol-1,3 geprüft. Die Ionenaustauschexperimente zeigen, dass sich *ca.* 50 % der Kationen schnell mit Ammonium-Ionen und Protonen austauschen lassen und saure Brønsted-Zentren (BS) bilden. Hohe Kalzinierungstemperaturen (>600°C) bzw. HCl-Konzentrationen haben einen großen Einfluss auf die Zeolithstruktur. Sie führen zu Materialverlust, sinkender Kristallinität und zu einer partiellen Amorphisierung. Andererseits bleibt die Struktur als solche erhalten (XRD, FTIR). Höchste Werte für die Azidität, Porosität und katalytische Aktivität wurden für NH_4-CIN-Katalysatoren nach Aktivierung bei 450°C gefunden. Bei dieser Temperatur erfolgt maximale Zersetzung der NH_4^+ -Ionen und Bildung von Säurezentren. Dennoch treten unterhalb 600°C nur geringe strukturelle Änderungen auf. Bei höheren Temperaturen nehmen die Azidität, Porosität und katalytische Aktivität wieder ab. Dies wird auf die Umwandlung von tetraedrisch koordiniertem Gerüst-Aluminium zu 5-fach koordinierten Al erklärt und durch ein Modell beschrieben. XRD und FTIR Daten zeigen, dass oberhalb von 700°C der strukturelle Kollaps des Zeoliths einsetzt. Für HCl behandelte Katalysatoren nehmen die Azidität und katalytische Aktivität mit steigender Säurekonzentration zu. Die Porosität nimmt nur leicht zu, aber der Masseverlust durch Auflösung des Zeoliths ist mit *ca.* 24 % hoch. Die Porosität, Aziditär und Aktivität nehmen nach erhitzen über 300-400°C wieder deutlich ab. Letzteres wird auf einen Abbau der BS durch Dehydoxylierung zurückgeführt. Die Ergebnisse zeigen, dass die katalytische Aktivität von H-CLIN sowohl von der Azidität als auch der Porosität abhängen. Letztere bestimmt die Zugänglichkeit der katalytischen Aktivzentren und den Stofftransport (Synthese-Struktur-Eigenschafts-Beziehung).

Table of content

List of Figures

List of Tables

List of Schemes

List of abbreviations

Ads.	Adsorption	**NH_4CLI**	NH_4^+-exchanged CLIN
BET	*Brunauer–Emmett–Teller*	**Ph**	Phenol
BS	Brønsted acid sites	**ppm**	Parts per million
ca.	Approximately	**SEM**	*Scanning electron microscopy*
CEC	Cation exchange capacity	**SSA**	*Specific surface area*
CLIN	Starting Clinoptilolite	**Ref.**	Reference
conc.	Concentration	**RT**	*Room temperature*
Des	Desorption	**T**	Temperature
DSC	*Differential Scanning Calorimetry*	**TG**	Thermogravimetry
		TPD	*Temperature programmed*
Eq.	Equation		*desorption*
GC	Gas chromatography	**V**	Volume
H-CLIN	Protonated CLIN, acid form	***vs.***	Versus
LS	Lewis acid sites	**XRD**	*X–ray diffraction*

Used units

Quantity	**Symbol**	**Name**	**Conversion**
Length	Å	Angstrom	1 Å = 10^{-10} m
	μm	Micrometer	1 μm = 10^{-6} m
	nm	Nanometer	1 nm = 10^{-9} m
Temperature	°C	Degree Celsius	x °C = (x + 273.15) K
Volume	ml	Milliliter	1 ml = 1cm^3 = 10^{-6} m^3
Wavenumber	cm^{-1}	Reciprocal centimeter	1cm^{-1} = 100 m^{-1}
Time	h	Hour	1 h = 3600 s
	min	Minute	1 min = 60 s
Pressure	Bar	Bar	1 bar = 100000 Pa
	hPa	Hectopascal	1 hPa = 100 Pa
Atom percent	at.-%	Weight percent	Wt.-%

1 Goals and objectives of the present work

Goals

Preparation of natural clinoptilolite heterogeneous catalysts with improved

- Acidity,
- Porosity,
- Catalytic activity, and
- To check the presence of possible Synthesis-Structure-Property relationships.

Objectives

The study aims the improvement of the performance of acid natural zeolite clinoptilolite, i.e. acidity, porosity, and activity in the formation of acetals by optimizing preparation and activation conditions. Two preparation ways for the acid functionalization of clinoptilolite are compared and optimized:

(1) Ammonium exchange followed by thermal activation,

And

(2) The treatment with hydrochloric acid and activation.

In detail:

- The harsh literature conditions were changed to soft treatment conditions. Therefore applying short cation exchange time, lower exchange temperature (0.5M NH_4NO_3 at 80°C, 1h and calcination temperature (300-600°C)) and low concentrated solution of acids (0.1-2M),
- Obtained acid clinoptilolite catalysts were characterized in detail regarding structure (XRD, FTIR), texture and porosity (SEM, nitrogen adsorption and desorption), thermal stability (TG/DSC, XRD), local structure and nature of aluminum (^{27}Al and ^{29}Si MAS NMR), acidity – strength and acid site concentration (ammonia-TPD, ^{1}H MAS NMR),
- The catalytic performance (activity and stability) of H-CLIN catalysts were studied in the acetalization of benzaldehyde with butandiol-1,3.
- A model for the observed transition of the coordination of tetrahedral framework aluminum to penta-coordination observed with thermal activation of ammonium-exchanged CLIN is proposed showing the Synthesis/Activation- Structure- Property relationship.

New Approach:

Using soft/mild conditions treatments, inclusion of ammonium CLIN and study of its impacts to identify optimized conditions for improving acidity and porosity:

- Acidity is responsible for more acidic sites and improving catalytic activities,

While,

- Porosity is important for easy access to active sites and for more mass transfer.

The strong acidity and high porosity of natural zeolites catalysts, together with their regular structure, is responsible for their widespread use as catalysts. Natural zeolite clinoptilolite are modified to an active porous catalyst by mild, cheap, economic and environment friendly treatment conditions.

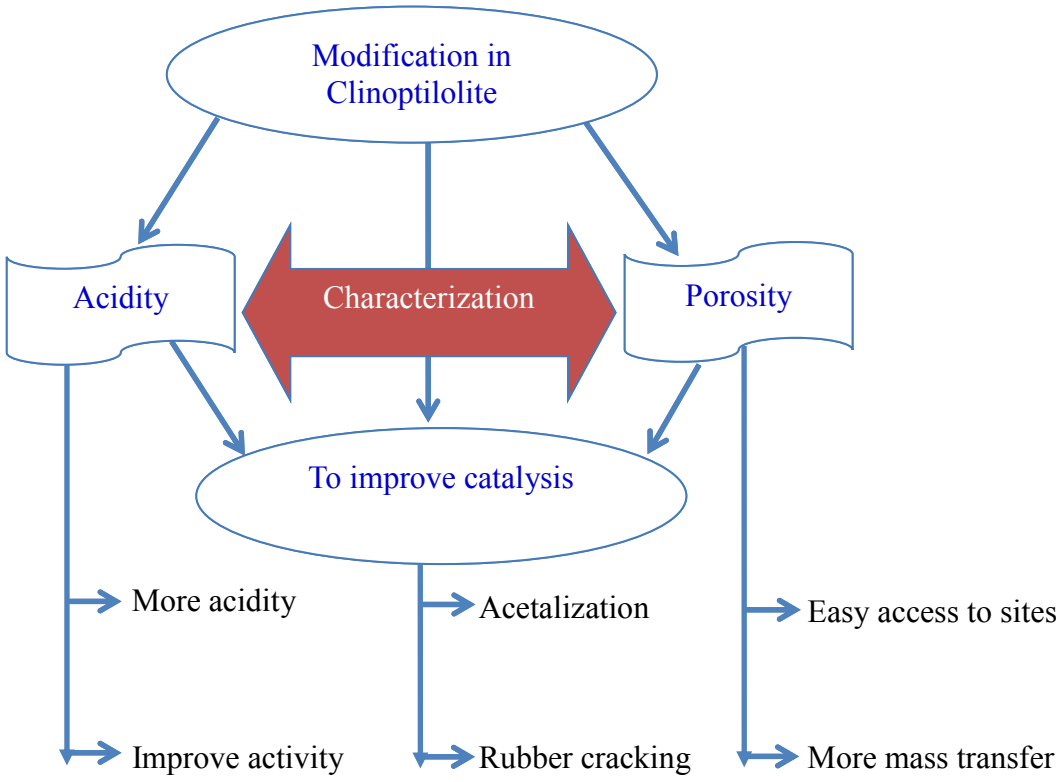

Scheme 1. Modification strategy for starting CLIN to get most, active, acidic and porous catalyst.

2 Introduction

Heavy oil feed stock is an available renewable source of fuel and chemicals to meet the challenge of sufficient energy supply. Zeolites after proper modification can be used as catalyst for converting heavy oil feed stock into valuable hydrocarbons. Zeolites are microporous crystalline solids, consisting of AlO_4 and SiO_4 tetrahedra which are linked at the corners by sharing all oxygen atoms, resulting in a three-dimensional silicate structure. Zeolites, discovered in 1756 by Axel Fredrik Cronstedt, have been used as catalysts, goods adsorbents, ion exchangers and molecular sieves.[1-3] Zeolites may be either obtained simply from natural mineral deposits or they can be synthesized. Beside 232 synthetic zeolites (molecular sieves), 67 different natural zeolites subdivided into 28 different framework types are currently known in large quantity and purity.[1,4-6] Synthetic zeolites are expensive, their synthesis is not environment friendly and cannot be used as spent catalyst. But their properties are unique. In contrast to synthetic zeolites, natural zeolites are abundant, easily available, cheap, environment friendly and can be used as spent catalyst. Natural zeolites as catalytic materials is much less studied compared to synthetic materials. They show a heterogeneous composition and material properties can vary due to different origins and may contain a lot of by-products. By exchange of extra-framework cations with protons (H^+), the tetrahedral framework is altered by loss of Al^{3+} and the zeolite become acidic producing Brønsted and Lewis acid sites with lattice defects responsible for increase in porosity.[7,8] Acidity is an important factor for improving catalytic activity, while porosity is important for the access to active sites and for enhanced mass transfer.

The aim of this study is to develop new natural zeolites based stable materials having potential catalytic applications and to know about in detail their chemical and physical characteristics. In this study natural zeolitic tuff containing *ca.* 94% of clinoptilolite is used. So far clinoptilolite is the most abundant natural zeolite having medium pore size channels like ZSM-5 with Si/Al=5-6. Clinoptilolite was modified to get a zeolite catalyst with high acidity (Brønsted and Lewis acidity) and increased porosity. Modification was done by ammonium ion exchange followed by calcinations and by direct treatment with inorganic acids in liquid medium. Ammonia-TPD measurements and acetalization experiments of 1, 3-butandiol with benzaldehyde were carried out to investigate the acidity and catalytic activity. XRD, FTIR, SEM, N_2-ads/des, TG/DSC, ^{27}Al and ^{29}Si MAS NMR investigations were done for characterizing the structure and porosity of prepared acidic clinoptilolite catalysts. Advanced highly acidic, porous and catalytic active clinoptilolite catalysts could be obtained

by optimized preparation conditions can be used for converting heavy oil feed stock, polyethylene and tube rubber into simple valuable hydrocarbon and fuel components.

2.1 Background

Zeolites are microporous crystalline hydrated metal aluminosilicates containing alkali and alkaline earth metals especially, sodium, potassium, calcium, magnesium, strontium and barium having an infinite, open, three-dimensional framework structures.[9,10] The name 'zeolite' is derived from two Greek words *zeo* and *lithos* which mean 'to boil' and 'a stone'. The phenomenon of melting and boiling at the same time is a novel property. The name 'zeolite' was first used by the Swedish mineralogist Cronstedt for stilbite, the first recognized mineral zeolite, which was discovered in 1756. The general chemical formula of zeolites is as follows:

$$Mx/n\ [(AlO_2)\ x\ (SiO_2)\ y].wH_2O$$

Where "n" is the valence of cation *M*, x and y are the total number of tetrahedral atoms per unit cell while the portion with [ ] defines the framework composition, and w is the number of water molecules per unit cell.

Zeolites remained strange for scientists and collectors for a long time until when their unique physicochemical properties attracted the attention of many researchers. In the late 1950s with the beginning of synthetic zeolites business, huge beds of zeolite-rich sediments were discovered in the western United States and other parts of the world, formed by the alteration of volcanic ash in lake and marine waters.[4]

2.2 Hydrothermal synthesis and formation of zeolites

Synthetic zeolites can be synthesized with a variety of chemical properties, pore sizes and high thermal stability. Typical zeolite synthesis includes the following reaction:

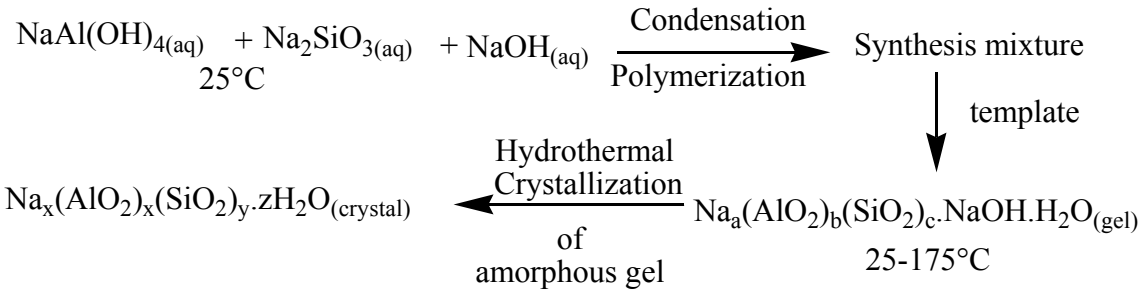

Scheme 2. Reaction mechanism and strategy of synthetic zeolite preparation.

Synthetic zeolite synthesis is affected by the composition of the reaction mixture (Si/Al ratio, hydroxide concentration inorganic cations), nature of reactants and their pretreatments, temperature of the process, reaction time and pH of the final reaction mixture (often medium alkaline pH>10).[11,12]

Natural zeolites are produced by volcanic activities due to converging and diverging of tectonic plates leading to the eruption of molten rocks. In cases where the hot lava and ash can flow into sea water and combine with salt from sea hydrothermal conditions are established which facilitate the natural formation of zeolites during long periods of time.[13-15]

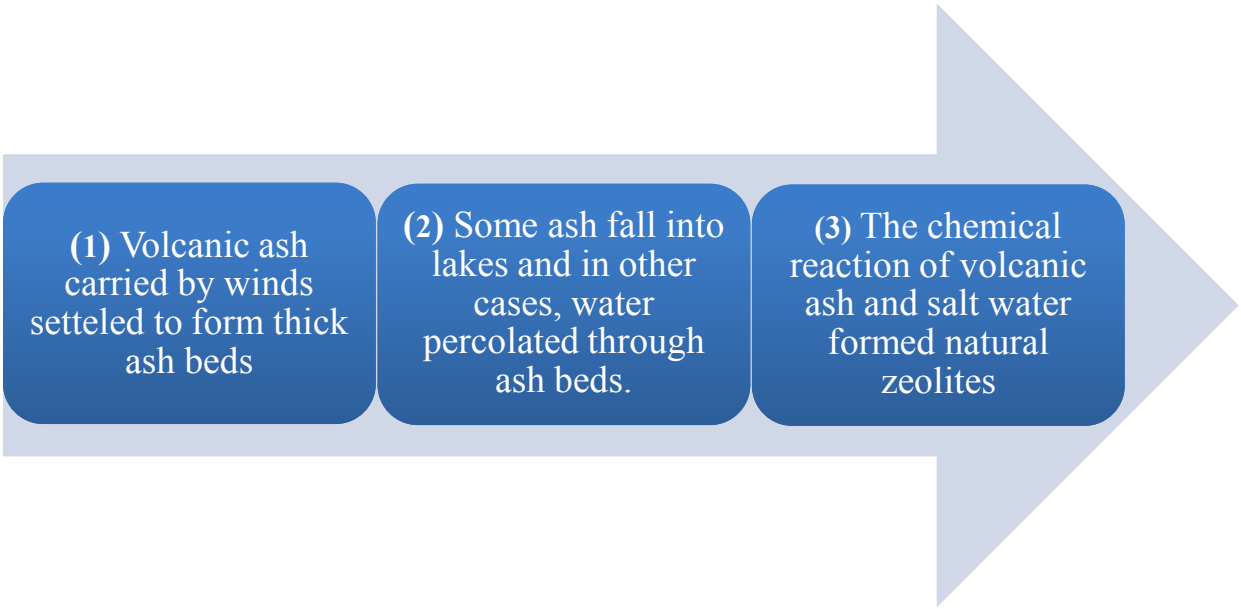

Figure 1. Different stages of natural zeolite formation.[15]

Zeolites have also crystallized in post-depositional environments over periods ranging from thousands to millions of years in shallow marine basins, and are found in some ocean sediments.[10,15,16]

2.2.1 Chemical composition and structure of zeolites

In 1997, the International Mineralogical Association, Commission on New Minerals and Mineral Names agreed that any framework structure with cavities occupied by freely movable ions and water molecules, having properties of ion exchange, molecular "sieving", absorption, diffusion, dehydration, reversible dehydration and catalysis be classified as a zeolite irrespective of its "Si" and "Al" content in tetrahedral sites. Zeolites may define as:

"Mineral of crystalline structure framework of linked tetrahedral, consisting of four O atoms surrounding a cation. Zeolite framework contains open cavities in the form of channels and

cages occupied by H_2O molecules and exchangeable extra-framework cations. Dehydration occurs at temperatures ca. 400 °C and is largely reversible".[17]

In zeolite, tetrahedral of AlO_4 and SiO_4 are linked at the corners by sharing all oxygen atoms. Each tetrahedron consists of four O atoms surrounding a Si or Al cation, resulting in a three-dimensional structure of aluminosilicate. The positive charge deficiency caused by substitution of Al^{3+} by Si^{4+} is compensated by monovalent or divalent cations located together with water molecules in the channels (Fig. 2c).[1,18]The crystal structure of zeolite consists of two types of units, primary building units (PBUs) and secondary building units (SBUs). The $(SiO_4)^{4+}$and $(AlO_4)^{5+}$ tetrahedra are called PBUs as represented in Figure 2a, b. PBUs combine in special geometric shape by sharing oxygen with adjacent tetrahedral to form SBUs. SBUs are basic units and building block of zeolite structure. 23 different types of SBUs are known until date.[1] SBUs link to each other as single rings, double rings and polyhedra in different ways to form a unique structure of zeolites. Some examples of SBUs linked by oxygen atoms in the structures are given in Figure 3.

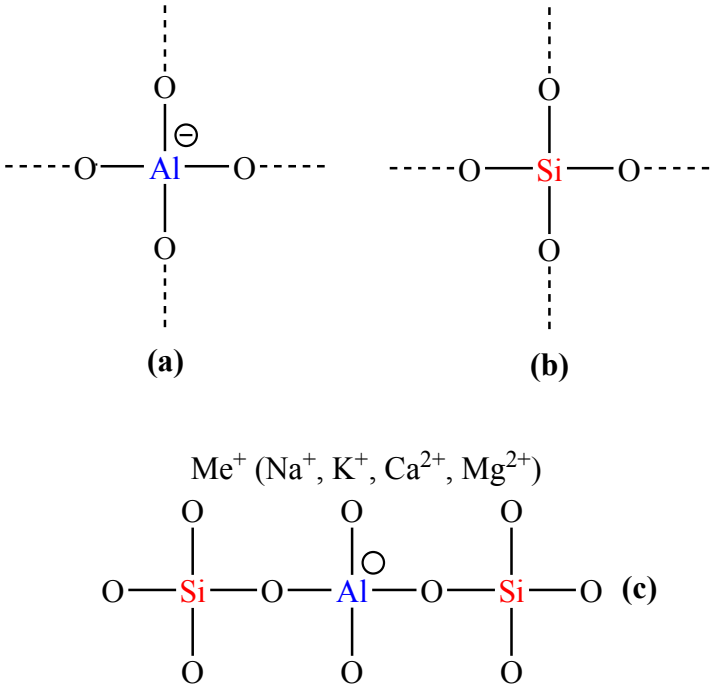

Figure 2. The tetrahedral arrangement of $(SiO_4)^{-4}$ or $(AlO_4)^{-5}$ molecules **(a)** and **(b)** primary building units (PBU) and **(c)** secondary building units (SBU) i.e. aluminosilicate structure.

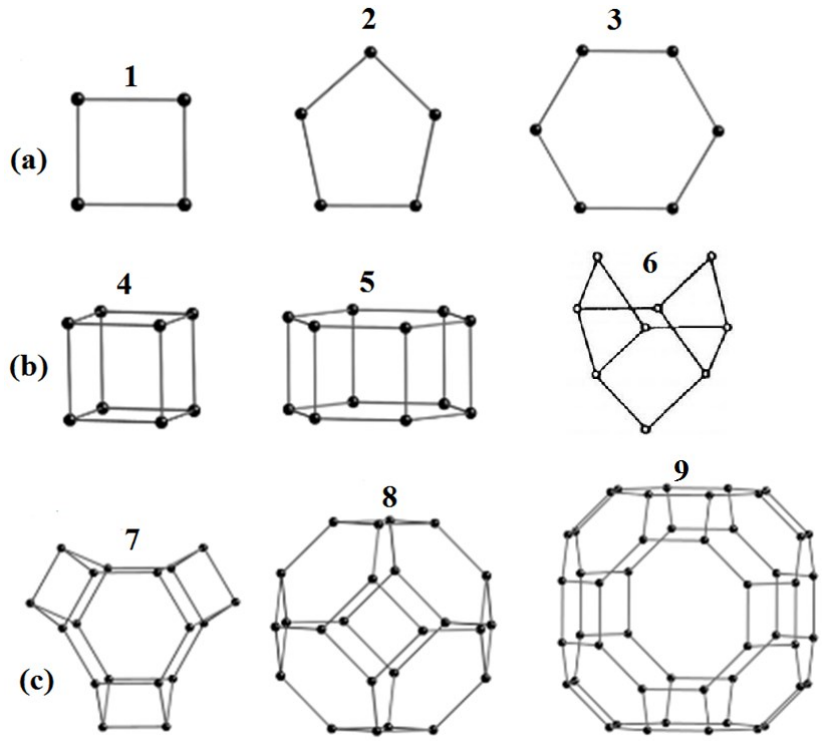

Figure 3. Different types of secondary building units of framework structures of zeolite groups. (**a**) Oxygen rings [O4R (1), O5R (2), O6R (3)], (**b**) Double or complex rings [double 4-membered ring, D4R (4),), D6R (5), 4-4-1 unit (6)], and (**c**) [polyhedra: cancrinite cage (7), sodalite or β-cage (8) and the α-cage (9)].[5,19,20]

2.2.2 Pores of zeolites

Zeolites are classified according to the pore size as small, medium and large pore systems:

- **Small pore zeolites**: contain the pore opening consisting of 8 TO_4 tetrahedra with free diameters of 3-4.2 Å. Examples are zeolite-A (4Å) and LTA (4.1 Å),
- **Medium pore zeolites**: contain the pore opening consisting of 10 TO_4 tetrahedra with free diameters of 4.5-6.0 Å. Examples are ZSM-5 (5.5-5.9 Å) and MFI (4-6Å),
- **Large pore zeolites**: contain the pore opening consisting of 12 TO_4 tetrahedra with free diameters of 6.0-8.0 Å. Examples are FAU (7.4 Å), zeolite-X and Y (7.3 Å), and
- **Extra-large pore zeolites**: contain the pore opening consisting of 14 TO_4 tetrahedra for example UTD-1 (7.5×10 Å).[21,22]

The pore size and shape of zeolite framework remain flexible to some extent, according to changes in temperature and guest species. For example 0.62 nm circular pore of ZSM-5 with sorption of neo-pentane changes to an elliptical shape pore diameter 0.45 to 0.70 nm, after substitution of aromatics as the guest species.[21]

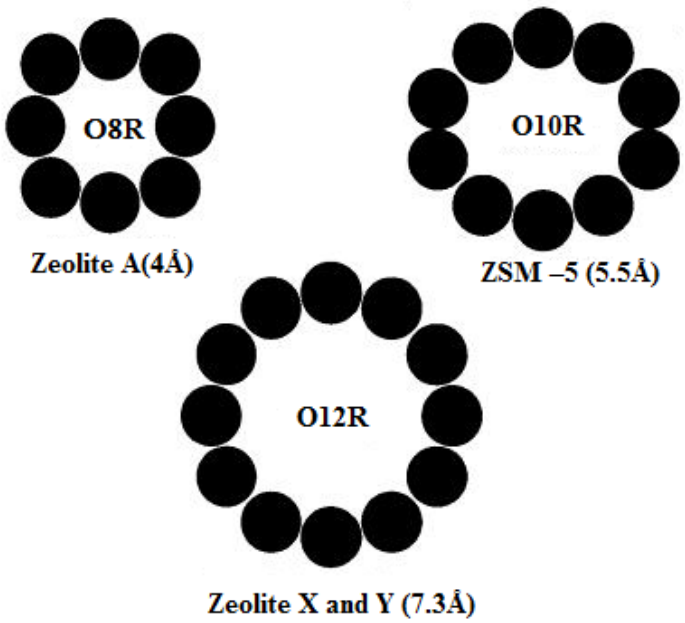

Figure 4. Composition and size of oxygen ring windows (openings) in the zeolite framework.[1,23]

Zeolites adsorb water reversibly and can undergo exchange of extra framework cations without changing the structure. The water molecules are associated with non-framework cations can be removed at 300-400°C, allowing access of molecules to the pores. The uniform size and shapes of pores and cavities give rise to the size selective adsorption of molecules of a specific size and shape which explain 'molecular sieve'' property of crystalline zeolites.[10,24,25]

2.2.3 Properties of zeolites

Compared to other crystalline inorganic oxide materials zeolites have some special properties that make them interesting for heterogeneous catalysis:

- Zeolites have microporous structure with uniform pore dimensions,
- Zeolites have molecular sieve property,
- Zeolites have ion-exchange ability (formation of solid acid by replacement of cation by protons H^+),
- Zeolites are used as catalysts, and
- Zeolites have high thermal stability.

2.2.4 Applications of zeolites

Zeolites have been used over years as adsorbents, ion exchangers and molecular sieves for removal of heavy metals, environmental and indoor air-quality monitoring, air separation, in industrial process control, the separation of straight-chain hydrocarbons from branched-chain hydrocarbons, chemical sensors, effluent and auto-exhaust control. Zeolites molecular sieve properties are extensively employed in catalysis and gas separation industries.[1,2,5,6,25,26-28]

Ion exchange applications

They allow the removal of radioactive ions from contaminated water by ion exchange. Ion exchange is mostly applicable in water softening devices, in detergents and soaps.[29]

Molecular sieve applications

In 1777, Fontana and Scheele used zeolites as adsorbents for NH_3, H_2S, NO, NO_2, SO_2, and CO_2 molecules. Zeolites extract the hazardous metal ion contaminations from (sludge) from waste water (sludge). Zeolites are used to decrease high level of ammonium ions, in the removal of ammonium ions from municipal, industrial, and agricultural waste and drinking waters.[30-33]

Catalysis applications

One of the main applications of zeolites is catalysis which adds high economic value. E.g., zeolites can be used as catalysts for reactions which require the participation of an acidic function. For example H-ZSM-5 is used for the production of synthetic gasoline from methanol by process (MTG), and for synthesis of fine chemicals.[34-37] Hydrogen-exchanged natural mordenite catalyst is used for the disproportionation of toluene to benzene and xylene.[38] Catalysis reaction mainly depends on the acidic sites and strength of acidic sites. In zeolites two types of acidic sites can be seen i.e. Brønsted acid sites and Lewis acid sites.

a) Brønsted acid sites

Substances which can donate protons (H^+) are called Brønsted acid sites. The Brønsted acidic sites of zeolites consist of protons bonded to the bridging oxygen atom connecting AlO_4 and SiO_4 tetrahedra (Si-OH-Al).[3]

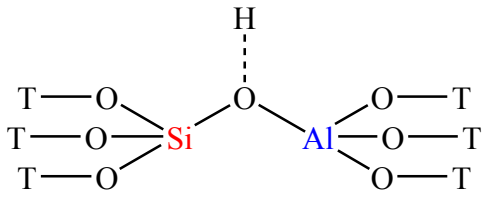

Figure 5. Schematic representation of Brønsted acid sites in zeolites.[3]

b) Lewis acid sites

Substances which can accept electron pairs are called Lewis acid sites. Some undefined sites such as AlO^{+} or charged $Al_xO_y^{n+}$ acceptor sites inside or outside the pore are formed during pretreatment, activation, reactivation and dehydroxylation of H-forms of zeolites acting as Lewis acid sites.[3]

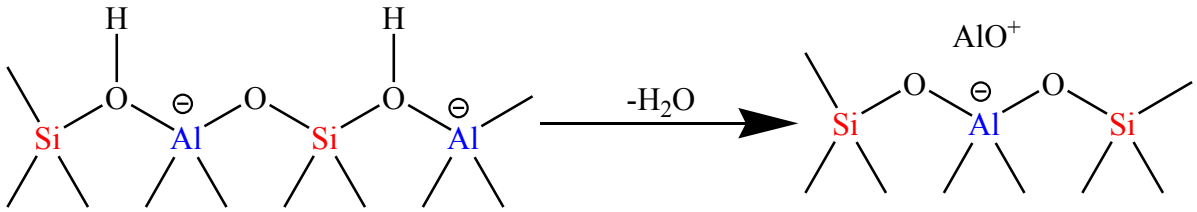

Figure 6. Schematic representations of Lewis acid sites in zeolites.[3]

In order to study the catalytic activity of zeolites it is important to know the structure, concentration, strength and accessibility of the Brønsted and Lewis acid sites. Protons can be incorporated into the zeolite framework by:

(i) Exchange with ammonium ions followed by calcination

And

(ii) Direct treatment with inorganic acid.

High structural selectivity and thermal stabilities are important for catalytic reactions of zeolites which proceed within the pores and cavities of zeolites in contrast to solid acid catalyst where reaction occurs at the surface. In catalysis with zeolites, both high selectivity and high catalytic activity can be achieved.

Shape Selectivity of zeolites

The ability to control the catalytic reactions on the basis of pore geometry is known as shape selectivity. Shape selective catalysis differentiates between reactants, products, or reaction intermediates according to their shape and size and can be used to increase yields of preferred products or to hinder undesirable reactions. Zeolite shows three types of shape selectivity:

(i) Reactant shape selectivity

Large size molecule cannot enter the small pore size zeolites to reach the active sites and cannot react. During reactant shape selectivity some of the reactant molecules are excluded, as they are too large to enter the pores. For example, n-hexane in mixtures of n-hexane and 3-methylpentane is easily cracked as 3-methylpentane is large enough to enter the pores of CaA. Similarly in a mixture of linear and branched paraffins, linear paraffins can be easily cracked in small pore zeolites.[39,40]

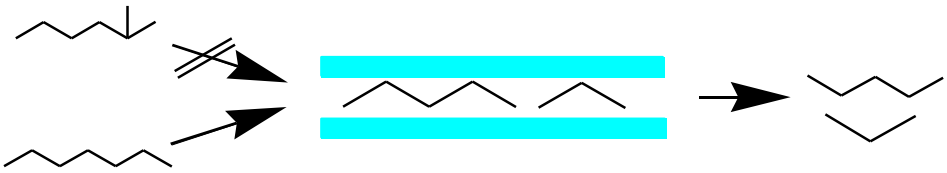

Figure 7. Reactant shape selectivity.[39,40]

(ii) Product shape selectivity

Small size molecules can easily enter the pore to reach the active sites and product is formed. Large size molecule that cannot diffuse out the small pore size zeolites are either converted to small size molecule or deactivate the catalyst by blocking the pores. For example in alkylation of toluene to xylene favors formation of para-xylene on medium pore size ZSM-5.[39,40]

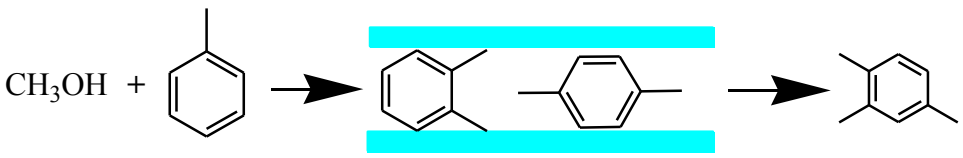

Figure 8. Product shape selectivity.[33,40]

(iii) Transition state shape selectivity

Transition state selectivity occurs for certain reactions that are prevented because the corresponding transition state requires more space than available in the cavities or pores. Neither reactant nor product molecules are prevented from diffusing through the pores. Reactions requiring smaller transition states can proceed easily. Bimolecular reactions with large intermediate proceed through transition state shape selectivity. Acid catalyzed trans-alkylation of dialkylbenzenes provides an example of transition shape selectivity.[39,40]

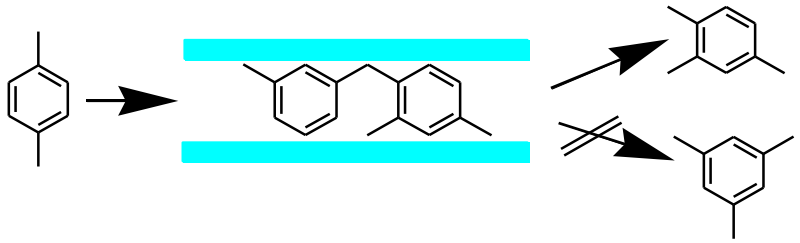

Figure 9. Transition state shape selectivity.[39,40]

Zeolites can be also classified according to the Si/Al ratio because it determines the thermal stability and acidity (Tab. 1).

Table 1: Classification of zeolites on the basis of Si/Al ratio.[4,5]

Zeolites grade	Si/Al molar ratio	Mineral names with framework codes
Low silica	≤ 2	Analcime (ANA), cancrinite (CAN), natrolite (NAT),
Intermediate silica	2 to 5	Chabazite (CHA), mordenite (MOR), Clinoptilolite (CLI)
High silica	10 to 100 (>5)	ZSM-5(MFI), zeolite-β (BEA)

In general for zeolites, an increase in Si/Al ratio from 1 (module 0.5) to infinity can result in the increase of acidic strength, acid resistivity, thermal stability, and hydrophobicity. While acid site density, cation concentration and hydrophilicity decreases.[3,5,41-42]

2.3 Clinoptilolite

Natural zeolites account for *ca.* 60 % of the total consumption is used for feed additives, soil amendment, water treatment, environmental uses, and construction.[43] Some of the most common natural zeolites are Clinoptilolite, chabazite, and mordenite. Clinoptilolite is one of the most abundant and economically important natural zeolite. Clinoptilolite is defined as the zeolite mineral having distinctive framework topology and Si/Al=5.[44] Its approximate chemical composition is as follows:

$$Ca\ (Na,\ K)_4\ (Al_6Si_{30}O_{72})\ 20H_2O$$

The clinoptilolite rich tuff can contain some impurities (depending on the origin) as low amounts cristobalite, chlorite, and sometimes mordenite as well as quartz, plagioclase, biotite and potassium feldspar. Along with the extra framework cations surrounded by water molecules in the channels, the H^+ ions may also be considered as exchangeable cations present in Si-OH and Al-OH.[4,45,46]

Structure and properties of Clinoptilolite

Clinoptilolite is a natural, medium pore size zeolite. It contains a 2-demensional pore system containing elliptical oxygen-10-membered rings of 4.1 × 7.5 Å size (channel-A) and two oxygen-8-membered rings of 3.6 × 4.6 Å and 2.81 × 4.7 Å size (channel B and C). Channel-A and B are alternating parallel arranged.[47,48] Both the channels are connected via perpendicular running C channels. Channel A and B are often occupied by sodium and calcium ions. Potassium ions are preferentially located in channel C whereas sodium and calcium ions are located in channel A and B (Fig. 11).[49]

In the structure of clinoptilolite, $(Si,Al)O_4$ tetrahedra are linked through oxygen atoms in layers . The secondary building unit (SBU) for clinoptilolite is the 4-4-1 unit. According to the results of X-ray diffraction study clinoptilolite unit cell parameters are as follows: a = 1.762 nm, b = 1.7911 nm, c = 0.7407 nm, α = 90°, β = 116°40′ and γ = 90°.[49-52]

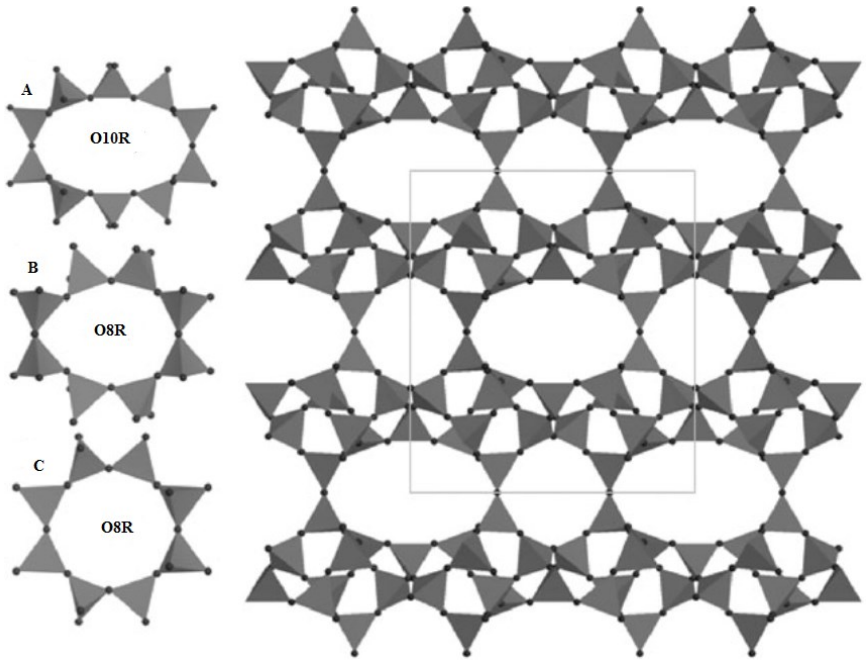

Figure 10. Tetrahedral model of clinoptilolite, indicating 10-membered A and 8-membered B channels that are bridged with 8-membered C.[49,52]

In clinoptilolite, ultra micropores (diameters <0.7 nm) and super micropores (diameters between 2 and 0.7 nm) exist. The presence of pores larger than super micropores in natural and modified clinoptilolite may be due to the existence of impurities or due to the partial destruction of the zeolite material during modification process.[44]

The structural view of clinoptilolite with cation site and water molecules is shown in Figure 11. In the clinoptilolite structure, Na^+ ions located at M (1) in channel A are coordinated with two framework oxygen and five water molecules, and Ca^{2+} ions in channel B at M (2) position are coordinated by three framework oxygen atoms and five water molecules in clinoptilolite lattice. K^+ situated in M (3) site has the highest coordination number among all the cation sites in the unit cell. These ions have a mixed coordination sphere of water molecules and framework oxygen atoms. Mg^{2+} is octahedrally coordinated only by water molecules in M (4) site.[45,49] The selectivity and uptake rate of molecules by clinoptilolite zeolites are influenced by the type, number, and location of the charge balancing cations residing in the A-C channels. Modifications in the cation composition and positions cause changes in amount and structural distribution of water molecules and water content in channels.[53]

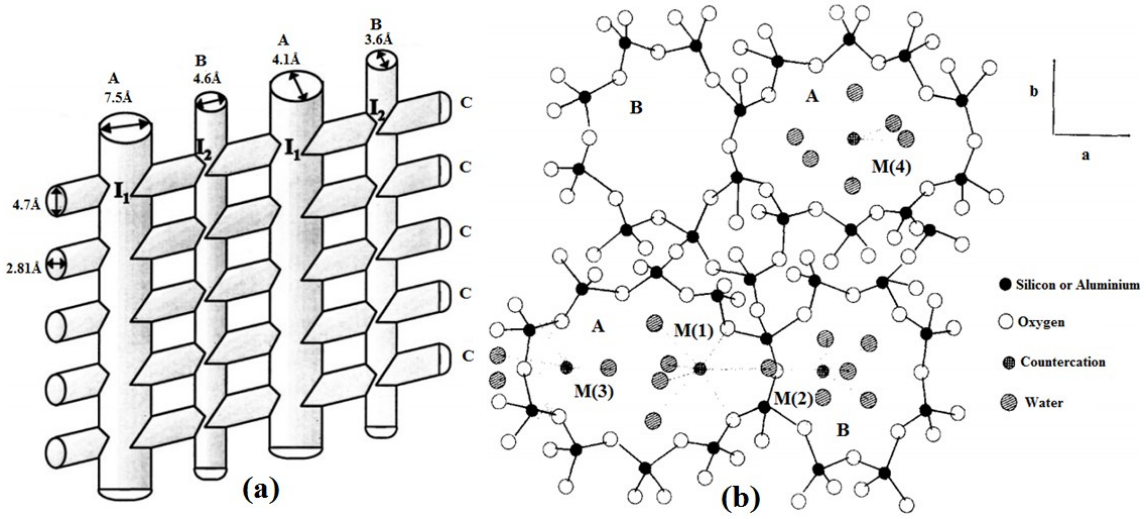

Figure 11. **(a)** Clinoptilolite structure showing channels A, B and C and intersections I_1 and I_2. Numbers represent pore dimensions in Å.[3] **(b)** The structural view of clinoptilolite with cation site and water molecules.[45,49,51]

2.4 State of the art

Zeolites, microporous solids are mostly used as catalyst, molecular sieves and active adsorbents.[54] The use of natural zeolites as catalytic materials is much less studied compared with synthetic materials due to the difficulty in obtaining homogenous material, the reproducibility of samples obtained from natural ores and the thermal and hydrothermal instability.

Clinoptilolite, the most abundant, cheap natural zeolite having medium pore size channels like ZSM-5, Si/Al=5-6, good thermal stability, worldwide availability, and easy to extract cannot adsorb large size molecules inside cavities, and channels due to small pore diameter, hindering their acidity and porosity.[55-58]

For the first time in 1964 clinoptilolite was treated with 0.25-30 N HCl for 4 h at 100°C for checking the adsorption capacity of H_2O, CH_3OH, C_2H_5OH, C_6H_6 and iso-C_5H_{12}. The BET surface area for sample treated with 1 N and 2 N HCl increased to 360 and 380 m^2/g respectively as compared to starting clinoptilolite (30 m^2/g). For 30 N acid treated samples the crystallinity is completely lost.[59] In 1993 clinoptilolite was treated with 1 M NH_4Cl and 5 M HCl solution for 5 hours at reflux temperature (5-fold), dried at 120°C and calcined at 400°C for 3 hours. The BET surface area, and pore volume for sample treated with 1 M NH_4Cl and 5 M HCl increases to 256 m^2/g, 0.162 cm^2/g and 200 m^2/g, 0.183 cm^2/g respectively as compared to starting clinoptilolite (51 m^2/g , 0.082 cm^2/g). The NH_3-TPD acidity value of 1.10, 2.1 and 1 meq NH_3/g was for starting material, calcined NH_4^+ exchanged and acid treated were reported respectively. Severe weight loss was observed by acid treatment followed by calcination.[55] In 2002, BET values of 36, 36, 220 and 50 m^2/g were noted for clinoptilolite treated with 0.5 N NaCl followed by treatment with 1 N NH_4Cl (2-fold) and calcined at 300, 400, 500 and 600°C for 3 hours respectively. The BET value 260, 220 and 315 m^2/g for samples Na-NH_4^++0.1 N HCl, Na-NH_4^+-0.1 N HCl at 350°C and Na-NH_4^+-1 N HCl at 350°C respectively. Nearly 40 % CLIN and feldspar phase intensity is lost by employing the 1 N HCl concentration.[56] In 2008 clinoptilolite was refluxed twice with 1 M of NH_4NO_3 overnight and calcined at 600°C for 6 h, for methanol conversion to dimethyl ether. The BET value of 214m^2/g and acidity values of 1.36 mmol/g were reported for modified sample. Loss in crystallinity was observed.[60] In 2010 clinoptilolite was treated with 1 M NH_4Cl (8-fold) at 100°C for 40 h, dried to get NH_4Z , calcined at 400°C for 16 h to get HZ. HZ was treated with 0.6 M HCl at 100°C for 2 h and washed 3 times in ultrasonic bath with 0.05 M HCl for each 15 mints at 70°C labeled as HZD1, with 3 times procedure as HZD3 and with 5 times as HZD5. The BET values of 20, 248, 259, 291 and 305 m^2/g were

noted for NZ, HZ, HZD1, HZD3 and HZD5 respectively. But nitrogen adsorption isotherms were not shown and obtained samples suffered from crystallinity.[61] In 2015 CLIN was treated with 10 % NH_4NO_3 (3-fold) at 80°C for 4 hours and calcined at 300°C for 6 h, 400°C and 500°C for 4 h and with 0.05 -11.5 M HCl for 4 h at 95-97°C. BET value of 143.4 and 164.7 m^2/g for 500°C calcined and 1 M HCl respectively and TPD values of 0.738 mmol/g for 300°C calcined were obtained. Treatment with 1M HCl causes *ca.* 50 % decrease in crystallinity. By applying more concentrated solutions of the acid, the samples became largely amorphous. NH_4^+ cations followed by high temperature calcination affect structural stability and result in decrease of crystallinity (Tab. 32).[62]

From the literature (Tab. 32), for improving ion exchange degree, acidity, activity and porosity, strategy of high concentration of NH_4NO_3 or NH_4Cl followed by high temperature calcination, concentrated acid treatment and long contact time of reaction were used. Different severe post-synthesis treatment by acid (HF, HCl) base (NaOH, KOH) and autoclave were applied. But achieved progress success is limited. From point of view of known zeolite chemistry these conditions are too harsh and can lead to severe damage of the zeolite structure and corresponding loss of wished properties like crystallinity, porosity, adsorption, and acidity. Presented data in the literature are not sufficient as sometime only BET values with no isotherm, only total acidity and no TPD curve, limited ^{29}Si MAS NMR and ^{27}Al MAS NMR about local structure, quantitative catalytic, acidity and activity data and influence of treatment conditions are not studied. Loss of the starting material was also not considered. Applied severe conditions of modifications in literature are expensive, energy and time consuming. Characterization of aluminosilicate framework of zeolites by ^{27}Al NMR and ^{29}Si NMR is needed to be considered for better understanding of framework changes after modifications.

Conclusion

So far used procedures are not optimal for the preparation of acidic clinoptilolite catalysts H-CLIN. Often the materials were not characterized in detail. Characterization data are not complete because they do not show nitrogen adsorption and desorption isotherms or ammonia-TPD curves. Often solid state NMR data are missed. Often markedly material loss occurs during acid treatment is not mentioned. Only some papers provide catalytic data. Obviously, the preparation conditions were very severe and too harsh for a zeolite. As a result framework damage, decrease in porosity and finally active sites are lost. Therefore this study focusses on the use of ”soft” preparation conditions, detailed structural, textural, and

qualitative and quantitative acidity characterization and catalytic testing of H-CLIN in order to improve preparation and properties of materials.

3 Results and Discussion

The acidic forms of the natural zeolite clinoptilolite were prepared in two ways, firstly by ammonium-exchange followed by calcination and secondly, by direct treatment with HCl in aqueous solution. The structural, textural, acidic properties of both types of acid catalysts were studied in detailed and catalytic performance in the acid catalyzed acetalization reaction and compared in order to derive possible property-catalysis relationships.

3.1 Ammonium exchanged and calcined Clinoptilolite

3.1.1 Material characterization

3.1.1.1 Chemical composition and Si/Al ratio

The ICP-AES elemental analysis data of the natural starting cation containing clinoptilolite CLIN and of calcined ammonium-exchanged NH_4-CLIN are shown in Table 2.

Table 2: Chemical composition of natural starting and ammonium-exchanged clinoptilolite CLIN determined by ICP-AES elemental analysis (ion exchange: 0.5M NH_4NO_3, 80°C, 1h; calcination: *ca.* 400°C for 1h, heating rate: 10K/min.)

Catalysts	Chemical composition (atom-%)							
	Si	Al	Ca	Mg	Na	K	Fe	Ti
Starting natural CLIN	31.00	5.88	1.00	0.20	0.51	2.90	0.99	0.08
Calcined NH_4^+-CLIN	30.15	5.48	0.24	0.26	0.29	1.70	0.95	0.08

According to chemical analysis Na^+, K^+, Mg^{2+}, Ca^{2+} were found as extra framework cations balancing the negative charge of the framework aluminum. The cation content is approximately in line with aluminum content the sample assuming that all aluminum is zeolitic (charge balance). Additional some Fe^{3+} and Ti^{3+} were found due to presence of small amounts of iron oxide, titanium oxide or iron titanate (not detectable by XRD). The total Si/Al ratio by chemical analysis of the natural CLIN is *ca.* 5.27. Assuming that the Si/Al ratio of the clinoptilolite compartment is 5 (according to IZA data base) and all aluminum is part of the zeolite, then the sample contains a 5 ma-% surplus of silica. So we arrive by zeolite content of the natural sample of *ca.* 95 %. Additional also *ca.* 1 % of Fe^{3+} and Ti^{3+} is present, so the final zeolite content is *ca.* 94 %. Taking into account that the sample contains *ca.* 5 % of non zeolitic silica, and then the Si/Al ratio of starting CLIN is 5.01 and calcined NH_4-CLIN is

5.23. This slightly increase is attributed to some dealumination occurring under the relative strong exchange conditions by temperature and ammonium salt concentration (80°C, 0.5 M, 1 h, pH = 6.8). Ammonium ion exchange followed by heating plays a key role in the variation of Si/Al ratio and are very effective in the removal of Fe^{3+}, Ca^{2+}, Na^{+} and Mg^{2+} cations. Potassium ions (K^{+}) are preferentially located in the center of 8-member ring (channel C- the window between channel A and B). They are hard to remove due to strong interaction with close framework oxygens of the small O8R. They play an important role in the thermal stability of clinoptilolite. Smaller cations such as Ca^{2+} and Na^{+} are too small to keep the channel expanded, whereas K^{+} due to its large size keep the structure expanded and prevents the structure from collapsing. Therefore, complete removal of K^{+} may cause a destruction of the framework.[49]

3.1.1.2 XRD pattern

XRD pattern of starting Natural CLIN vs Simulated CLIN are shown in Figure 12.

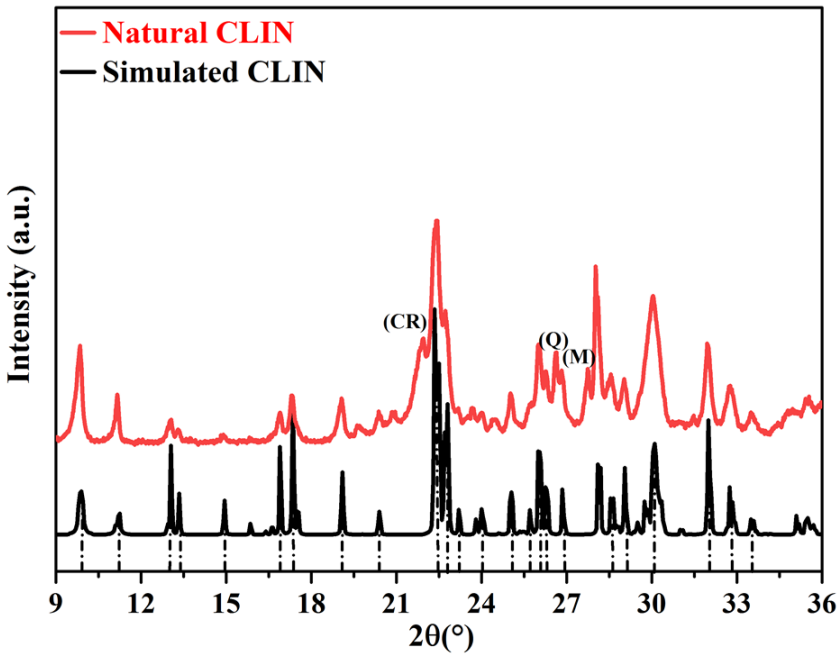

Figure 12. XRD patterns of simulated clinoptilolite (black) and natural zeolite clinoptilolite (Red). "C"-clinoptilolite, "Q"-α-quartz, "M"-mordenite and "CR"-cristobalite reflections.

The observed XRD pattern of CLIN agrees with the simulated clinoptilolite pattern. CLIN pattern shows all the main reflections present in simulated pattern and some additional reflections for Cristobalite (CR), Mordenite (M), and α-Quartz (Q), which are present in the

natural material as impurity. Compared to simulated diffraction pattern, the reflections in XRD pattern of CLIN are somewhat broader and the background increases between 2θ valve 18° and 35° due to lower crystallinity. Characteristics reflections for CLIN (C) are observed at 2θ = 9.85°, 11.2°, 13.05°, 16.95°, 17.34°, 19.10°, 22.44°, 26.64°, 28.08°, 30.15° and 31.94°. Additionally some non zeolitic reflections were observed at 2θ = 27.75°, 26.61° and 21.95° belonging to mordenite, cristobalite and α-quartz respectively. The same characteristics peak lines have also been confirmed by other authors.[55,60-63] The chemical analysis showed already that the material contains *ca*. 94 % of clinoptilolite, indicating the presence of some non zeolitic silica which is now confirmed by XRD.

XRD patterns of NH_4^+-exchanged and calcined CLIN are shown in Figure 13. Some shifts in peak positions and peak broadening can be seen for calcined NH_4-CLIN, but the overall structure is maintained.

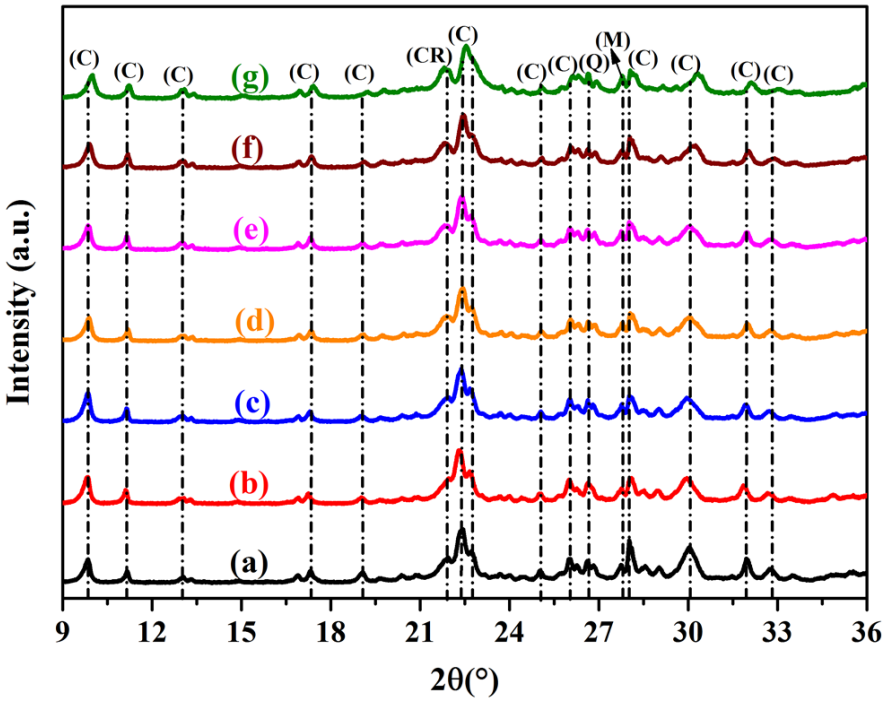

Figure 13. XRD patterns of starting CLIN and calcined rehydrated NH_4-CLIN (exchange condition: 0.5 M NH_4NO_3 at 80°C for 1 hour; calcination at 400-600°C, rehydration in humid air at r.t.). **a)** CLIN, **b)** NH_4-CLIN, **c)** H-CLIN-400°C, **d)** H-CLIN-450°C, **e)** H-CLIN-500°C, **f)** H-CLIN-550°C, **g)** H-CLIN-600°C. H-CLIN means protonic sample, calcined after NH_4^+-exchange at (400-600°C). "**C**"-clinoptilolite, "**Q**"-α-quartz, "**M**"-mordenite and "**CR**"-cristobalite reflections.

An increase in the background was observed for NH_4-CLIN after heating to *ca*. 400°C, 450°C, 500°C, 550°C and 600°C, respectively. The narrow-shaded reflections and small variation of their position after the thermal treatment confirms the structural and thermal

stability of all modified zeolite samples. Heating up to 400°C causes a shift of the reflections to higher angle due to shrinkage of the framework. Such shifts are typically observed with zeolites and are related to the dehydration of the zeolite framework and the decomposition of the ammonium ions. However, heating beyond 500°C causes stronger high angle shifts. E.g. the reflections at 2θ=9.85°, 17.34°, 30.15° and 31.94° shift to higher valves of 9.99°, 17.44°, 30.34° and 32.10° respectively by *ca*. 0.1° to 0.2° indicating more severe changes in the zeolite framework, e.g. dealumination or dehydroxylation.[64] These changes are accompanied by an increase of the background between 20° and 35° (deg.) and the relative increase of the cristobalite peak at 2θ=21.9° compared to neighbored clinoptilolite peaks. The crystallite size decreases (Tab. 4). These findings point to a loss of crystallinity and partial damage (amorphization) of the zeolitic framework due to calcination at high temperature.

Table 3: Influence of calcination temperature on position of selected diffraction peaks-2θ (°) of starting CLIN and calcined rehydrated NH_4-CLIN (exchange condition: 0.5 M NH_4NO_3 at 80°C for 1 hour; calcination at 300-600°C, rehydration in humid air at r.t.). H-CLIN means protonic sample, calcined after NH_4^+-exchange at (300-600°C).

Catalysts	**CLIN and calcined NH_4-CLIN samples 2θ (°)**				
CLIN	9.85	22.44	28.08	30.06	31.94
NH_4-CLIN	9.81	22.33	28.10	29.93	31.83
H-CLIN-300°C	9.81	22.36	28.03	29.93	31.90
H-CLIN-350°C	9.81	22.39	28.03	29.96	31.90
H-CLIN-400°C	9.85	22.39	28.00	29.93	31.94
H-CLIN-450°C	9.88	22.43	28.10	30	31.96
H-CLIN-500°C	9.88	22.45	28.10	30	31.96
H-CLIN-550°C	9.92	22.50	28.13	30.20	32.03
H-CLIN-600°C	9.98	22.60	28.16	30.33	32.16

The calcined NH_4-CLIN, i.e. the partial protonic H-form is stable until 600°C. Heating to 700°C and 800°C (Fig. 14) leads a collapse of zeolite framework. The background increases markedly and characteristics reflections of clinoptilolite (C) at 2θ=9.85°, 11.2°, 13.05°, 16.95°, 17.34°, 19.10°, 22.44°, 26.64°, 30.15° and 31.94° disappear due to amorphization. Mainly, XRD peaks characteristic for cristobalite and α-quartz remain (Fig. 14)

Table 4: Crystallite size of starting CLIN and calcined rehydrated NH_4-CLIN (exchange condition: 0.5M NH_4NO_3 at 80°C for 1 hour; calcination at 300-600°C, rehydration in humid air at r.t.). H-CLIN means protonic sample, calcined after NH_4^+-exchange at (300-800°C)

Catalysts	Crystallite size (nm)
CLIN	40.16
NH_4-CLIN	35.23
H-CLIN-300°C	37.13
H-CLIN-350°C	38.71
H-CLIN-400°C	37.20
H-CLIN-450°C	36.20
H-CLIN-500°C	36.28
H-CLIN-550°C	34.92
H-CLIN-600°C	28.42
H-CLIN-700°C	14.33
H-CLIN-800°C	12.75

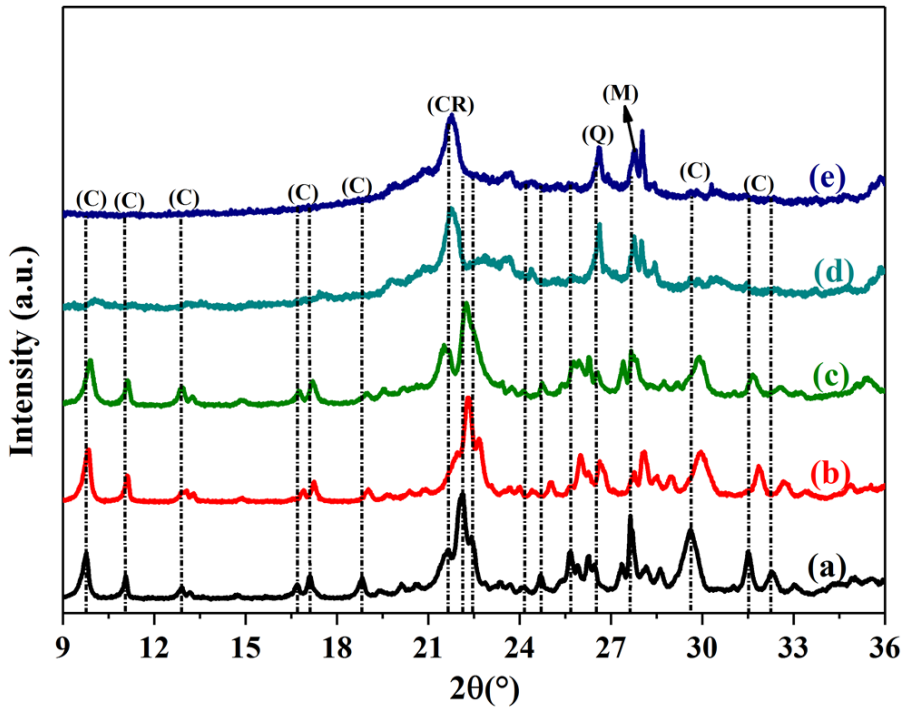

Figure 14. XRD patterns of CLIN-starting material and calcined rehydrated NH_4-CLIN (exchange condition: 0.5 M NH_4NO_3 at 80°C for 1 hour; calcination at 600-800°C, rehydration in humid air at r.t.). **a)** CLIN, **b)** NH_4-CLIN, **c)** H-CLIN-600°C, **d)** H-CLIN-700°C, **e)** H-CLIN-800°C. H-CLIN means protonic sample, calcined after NH_4^+-exchange at (600-800°C). "**C**"-clinoptilolite, "**Q**"-α-quartz, "**M**"-mordenite and "**CR**"-cristobalite reflections.

3.1.1.3 Fourier-transform infrared spectroscopy (FTIR)

FTIR spectra for CLIN and calcined NH_4- CLIN are shown in Figure 15 and wavenumbers of the different lattice and OH vibrations bands in the spectral range of 400-1800 cm^{-1} are given in Table 6. They are consisting with spectra typically observed with zeolites showing main absorbance at *ca*. 1200-900, 800-700 and at *ca.* 450 cm^{-1}, confirming the mainly zeolitic nature of the natural material (Tab. 5). These vibration bands are assigned as anti-symmetric at 1025 cm^{-1}, symmetric T-O-T at 794 cm^{-1} and tetrahedral TO_4 deformation vibrations of aluminosilicate framework at 446 cm^{-1} and structural sensitive double ring vibration band at 600 cm^{-1}. Additional absorbance at 1640 and 1450 cm^{-1} belong to deformation bands adsorbed water and ammonium ions respectively. The latter disappear after heating to 450°C due to the decomposition of the ammonium ions to protons (consistent with the formation of the partial H-form) by release of ammonia, whereas the water vibration band decreases only somewhat and remains even after heating to 600°C.

Table 5: Assignment of IR bands for natural zeolite clinoptilolite-CLIN.[56,61,62,65]

Vibration modes	Wavenumber (cm^{-1})	Intensity
Internal tetrahedral T-O bending vibrations	446	Strong
External tetrahedral double ring vibrations	600	Medium
External symmetric T-O-T vibrations	794	Medium
External anti-symmetric T-O-T vibrations	1025	Very strong
NH_4^+ ions located in the framework	1450	Medium
Bending deformation vibrations of adsorbed H_2O	1625	Weak

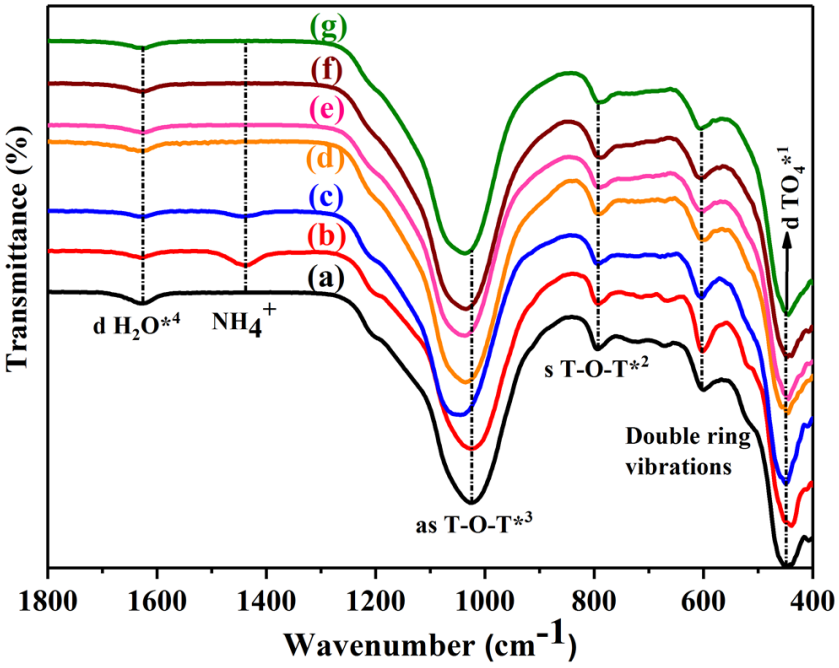

Figure 15. FTIR spectra of starting CLIN and calcined rehydrated NH_4-CLIN (exchange condition: 0.5M NH_4NO_3 at 80°C for 1 hour; calcination at 400-600°C, rehydration in humid air at r.t.). **a)** CLIN, **b)** NH_4-CLIN, **c)** H-CLIN-400°C, **d)** H-CLIN-450°C, **e)** H-CLIN-500°C, **f)** H-CLIN-550°C, **g)** H-CLIN-600°C.H-CLIN means protonic sample, calcined after NH_4^+-exchange at (400-600°C). **d TO_4*^{1}**-tetrahedral deformation vibration, **s T-O-T*^{2}**-symmetric T-O-T vibration, **as T-O-T*^{3}**-anti-symmetric stretching T-O-T vibration and **d H_2O*^{4}**-deformation vibrations of adsorbed H_2O.

Hence, residual water is strongly bound in the framework. The maintenance of the double-ring vibration band until 600°C confirms the structural stability of the partial H-form of NH_4-CLIN. It disappears after heating to 700-800°C indicating structural collapse (Fig. 16). The thermal treatment causes changes in the wavenumbers of IR vibration bands (Tab. 6). Specifically the wavenumber of anti-symmetric T-O-T vibration shows an unusual behaviour. The ammonium exchange has nearly no influence on its position and increases from 1025 to 1026 cm^{-1} only. Heating to 400°C causes a gradual and markedly increase of its wavenumber to 1044 cm^{-1}. This can be explained by the removal of water and mainly by the decomposition of NH_4^+ ions. Obviously, the ammonium ions strongly interact with the neighboured oxygen atoms located in the oxygen rings via strong hydrogen bonding. Therefore, the removal of the ammonium ions lead to a decrease of the T-O bond length and correspondingly to an increase of wavenumber of the anti-symmetric T-O-T band to 1044 cm^{-1} at 400°C. The FTIR spectroscopy is more sensitive to local changes in the structure than the XRD pattern. Distinct band shifts of the as-TOT band occur during heating from r.t. and to 400°C (Tab. 6). Other authors also reported similar results.[55,56,61,62,66-69]

Table 6: Position of the main vibration modes in CLIN- starting material and calcined rehydrated NH_4-CLIN (exchange condition: 0.5M NH_4NO_3 at 80°C for 1 hour; calcination at 300-600°C, rehydration in humid air at r.t.). H-CLIN means protonic sample, calcined after NH_4^+-exchange at (300-600°C). **d TO_4*[1]**-the tetrahedral deformation vibration, **s T-O-T*[2]** -symmetric T-O-T vibrations and **as T-O-T*[3]** - anti-symmetric stretching T-O-T vibrations.

Catalysts	d TO_4*[1]	Double ring vibration	s T-O-T*[2]	as T-O-T*[3]
CLIN	446	600	794	1025
NH_4-CLIN	445	601	792	1026
H-CLIN-300°C	447	602	793	1032
H-CLIN-350°C	447	602	793	1036
H-CLIN-400°C	448	603	792	1044
H-CLIN-450°C	448	604	792	1038
H-CLIN-500°C	446	605	791	1040
H-CLIN-550°C	445	605	790	1038
H-CLIN-600°C	444	607	788	1036
H-CLIN-700°C	446	n.a.	790	1052
H-CLIN-800°C	448	n.a.	789	1055

The XRD show a small expansion of the crystal lattice in this temperature range visible in the high angle shift of reflections. Heating beyond 400° causes small decrease of the $\nu_{.asTOT}$ accompanied by small contraction of the zeolite lattice. Beyond 500°C the $\nu_{.asTOT}$ decreases more rapidly and also the lattice contraction is stronger. Interestingly, then shifts to lower wavenumber of 1036 cm^{-1} again with heating to 600°C.This behaviour violates common knowledge. At high temperature zeolites undergo dealumination or de-hydroxylation which causes a decrease of the T-O bond length due to the increased Si/Al ratio. Therefore, these processes are connected with an increase of the vibration frequencies and not with a decrease. The double-ring vibration band and the symmetric vibration bands show a different behaviour. They continuously increase or decrease, respectively, with increasing temperature (Tab. 6). These contradictory findings points to more complex changes in the framework of NH_4-CLIN during heating to 600°C.

FTIR spectra for calcined NH_4-CLIN samples at 700°C and 800°C are shown in Figure 16. Two most pronounced changes are observed. The structure sensitive double-ring vibration band at 607 cm^{-1} disappears. Obviously, the zeolite structured is damaged. At the same time the wavenumber of the antisymmetric T-O-T vibrations increases from 1036 to 1052 cm^{-1} and 1055 cm^{-1}, respectively, this originates from the amorphous aluminosilicate phase.

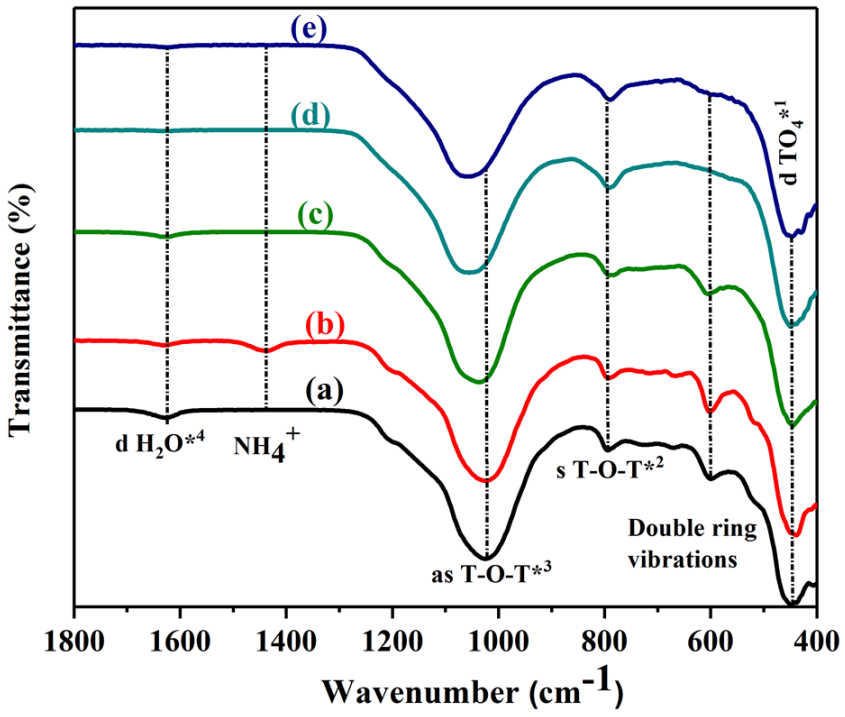

Figure 16. FTIR spectra of CLIN- starting material and calcined rehydrated NH_4-CLIN (exchange condition: 0.5M NH_4NO_3 at 80°C for 1 hour; calcination at 600-800°C, rehydration in humid air at r.t.).**a)** CLIN, **b)** NH_4-CLIN, **c)** H-CLIN-600°C, **d)** H-CLIN-700°C, **e)** H-CLIN-800°C. **d TO_4*[1]**-the tetrahedral deformation vibration, **s T-O-T*[2]**-symmetric T-O-T vibration, **as T-O-T*[3]**-anti-symmetric stretching T-O-T vibration and **d H_2O*[4]**-deformation vibrations of adsorbed H_2O.

The FTIR lattice vibration spectra confirm the XRD results. The FTIR is more sensitive to local changes in the structure. Distinct band shifts of the as-TOT band occur during heating from r.t. and to 400°C. Beyond 500°C the ν_{asTOT} decreases again, which is usually assigned to a decrease in the T-O bond distance. However, the XRD pattern shows mainly shrinkage of the zeolite framework between 500 and 600°C (Tab. 3). The reflection at 2θ=30° is shifted by *ca.* 0.3 degree to 30.33°.

3.1.1.4 Thermal Analysis (TG-DSC)

TG/DSC curve of starting CLIN are shown in Figure 17. In Figure 17a is shown the TG curve. Generally, the low temperature (25-180°C ± 10) weight loss represents the desorption of loosely bound water from the surface of the powdered sample (external water) and external and internal pores of the zeolite. The middle part of TG curve (180-430°C ± 20), represents desorption of cationic bound water. High temperature loss curve (430-600°C), represents desorption of tightly bound water from inner parts of the clinoptilolite pore system as e.g. small windows or the double ring cage.

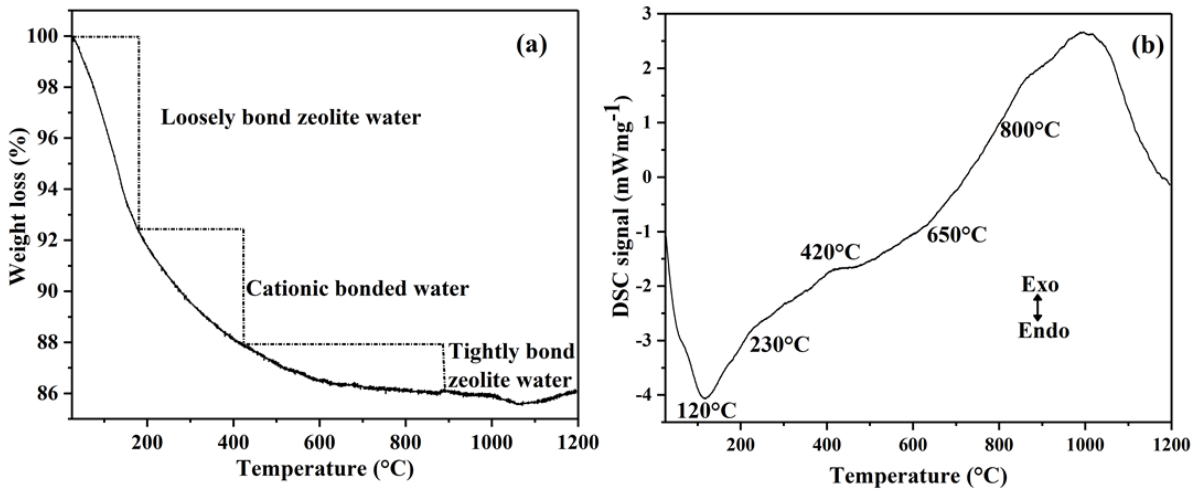

Figure 17. **(a)** TG curves of starting CLIN with different dehydration stages. **(b)** DSC curve of starting CLIN with endothermic DSC peaks. TG/DSC curves are recorded by heating CLIN sample up to 1200°C at 10°C/min under Argon.

The DSC curve (Fig. 17b) shows a large and a broad large endothermic peak at 50-230°C, belongs to desorption of external and zeolitic water. The endothermic peak at 230-420°C (shoulder) is assigned to desorption of cationic bonded zeolite water. A very broad endothermic DSC peak at 420-650°C, represents desorption of tightly bound zeolite water and also some dehydroxylation may occur in this temperature range. Thereafter (>650°C) very strong exothermic peak appears with a temperature maximum at *ca.* 1030°C due to the amorphization of the zeolite and formation of e.g. cristobalite.

TG/DSC curves of NH_4^+-exchanged and calcined re-hydrated NH_4-CLIN is shown in Figure 18. Two main broad, but well-defined, weight loss steps are observed with NH_4-CLIN between r.t. and 350°C and between 360 and 650°C. They are assigned desorption of loosely bound water and medium strong bound water in the cage. The second weight loss is assigned to the desorption of strong bound cationic water, the release of ammonia from decomposition of NH_4^+ ions as well as tightly fixed water confined in cages or windows.[75] Both losses are strongly endothermic as typical water desorption.

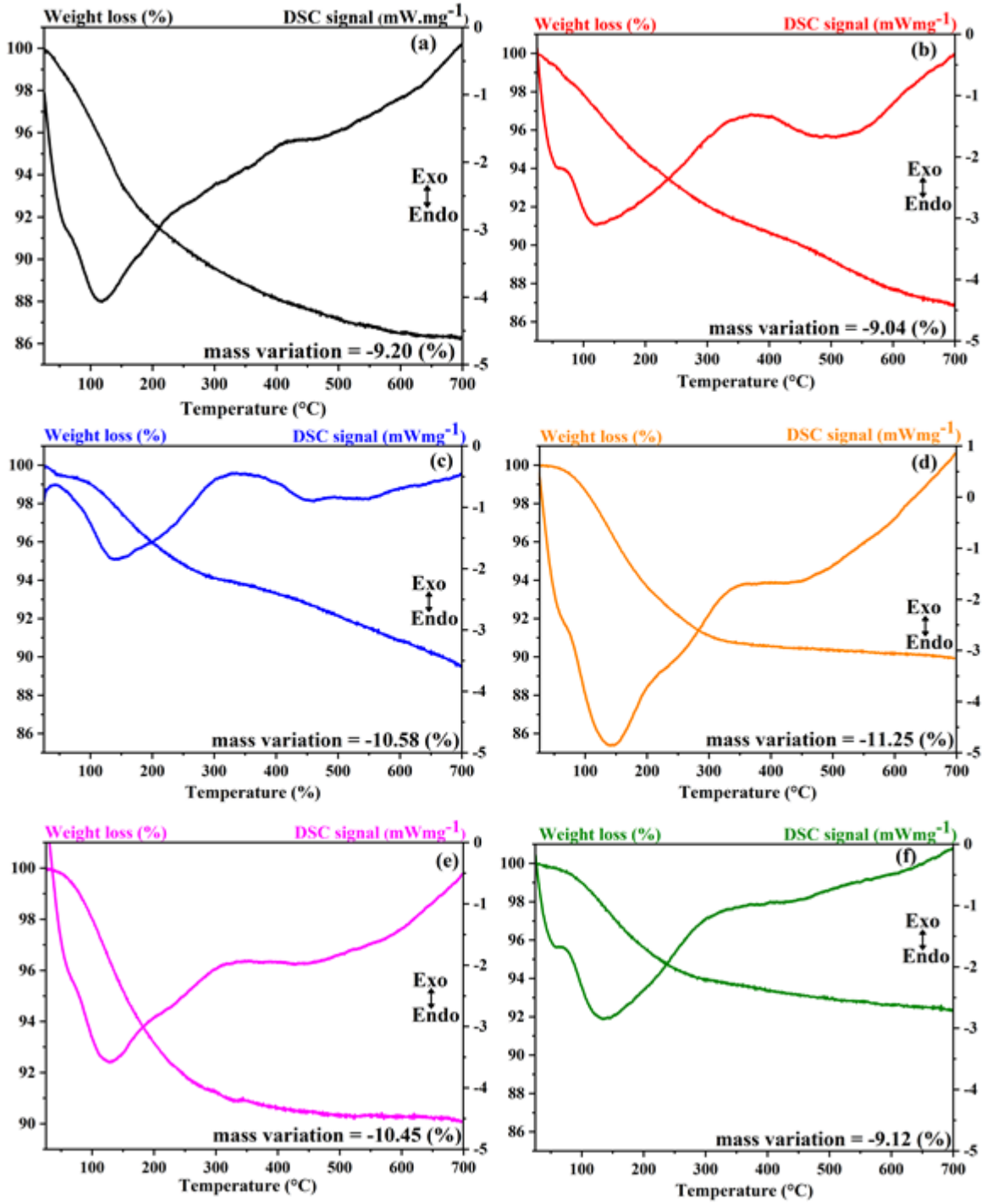

Figure 18. TG/DSC curves of starting CLIN and calcined rehydrated NH_4-CLIN (exchange condition: 0.5 M NH_4NO_3 at 80°C for 1 hour; calcination at 300-600°C, rehydration in humid air at r.t.). **a)** CLIN, **b)** NH_4-CLIN, **c)** H-CLIN-400°C, **d)** H-CLIN-450°C, **e)** H-CLIN-500°C, **f)** H-CLIN-600°C. H-CLIN means protonic sample, calcined after NH_4^+-exchange at (400-600°C).

The DSC curves show that the maximum temperatures of the weight losses are *ca*. 120°C and *ca.* 530°C. The shoulder at 50°C is characteristic of loosely bound external water. The overall appearance of the TG and DSC curves are maintained also after calcination and rehydration.

Samples calcined beyond 400°C, show only one large weight loss step up to 360°C with a continuous tailing to high temperature. Calcination at 400°C for 1 h leads already to a partial decomposition ammonium ions already (Scheme 3). Therefore, the second weight loss at higher temperature is not so pronounced.

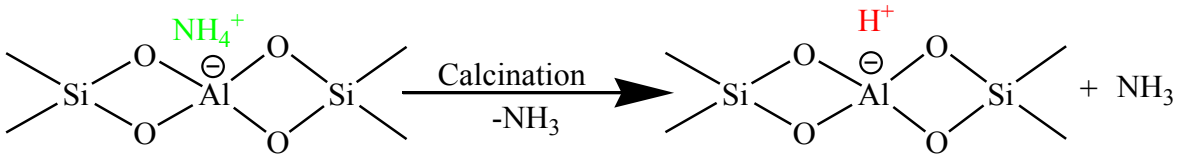

Scheme 3. Decomposition of NH_4^+ ions to NH_3 gas and H^+ during calcination (300-600°C) releasing protons to acid sites forming Brønsted acid sites i.e. bridging (OH) group Si-O(H)-Al.

Table 7: Influence of the calcination temperature on the weight loss of rehydrated ammonium-exchanged clinoptilolite and calcined NH_4-CLIN. Total weight loss and weight losses for loosely, medium- strong, and tightly bound water. Starting CLIN and calcined rehydrated NH_4-CLIN (exchange condition: 0.5 M NH_4NO_3 at 80°C for 1 hour; calcination at 300-600°C, re-hydration in humid air at r.t.). H-CLIN means protonic sample, calcined after NH_4^+-exchange at (300-600°C). Water is used as test molecule for pore volume and the change of the sample after NH_4-exchange and calcination.

Catalysts	**Total weight loss (%)***	**Loosely bond H_2O**	**Medium strong bound**	**Tightly bond H_2O**
		25-180°C	**180-430°C**	**430-700°C**
CLIN	9.20	3.41	3.70	2.09
NH_4-CLIN	9.04	3.22	3.58	2.24
H-CLIN-300°C	9.63	3.60	3.68	2.55
H-CLIN-350°C	10.10	4.10	3.90	2.60
H-CLIN-400°C	10.58	4.30	4.06	2.62
H-CLIN-450°C	11.25	5.34	4.83	2.08
H-CLIN-500°C	10.45	4.62	4.20	3.30
H-CLIN-550°C	9.88	4.00	3.78	2.80
H-CLIN-600°C	9.12	3.21	3.40	2.51

*The measurement error is < 0.1%.

The increase in the total water content of *ca.* 11 % by rising the calcination temperature to 450°C can be explained by the increase of the accessible pore volume due to the decomposition of the ammonium ions. Further rising the calcination temperature causes a decrease of the total amount of adsorbed water. This could be an indication for some crystallinity loss, pore blockage or other changes affecting the water adsorption capacity. The weight losses of loosely, cationic and tightly bound water show a similar behavior with rising

calcination temperature. The total weight loss is in line with former results observed with clinoptilolite minerals from different origins.[67,70-74] The observed total weight loss and weight losses at low, medium and high temperature are summarized in Table 7. The total weight loss, mostly due to water desorption, is similar (9-11 wt.-%) for all samples confirming the stability of the zeolite structure until 600°C. No structure transition signal is observed in the DSC curve. Usually it is narrow and exothermic.

3.1.1.5 Framework local structure analysis by ^{29}Si, ^{27}Al and ^{1}H MAS NMR

^{29}Si MAS NMR spectra of CLIN and calcined NH_4-CLIN

^{29}Si MAS NMR spectra of starting CLIN and calcined NH_4-CLIN are shown in Figure 20. Zeolites such as clinoptilolite consist of 3-dimensional frameworks of 4-fold connected $(Si,Al)O_4$- tetrahedra. The tetrahedra are connected via Si-O-Si and Si-O-Al aluminosiloxane bridges. Al-O-Al connections are forbidden according to the Löwenstein rule. Therefore, five different aluminum environments exist for the tetrahedral silicon denoted Si(nAl), with n=0-4 (Fig. 19). Here, n corresponds to the number of nearest next neighbored aluminum atoms in the second coordination sphere of silicon atoms. They give rise to appearance of selective characteristic signals in the ^{29}Si MAS NMR spectra of zeolites appearing at different chemical shifts (Tab. 8).

Table 8: General ^{29}Si MAS NMR chemical shifts trend in zeolites.[75]

Coordination	Notation	Chemical shift (ppm)
$Si(OSi)_4$	$Q^4(0Al)$	(-106.5) – (-116.5)
$Si(OSi)_3(OAl)$	$Q^4(1Al)$	(-97.5) – (-107)
$Si(OSi)_2(OAl)_2$	$Q^4(2Al)$	(-92.5) – (-99.5)
$Si(OSi)(OAl)_3$	$Q^4(3Al)$	(-85) – (-94.5)
$Si(OAl)_4$	$Q^4(4Al)$	(-81) – (-90.5)

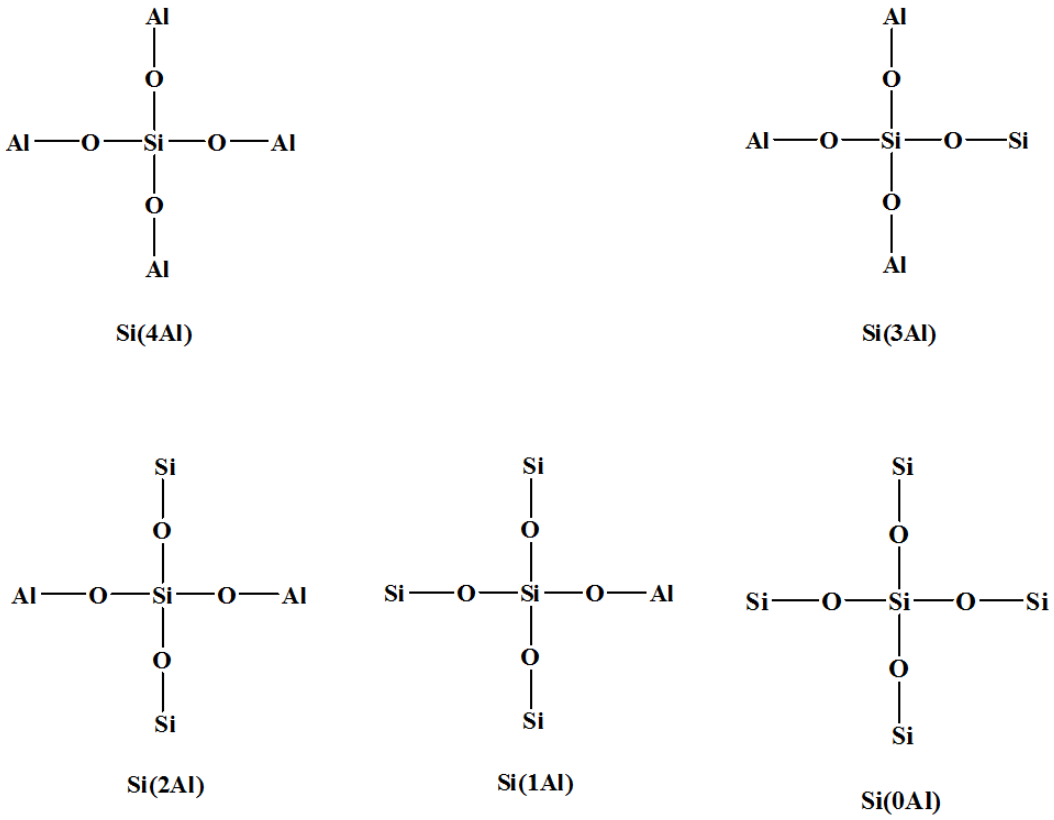

Figure 19. Silicon environments in zeolite frameworks which differ in the number of next nearest neighboured aluminum atoms connected to silicon by oxygen bridges. Si (nAl) units, n= 4, 3, 2, 1, 0.

Starting CLIN and calcined NH_4-CLIN spectra consist of three overlapping resonances located at *ca*. -101, -107 and -113 ppm which are assigned to Si(2Al), Si(1Al) and Si(0Al) units respectively (Tab. 9). The low field tailing of the spectrum *ca.* -97 ppm might indicate the presence of some Si(3Al) unit. The occurrence of thermally stable Si(2Al) units, which do not disappear with calcination, points to the presence of isolated stable bridged Si-O(H)-Al-O-Si-O-Al-O(H)-Si Brønsted acidic units in the protonated H-CLIN (medium silica-rich).[61,75-82] The spectra of the starting CLIN and NH_4-CLIN are very similar and do not change after heating to 400°C (Tab. 9). Heating beyond 400°C causes a broadening of the observed NMR signals indicating loss of local structural order. The spectra are no more structured and show a broad signal with an increased intensity located at *ca.* -110 ppm. The apparent shift in the peak maximum the ^{29}MAS NMR spectrum to lower ppm (Fig. 20d, e) is due to a new arising signal -109 ppm. This signal is assigned to the formation of cristobalite by partial destruction of zeolite framework at high temperature. These results are in line with XRD analysis and FTIR analysis.

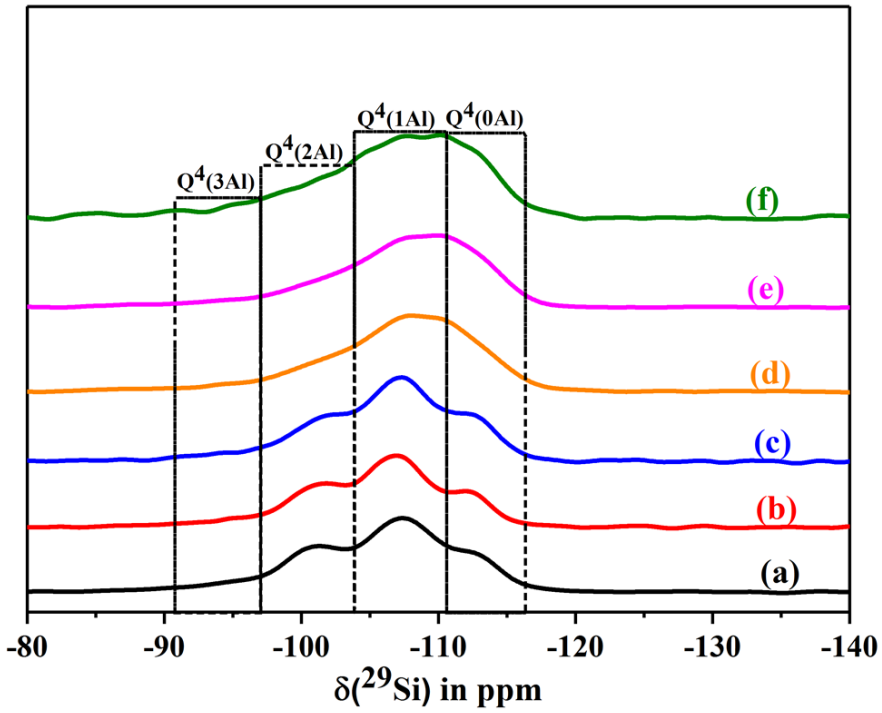

Figure 20. ^{29}Si MAS NMR spectra of dehydrated CLIN, and calcined NH_4-CLIN (0.5 M NH_4NO_3 at 80°C for 1 hour, 400-600°C) samples in dehydrated state. **a)** CLIN, **b)** NH_4-CLIN, **c)** H-CLIN-400°C, **d)** H-CLIN-450°C, **e)** H-CLIN-500°C, **f)** H-CLIN-600°C. All samples were activated at 400°C for 1 hour, heating rate of 5°C/min.

Table 9: Influence of calcination temperature on intensities and shifts of ^{29}Si NMR peaks of calcined NH_4-CLIN (Intensity roughly estimated from the intensity in the signal maximum are given in the brackets)

Catalysts	Q^4(2Al)		Q^4(1Al)		Q^4(0Al)	
	Intensity	Shift	Intensity	Shift	Intensity	Shift
CLIN	1.1	(-100.65)	1.9	(-107.37)	1.1	(-113.2)
NH_4-CLIN	1.1	(-100.97)	1.6	(-107.25)	1	(-113.04)
H-CLIN-400°C	1.2	(-101.33)	2.2	(-107.45)	1.3	(-113.27)
H-CLIN-450°C	0.9	(-102)	2	(-107.52)	1.4	(-113.42)
H-CLIN-500°C	0.8	(-102.71)	1.8	(-107.66)	1.5	(-113.5)
H-CLIN-600°C	1.2	(-103.65)	2.1	(-107.73)	1.8	(-113.85)

^{29}Si MAS NMR spectra calcined NH_4-CLIN at 600°C, 700°C and 800°C are shown in Figure 21. Rising the calcination temperature from 600°C to 700°C and 800°C results in markedly change in the ^{29}Si spectra of the calcined materials. The spectra are broadened and the signal maximum to *ca.* -109 to -110 ppm. The pronounced maximum points to the formation of

cristobalite[92]. The overall appearance is similar to amorphous silica and aluminosilicate material. These findings are in line with XRD results which show the amorphization (destruction) of zeolite structure and additional formation quartz after calcination at 700 and 800°C (compare Fig. 14- XRD-700,800°C).

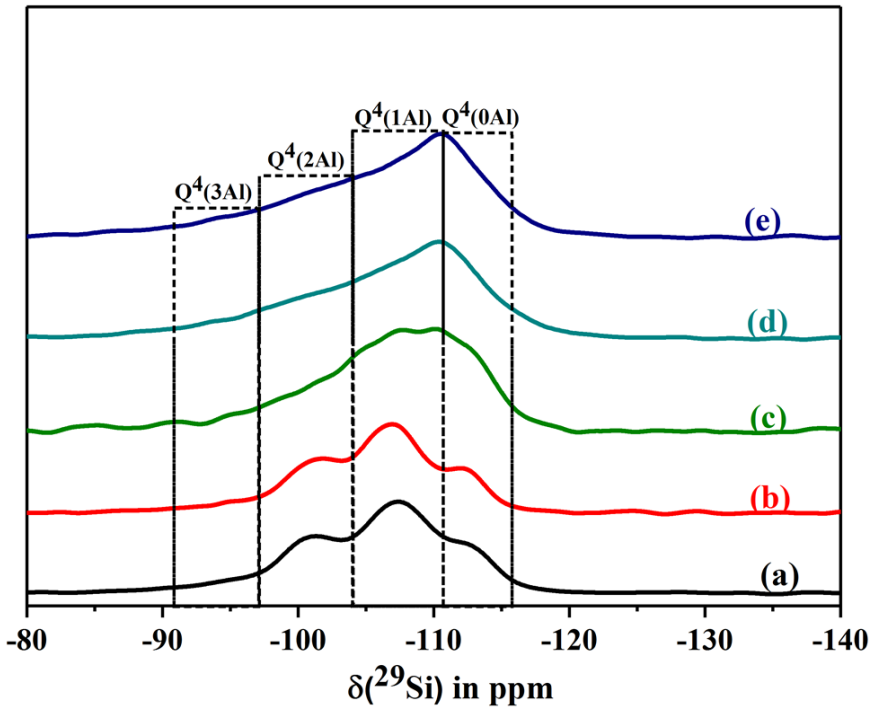

Figure 21. ^{29}Si MAS NMR spectra CLIN, and calcined NH_4-CLIN (0.5 M NH_4NO_3 at 80°C for 1 hour, 400-600°C) samples. **a)** CLIN, **b)** NH_4-CLIN, **c)** H-CLIN-600°C, **d)** H-CLIN-700°C, **e)** H-CLIN-800°C.

^{27}Al MAS NMR spectra of CLIN and calcined NH_4-CLIN

The ^{27}Al MAS NMR spectra of CLIN and calcined NH_4-CLIN are shown in Figure 22. The spectrum of the starting CLIN, which contains potassium, sodium, calcium and some magnesium cations, shows a strong signal at *ca.* 55 ppm with a shoulder at *ca.* 59 ppm, which is assigned to tetrahedral framework aluminum atoms $Al^{[IV]}$. There is no indication for the presence of octahedral coordinated extra-framework aluminum $Al^{[VI]}$, which usually give rise to a signal in the range of *ca.* +10 to -10 ppm. The ^{27}Al MAS NMR spectrum nearly not changes after partial exchange of the present cations, which are located in the pore system of the clinoptilolite, by ammonium ions. Subsequent calcination of the NH_4^+-exchanged CLIN at 400°C causes some changes in the spectrum by the appearance of a weak broad signal at *ca.* 30-50 ppm. This resonance is assigned to penta-coordinated $Al^{[V]}$. It is formed on the expense of tetrahedral-coordinated framework $Al^{[IV]}$. Additionally, the signal of the tetrahedral framework aluminum broadens indicating increasing disorder in the zeolite lattice. Obviously,

the lattice disorder originates from the partial decomposition of the NH_4^+-ions with corresponding formation of protons. They are located at the Si-O(H)-Al bridges and cause local structural changes, e.g. of the TOT-angles and T-O-bond distances (lattice distortion). Additionally the appearance of a very weak signal at *ca*. 0 ppm shows the presence of some octahedral coordinated extra-framework aluminum $Al^{[VI]}$. Further heating during calcination to 450, 500 and 600°C causes a markedly broadening of the signal of tetrahedral coordinated aluminum, indication increasing disorder in the clinoptilolite framework. This broadening is accompanied by a substantially increase of the signal intensity of penta-coordinated aluminum. H^+ ions produced are getting attached to the framework to balance the negative charge of the framework instead of staying in the lattice, causing shrinkage of the framework and more appearance of extra framework octahedral aluminum and penta-coordinated aluminum at around 0 ppm and *ca.* 30-40 ppm respectively can be seen. Hence, a noticeable transition of tetrahedral coordinated aluminum to penta-coordinated aluminum occurs during calcination at high temperature. Additionally, amount of extra-framework remains small as shown by the low intensity of the AlO_6 signal in the ^{27}Al MAS NMR spectrum i.e. some octahedral aluminum is formed (signal at 3 ppm).[61,75,76,83,84]

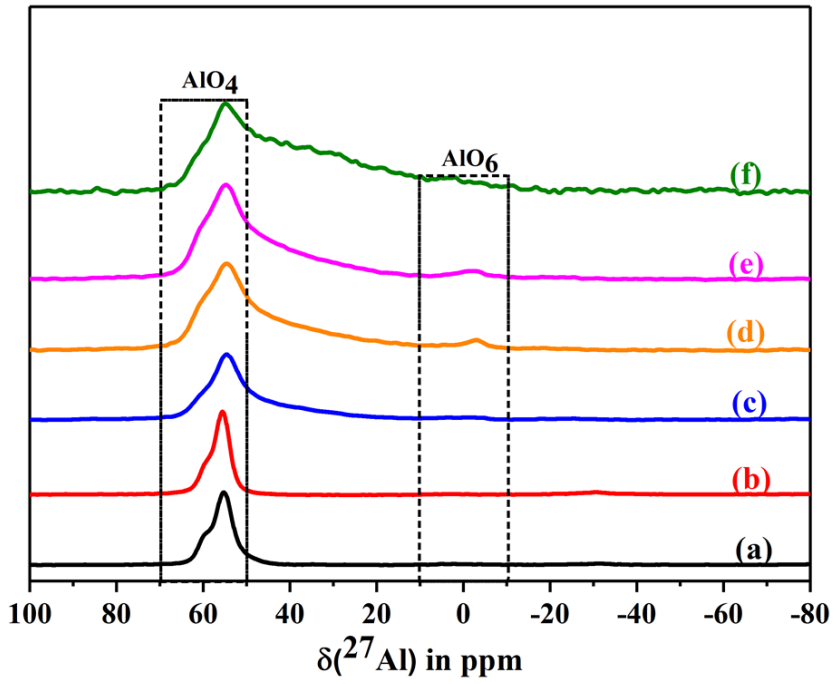

Figure 22. ^{27}Al MAS NMR spectra of dehydrated CLIN, and calcined NH_4-CLIN (0.5M NH_4NO_3 at 80°C for 1 hour, 400-600°C) samples. **a)** CLIN, **b)** NH_4-CLIN, **c)** H-CLIN-400°C, **d)** H-CLIN-450°C, **e)** H-CLIN-500°C, **f)** H-CLIN-600°C. All samples are activated at 400°C for 1 hour, heating rate of 5°C/min.

Calcination of sample at 600°C causes the formation of framework defects, breaking of Al-O bonds and local lattice shrinkage is induced and causes a shift of the distinct reflections. The action is locally, therefore, only selected reflections are shifted to higher 2θ value (XRD), i.e., lattice plane distance decreases in this area. It is concluded, that the transition of the NH_4-CLIN to protonic H-CLIN and following transition of framework $Al^{[IV]}$ to penta-coordinated $Al^{[V]}$, which likely remains in the framework. Otherwise, also larger amounts of octahedral coordinated extra-framework aluminum $Al^{[VI]}$ should be formed and also the intensities of ^{29}Si MAS NMR signals of the Si(1Al) and Si(0Al) units should be increased markedly, which is not the case.

The ^{27}Al MAS NMR spectra of NH_4-CLIN calcined at 600°C, 700°C and 800°C are shown in Figure 23. After calcination beyond 600°C to 700 and 800°C, the signal of $Al^{[V]}$ remains in the spectrum and further broadens, whereas the elative signal intensity of penta-coordinated $Al^{[V]}$ decreases. Also the shoulder at *ca.* 59 ppm is lost. The signal of octahedral $Al^{[V]}$ is still low and very broad ranging from *ca.* +10 to -10 ppm. These observed changes are consistent with the XRD and ^{29}Si MAS NMR results showing a destruction of the zeolite framework structure and formation of amorphous phases.

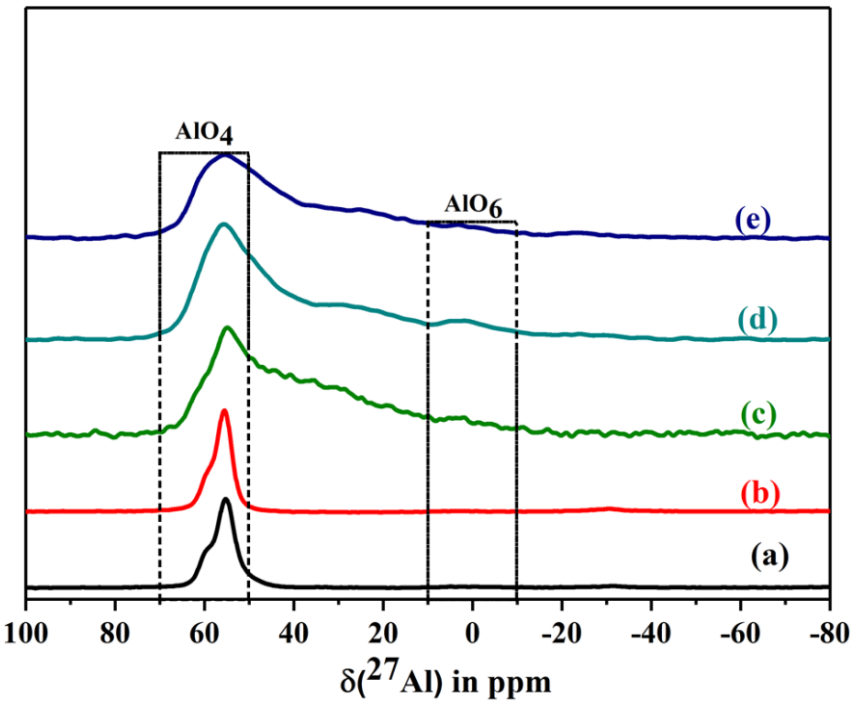

Figure 23. ^{27}Al MAS NMR spectra of CLIN, and calcined NH_4-CLIN (0.5M NH_4NO_3 at 80°C for 1 hour, 600-800°C) samples. **a)** CLIN, **b)** NH_4-CLIN, **c)** H-CLIN-600°C, **d)** H-CLIN-700°C, **e)** H-CLIN-800°C.

^{1}H MAS NMR spectra of CLIN and calcined NH_4-CLIN

The ^{1}H MAS NMR spectra of CLIN and calcined NH_4-CLIN are shown in Figure 21. The Chemical shifts of protons located on different sites in zeolite frameworks in Table 10. ^{1}H MAS NMR spectra of CLIN show a broad signal at *ca.* 4 ppm due to adsorbed water. NH_4-CLIN spectra show two broad signals at *ca.* 4 ppm and 6.6 ppm due to adsorbed water and exchanged NH_4^+ ions, respectively. In case of the dehydrated and NH_4-CLIN (400°C) an intense narrow signal at *ca.* 6.6 ppm is observed due to remaining NH_4^+ ions. Additionally, a broad signal arises at *ca.* 4.3 ppm which is assigned to acidic bridging OH groups, due to starting decomposition of ammonium ions. Also the presence (contribution) of some traces of water cannot be excluded. After calcination at 450°C, a broad signal with a maximum at *ca.* 5.6 ppm appears which assigned to Brønsted acid sites. Additionally, a signal appears at *ca.* 8.5 ppm which is assigned to distributed Brønsted acid sites (Tab. 10). The shoulder at *ca.* 6.5 ppm is caused by traces of not decomposed NH_4^+ ions. The weaker signal at *ca.* 1.6 ppm indicates the presence of silanol groups (SiOH). After calcination at 500°C, significant changes in the ^{1}H MAS NMR spectrum are observed. The intensity of Brønsted sites with former maximum at 5.6 ppm disappears and only a broad shoulder remains in the BS chemical shift range (3.8-6 ppm). Also the signals of distributed acid sites and ammonium ions disappear. The intensity of SiOH signal at *ca.* 1.6 ppm increases markedly. Additionally, a new intense dominating signal is appears at *ca.* 2.45 ppm. It assigned to AlOH species.

Table 10: Chemical shifts of protons located on different sites in zeolite frameworks.[85]

^{1}H MAS NMR shifts (ppm)	**Abbreviation**	**Types of hydroxyl group**
(-0.5)-(+0.5)	MeOH*	Metal or cation OH groups in large cavities or outer surface
1.3-2.2	SiOH	Silanol groups at the external surface or lattice defects
2.6-3.6	AlOH	OH groups bounded to extra framework aluminum species located in cavities or channels involved in hydrogen bonds
3.8-4.3	SiOHAl, SiO_1HAl	Bridging OH groups in large cavities or channels of zeolites
4.6-5.2	SiOHAl, SiO_3HAl	Bridging OH groups in small channels and cages of zeolites
6.1-7.0	SiOHAl	Distributed bridging OH groups in zeolites

*Me = metal cations

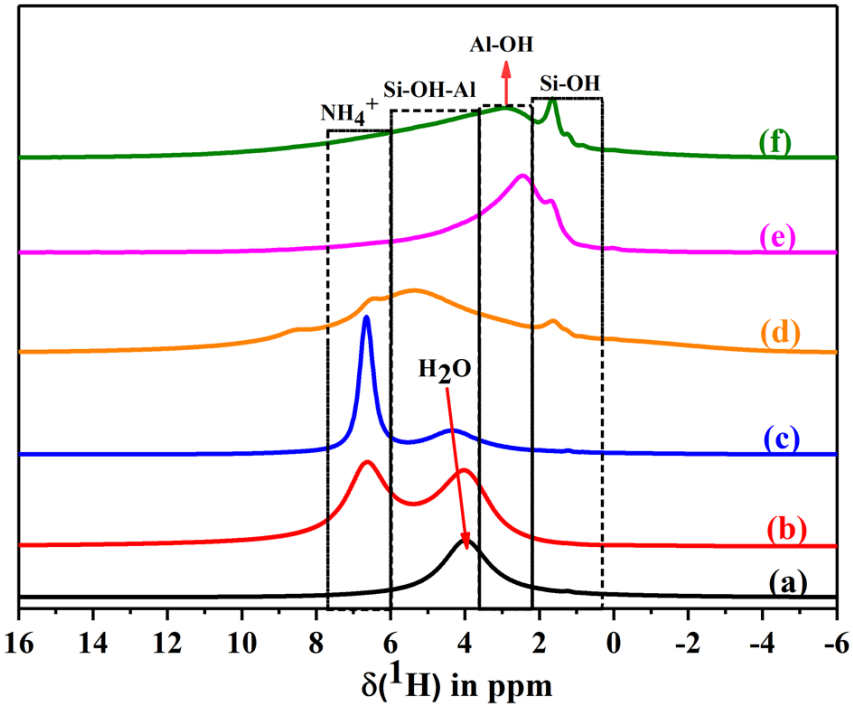

Figure 24. ^{1}H MAS NMR spectra of dehydrated CLIN, and calcined NH_4-CLIN (0.5M NH_4NO_3 at 80°C for 1 hour, 400-600°C) samples. **a)** CLIN, **b)** NH_4-CLIN, **c)** H-CLIN-400°C, **d)** H-CLIN-450°C, **e)** H-CLIN-500°C, **f)** H-CLIN-600°C. All samples were activated at 400°C for 1hour, heating rate of 5°C/min.

However, ^{27}Al MAS NMR spectra confirmed that the relative amount of octahedral EFAL is low. In contrast, formation of a large portion of penta-coordinated aluminum $Al^{[V]}$ is observed (signal at *ca.* 30 ppm). Therefore, it is concluded that the high intense AlOH signal at *ca.* 2.45 ppm belongs to penta-coordinated. Further heating to 600°C, leads to a decrease of the intensity and shift of the AlOH signal to *ca.* 2.9 ppm due to dehydroxylation and removal of tightly bound water as shown by TG/DSC measurements (Fig. 18). The high field tailing of the AlOH signal to *ca.* 6 ppm may indicate that Brønsted acid sites are still present. Also a well-resolved signal at *ca.* 0.5 ppm is observed which belongs to cationic MeOH groups.

3.1.2 Textural characterization

3.1.2.1 Scanning electron microscopy (SEM)

SEM images of the starting mineral clinoptilolite CLIN, of its ammonium exchanged form and NH_4-CLIN after calcination are shown at different magnification in Figure 25. They show that the starting clinoptilolite natural is in the form of very heterogeneous agglomerate and consists of µm-sized irregular shaped bulky agglomerated particles (submicron size).

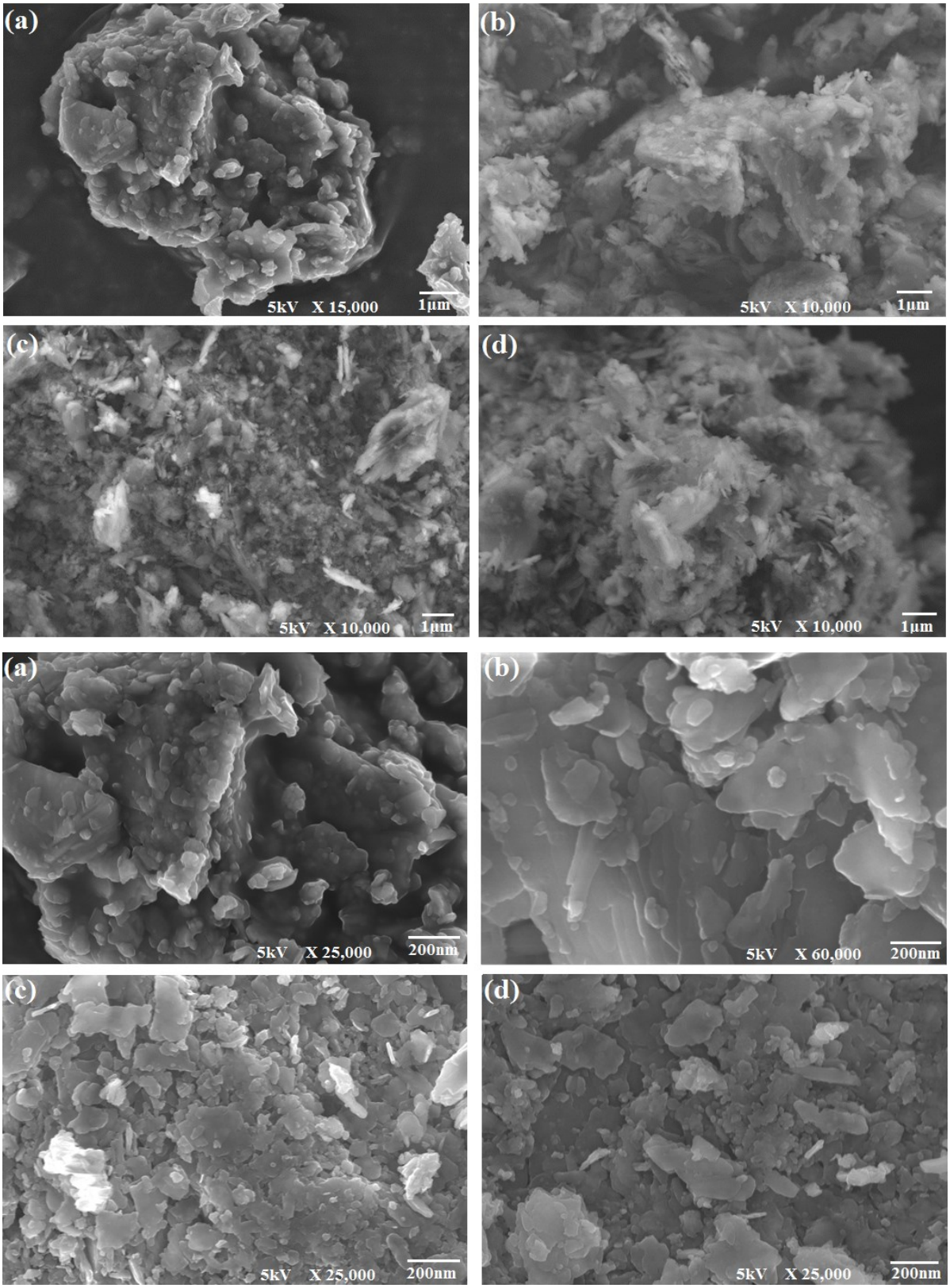

Figure 25. SEM images of CLIN- starting material and calcined rehydrated NH_4-CLIN (exchange condition: 0.5M NH_4NO_3 at 80°C for 1 hour; calcination at 300-600°C, rehydration in humid air at r.t.). **a)** CLIN, **b)** NH_4-CLIN, **c)** H-CLIN-450°C, **d)** H-CLIN-600°C. H-CLIN means protonic sample, calcined after NH_4^+-exchange at (450-600°C).

In starting CLIN pores of fracture-type 25-50 nm to 100 nm in size between clinoptilolite grains as well as pores between crystal aggregates up to 500 nm in size are reported.[58,67,68,70,86] After ammonium-exchange in aqueous solution of ammonium nitrate at 80°C for 1 h, i.e. under hydrothermal conditions, the particle size is little bit growing and particle surfaces become more flat. Obviously small material parts dissolve under exchange conditions or are removed after centrifugation. Calcination at 450°C causes a markedly de-agglomeration, probably due to sudden decomposition of ammonium ions and creates inter particle textural porosity ("Popcorn effect"). The sample is more homogeneous and composed of small particles. Clearly are visible the agglomerated small particles and the textural porosity, large meso and macropores in between the particles. The small primary nanoparticles have a size 30-100(200) nm as seen with higher magnification. Mesopores are not in the nanoparticles. Sample show hierarchical textural porosity with pore size rages from 30 nm to 0.5-1 µm. Compared to the starting material, the access of molecules to the catalyst surface is markedly increased. After calcination at 600°C, the surface seems more rough and a large number of small distributed particles are visible. Due to high temperature calcination the sample surface seems more damaged.

3.1.2.2 Nitrogen adsorption-desorption

The N_2 adsorption-desorption isotherms of CLIN and calcined NH_4-CLIN are shown in Figure 26 and the specific surface areas and pore volumes are summarized in Table 11. All clinoptilolite samples show the same type IV isotherm according to IUPAC classification. They show a steep nitrogen uptake at very low relative pressure (of p/p_0 <0.01) and a less steep increase up to of p/p_0=0.05 due to the adsorption in small and larger zeolitic micropores. It is followed by slow increase of the adsorption isotherm with growing relative pressure until of p/p_0 of *ca.* 0.8 due to adsorption in mesopores or multilayer adsorption. Beyond this value adsorption of nitrogen in textural larger meso-nano or macropores starts, located in between the crystals. The N_2 adsorption-desorption isotherms of CLIN and NH_4-CLIN show low uptake in the micropore range. The zeolite pores are blocked by extra framework cations i.e. Na^+, K^+, Ca^{2+}, Mg^{2+} ions. As a result low BET surface areas of *ca.* 43 to 52 m^2/g and micropore volumes V_{micro} of 0.018 to 0.022 cm^3/g was observed for starting CLIN and NH_4-CLIN. These values agree with data reported in the literature. The BET values of 33.5, 29.7, 84.45, 13.4, and 7.9 m^2/g and V_{micro} values of 0.003, 0.053, 0.0254, 0.003 and 0.002 cm^3/g were reported for natural clinoptilolites from different origins.[56,60-62,67-70]

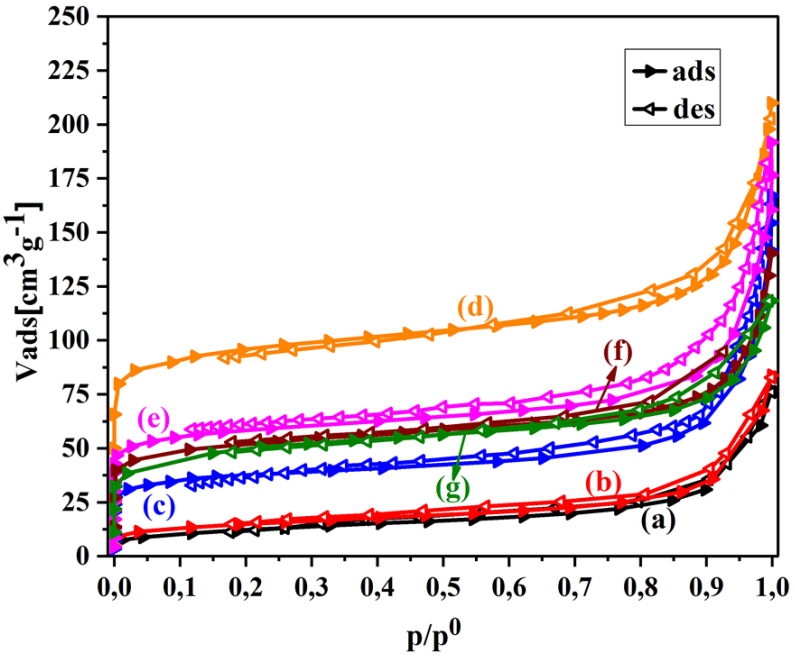

Figure 26. N_2-adsorption desorption isotherm of starting CLIN and calcined rehydrated NH_4-CLIN (exchange condition: 0.5M NH_4NO_3 at 80°C for 1 hour; calcination at 300-600°C, rehydration in humid air at r.t.). **a)** CLIN, **b)** NH_4-CLIN, **c)** H-CLIN-400°C, **d)** H-CLIN-450°C, **e)** H-CLIN-500°C, **f)** H-CLIN-550°C, **g)** H-CLIN-600°C. H-CLIN means protonic sample, calcined after NH_4^+-exchange at (400-600°C). Samples are dried by heating at 300 °C for 2 h at 3 K/min and pumping under the reduced pressure and measurement was carried out at 77 K (-196 °C).

N_2 is mainly adsorbed in mesopores, slight increase of the adsorption isotherm until p/p_0 of *ca.* 0.8, and in textural nano and macropores filled at $p/p_0 > 0.8$. Calcination at elevated temperature causes the decomposition of the NH_4^+-ions leaving structural Brønsted protons. The removal of the cations and the loss of adsorbed zeolite water results in an opening of the pores. The micropore system becomes available for adsorbed molecules resulting in strong increase of the nitrogen uptake at very low relative pressure. It reaches maximum after calcinations at 450°C. At this temperature pore blocking ammonium ions are nearly completely removed. The BJH micropore area and volume increase to *ca.* 334 m^2/g and 0.148 cm^3/g (Tab. 11). The BET surface area reaches 409 m^2/g and the pore volume 0.374 cm^3/g. These values are in agreement to that achieved with zeolite ZSM-5 [Si/Al 32, 377 m^2/g, 0.15 cm^3/g].[86,88,89] The calcination causes also an increase in the adsorption at high relative pressure which is related to adsorption in larger textural pores. This finding is in line with the SEM images, which show formation of textural porosity by de-agglomeration (popcorn effect -micro explosion of ammonia gas formed by the sudden decomposition of ammonium ions confined in the micropores).

Table 11: Structural parameters calculated from adsorption–desorption isotherms of nitrogen for starting CLIN and calcined rehydrated NH_4-CLIN (exchange condition: 0.5 M NH_4NO_3 at 80°C for 1 hour; calcination at 300-600°C, rehydration in humid air at r.t.). H-CLIN means protonic sample, calcined after NH_4^+-exchange at (300-600°C). Samples are dried by heating at 300 °C for 2 h at 3 K/min and pumping under the reduced pressure and measurement was carried out at 77 K (-196 °C).

Catalysts	SSA (m^2g^{-1})[a]	Micropore area (m^2g^{-1})	Mesopore area (m^2g^{-1})[b]	Pore volume (cm^3g^{-1})[c]	Micropore vol. (cm^3g^{-1})[b]	Mesopore vol. (cm^3g^{-1})	Nanopore vol. (cm^3g^{-1})
CLIN	44.3	15.79	28.51	0.12	0.018	0.017	0.085
NH_4-CLIN	51.77	23.26	28.51	0.13	0.022	0.018	0.09
H-CLIN-300°C	63.65	36.63	27.02	0.14	0.02	0.016	0.104
H-CLIN-350°C	81.08	46.47	34.608	0.19	0.034	0.02	0.136
H-CLIN-400°C	170.27	137.66	32.61	0.26	0.058	0.02	0.182
H-CLIN-450°C	409.14	333.81	75.33	0.374	0.148	0.031	0.195
H-CLIN-500°C	244.21	202.95	41.26	0.29	0.09	0.02	0.18
H-CLIN-550°C	204.79	157.18	47.61	0.22	0.08	0.02	0.12
H-CLIN-600°C	199.35	153.12	46.23	0.183	0.076	0.023	0.084

[a]Specific surface area BET, [b]t-Method, [c]Gurvich at $p/p^0 = 1$.

The rise of the calcination temperature from 450°C to 600°C results in markedly decrease of specific pore areas and pore volumes of calcined NH_4-CLIN (Tab. 11 and Fig. 27). These finding are in line with the observed decrease in the crystallinity of these samples with increasing calcination temperature: increase of the background and widths of XRD reflections, i.e. decrease of crystallite size and shift of selected reflections to higher diffraction angles (lattice shrinkage), broadening of the ^{29}Si MAS NMR spectra indicating local structural disorder, and increased intensity of the penta-coordinated ^{27}Al MAS NMR signal. Figure 28 shows the effect of calcination temperature on the micropore, mesopore and nanopore volumes. With increasing calcination temperature to 400-450°C the pore volumes of micro and nanopores increases and decreases again with rising temperature. Both have a similar contribution to the total porosity. The micropores contribute mostly to the total specific surface areas. The mesopores are nearly not affected and show lowest contribution to porosity.

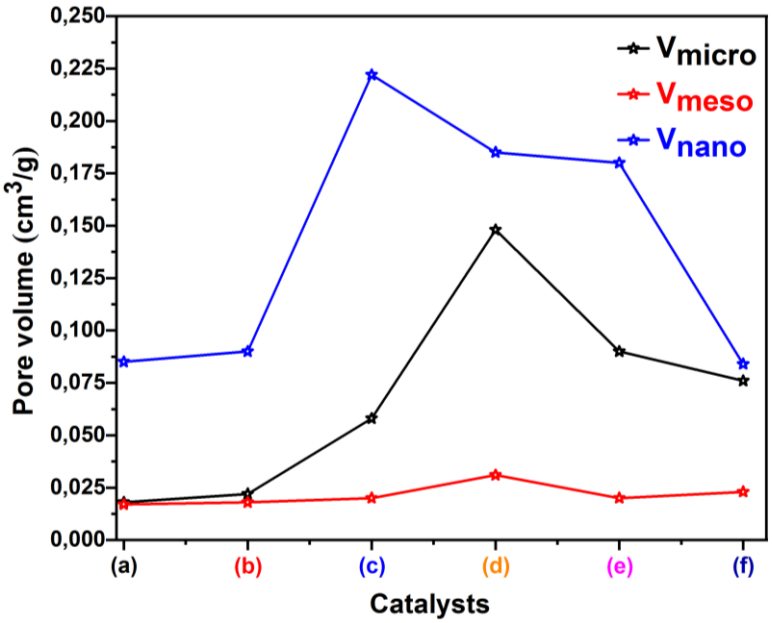

Figure 27. Micropore, mesopore and nanopore volumes of starting CLIN and rehydrated calcined NH_4-CLIN (exchange condition: 0.5 M NH_4NO_3 at 80°C for 1 hour; calcination at 300-600°C, rehydration in humid air at r.t.). **a)** CLIN, **b)** NH_4-CLIN, **c)** H-CLIN-400°C, **d)** H-CLIN-450°C, **e)** H-CLIN-500°C, **f)** H-CLIN-550°C, **g)** H-CLIN-600°C. H-CLIN means protonic sample, calcined after NH_4^+-exchange at (400-600°C).Sample are dried by heating at 300°C for 2 h at 3 K/min and pumping under the reduced pressure and measurement was carried out at 77 K (-196 °C).

3.1.3 Acidity of NH_4-CLIN and calcined NH_4- CLIN at 400°C

The temperature-programmed desorption of ammonia from starting NH_4-CLIN and calcined NH_4-CLIN at 400°C (H-CLIN-400°C), releasing structural bridging Si-O(H)-Al Brønsted acid sites (BS) are shown in Figure 28. The desorption profile is structured into low medium and high temperature peaks which can be related to weak, medium, strong and very strong bound ammonium ions. The low temperature shoulder below 300°C and the peak at *ca.* 330°C is assigned to weak and medium strong BS. The high temperature peaks (HTP) between 400°C to 600°C, with maxima at *ca*. 450°C and 520°C can be related to strong and very strong BS, respectively. Calcination of the sample at 400°C diminishes markedly the TPD-peak intensities. Medium Weak and medium strong bound ammonium ions are completely released. Strong bound ammonium ions are only partially decomposed into ammonia. Weak and medium strong BS as well as some strong BS sites are formed. Calcination at 400°C is not sufficient for the complete decomposition of exchanged ammoniums (activation) in order to achieve maximum acidity (number of BS). The total ammonium content of NH_4-CLIN amounts to *ca.* 1.4 mmol/g. The cation exchange capacity CEC of the natural CLIN material

is *ca.* 2.25 mmol/g i.e. CEC degree *ca.* 62 % is reached after ammonium exchange with aqueous 0.5 M NH_4NO_3 solution at 80°C for 1 h.

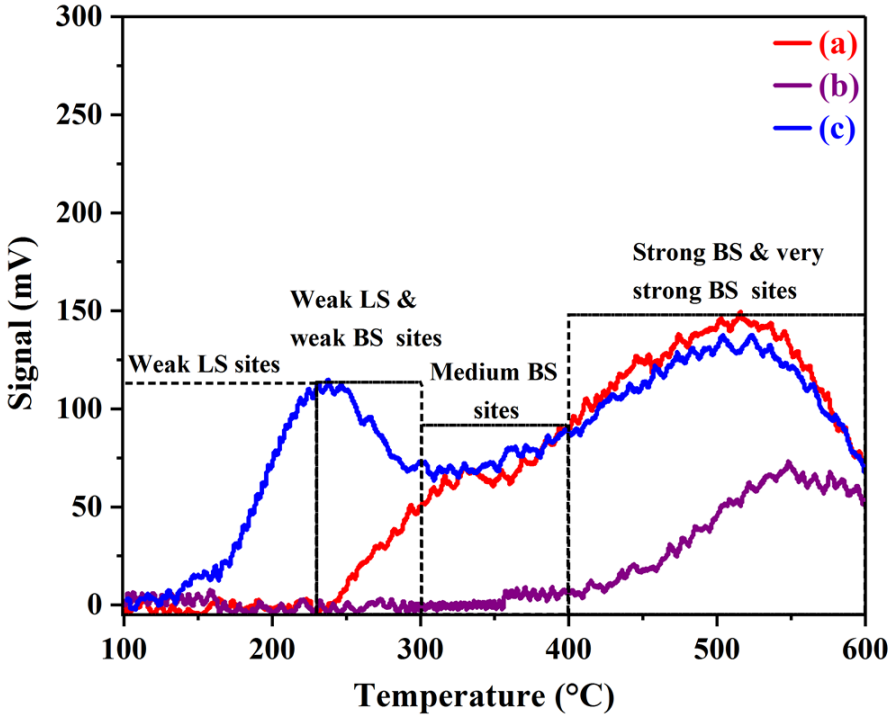

Figure 28. Temperature programmed desorption profiles of rehydrated NH_4-CLIN and calcined rehydrated NH_4-CLIN (exchange condition: 0.5M NH_4NO_3 at 80°C for 1 hour; calcination at 400°C, rehydration in humid air at r.t.). **a)** NH_4-CLIN without NH_3-loading, **b)** H-CLIN-400°C without NH_3-loading, **c)** H-CLIN-400°C with NH_3-loading, H-CLIN means protonic sample, calcined after NH_4^+-exchange at (400°C). Pretreatment of samples at 180°C, NH_3 gas loading at 100°C and desorption analysis at 600°C.

After calcination at 400°C remains 0.425 mmol/g of ammonium ions (Tab. 12). All samples contain residual, hardly to exchange, cations. These finding are in line with the chemical analysis. The re-adsorption ammonia on NH_4-CLIN calcined at 400°C nearly retains the TPD-profile of the starting NH_4-CLIN. The zeolite structure is not affected at this temperature. Additionally, a broad low temperature peak appears with a peak maximum near 230°C. It is assigned to ammonia adsorb at weak Lewis sites (LS) as cations and framework sites (Tab. 13). Heating to 450°C (Fig. 29) leads to the complete decomposition and desorption of ammonium ions and formation of the BS acidic H-form (H-CLIN). Only some ammonium ions remain (0.08 mmol/g), which is line the ^{1}H MAS NMR and FTIR results presented before (Fig. 15 and 24).

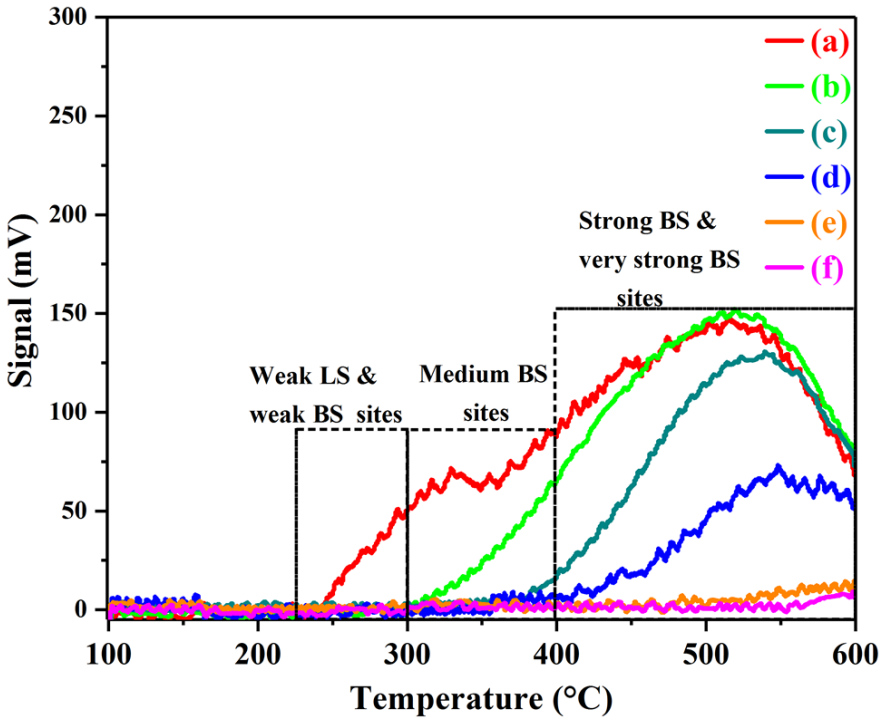

Figure 29. Temperature programmed desorption profiles of rehydrated NH_4-CLIN and calcined rehydrated NH_4-CLIN (exchange condition: 0.5M NH_4NO_3 at 80°C for 1 hour; calcination at 300-600°C, rehydration in humid air at r.t.). **a)** NH_4-CLIN without NH_3-loading, **b)** H-CLIN-300°C without NH_3-loading, **c)** H-CLIN-350°C without NH_3-loading,**d)** H-CLIN-400°C without NH_3-loading, **f)** H-CLIN-450°C without NH_3-loading, **g)** H-CLIN-500°C without NH_3-loading. H-CLIN means protonic sample, calcined after NH_4^+-exchange at (300-500°C). Pretreatment of samples at 180°C and desorption analysis at 600°C.

The TPD profiles of starting NH_4-CLIN and H-CLIN obtained after calcination at 450°C to 600°C are shown in Figure 30. The distributions of weak, medium, strong and very strong Lewis sites (LS) and Brønsted acid sites (BS) are shown in Table 12 and 13. With increasing calcination temperature weak, medium, strong and very strong BS sites are created by successive removal by ammoniums ions. Calcination at 300°C liberates weak and medium strong BS, weak to strong BS are liberated at 350°C to 400°C, Strong BS become available after calcination 450°C (Fig. 30). The broad low temperature peak LTP located at *ca.* 200°C belongs to ammonia desorbed from weak Lewis sites (Tab. 13). It overlaps the low intense peak of weak BS located between 230-300°C. Ammonia desorption from 300°C to 600°C clearly belongs to BS, namely medium strong (300-400°C), strong as well as very strong (400-600°C) BS. Remarkably, a strong decrease of the HTP by about 50 % is observed after heating to 450°C compared to ammonia loaded H-CLIN-400°C.

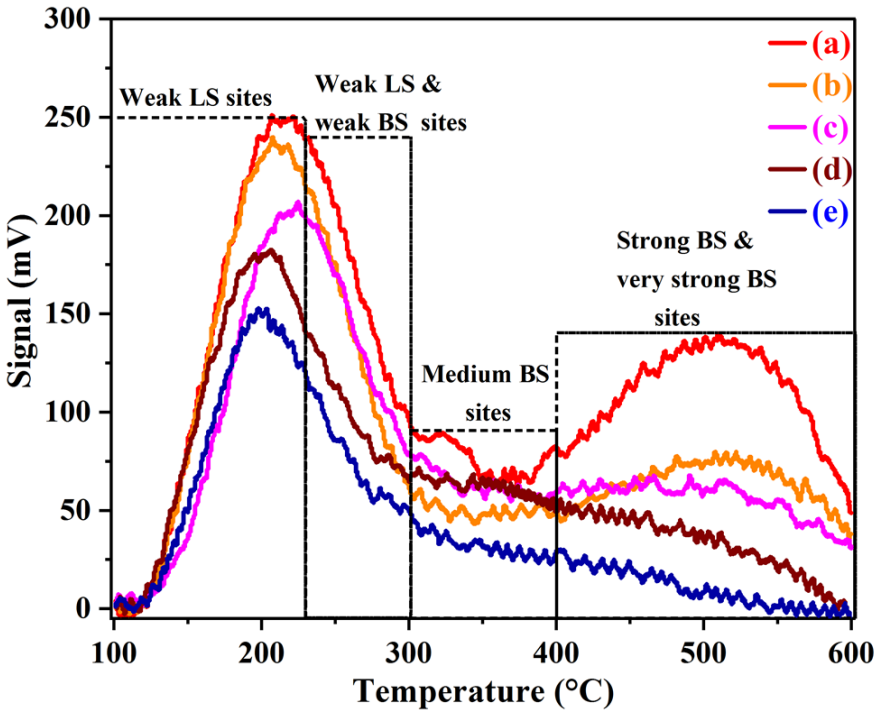

Figure 30. Temperature programmed desorption profiles of rehydrated NH_4-CLIN and calcined rehydrated NH_4-CLIN (exchange condition: 0.5M NH_4NO_3 at 80°C for 1 hour; calcination at 300-600°C, rehydration in humid air at r.t.). **a)** NH_4-CLIN, **b)** H-CLIN-450°C, **c)** H-CLIN-500°C, **d)** H-CLIN-550°C,and **e)** H-CLIN-600°C. H-CLIN means protonic sample, calcined after NH_4^+-exchange at (450-600°C). Pretreatment of samples at 180°C, NH_3 gas loading at 100°C and desorption analysis at 600°C.

Table 12: Total BS sites (mmol/g) and distribution of medium, strong and very strong BS acidic sites for rehydrated NH_4-CLIN (exchange condition: 0.5M NH_4NO_3 at 80°C for 1 hour) and calcined rehydrated NH_4-CLIN (calcination at 300-600°C, rehydration in humid air at r.t.). H-CLIN means protonic sample, calcined after NH_4^+-exchange at (300-600°C). Pretreatment of samples at 180°C, NH_3 gas loading at 100°C and desorption analysis at 600°C.

Catalysts	Remaining NH_4^+ content	Medium BS* sites	Strong and very strong BS sites	Total BS Sites
		300-400°C	400-600°C	300-600°C
NH_4-CLIN	1.40***	0.27	1.09	1.35
H-CLIN-300°C	1.16	0.25	0.99	1.24
H-CLIN-350°C	0.98	0.20	0.96	1.16
H-CLIN-400°C	0.42	0.15	0.93	1.08
H-CLIN-450°C	0.08	0.11	0.80	0.91
H-CLIN-500°C	0	0.13	0.65	0.78
H-CLIN-550°C	---------	0.13	0.38	0.51
H-CLIN-600°C	---------	0.27	0.13	0.40

Note Table 12.: LS** Lewis acid sites by interaction with cations and framework oxygen, BS* Brønsted acid sites, 1.4***-Maximum NH_4^+ content achieved by ion exchange with $NH4NO_3$ at 80°C, equal to the possible maximum amount of BS sites. Ion exchange capacity (CEC) of the parent natural zeolite CLIN normalized to cation charge +1 (mval(g), CEC. Calculated CEC for starting CLIN material is 2.25mmol/g. Therefore, achieved ion exchange degree is *ca.* 62%.

Table 13: Total BS sites (mmol/g) and distribution of weak LS, medium and strong BS acidic sites for rehydrated NH_4-CLIN (exchange condition: 0.5 M NH_4NO_3 at 80°C for 1 hour) and calcined rehydrated NH_4-CLIN (calcination at 300-600°C, re-hydration in humid air at r.t.). H-CLIN means protonic sample, calcined after NH_4^+-exchange at (300-600°C). Pretreatment of samples at 180°C, NH_3 gas loading at 100°C and desorption analysis at 600°C.

Samples	Total BS sites	Weak LS** sites	Weak LS & BS sites	Total adsorbed
	300-600°C	100 -230°C	230-300°C	NH_3 (mmol/g)
NH_4-CLIN	1.35	0.49	0.39	2.23
H-CLIN-300°C	1.24	0.48	0.48	2.20
H-CLIN-350°C	1.16	0.46	0.45	2.07
H-CLIN-400°C	1.08	0.21	0.30	1.56
H-CLIN-450°C	0.91	0.38	0.39	1.68
H-CLIN-500°C	0.78	0.25	0.42	1.44
H-CLIN-550°C	0.51	0.12	0.27	0.9
H-CLIN-600°C	0.40	0.11	0.21	0.71

Further heating to 600°C causes additional loss of BS acidity by total *ca.* 85 % as indicated by the markedly loss of the intensity of the corresponding TPD curve. Very strong BS (signal intensity at 500-600°C nearly disappears and mainly medium strong to strong BS remains. The zeolite framework is maintained until 600°C. The decrease in acidity and catalytic activity can be related to maximum conversion to penta-coordinated aluminum responsible due to loss of active sites. Formation of penta-coordinated $Al^{[V]}$ drops the portion of framework $Al^{[IV]}$ and, therefore, of Brønsted acid sites. The loss of potential BS between 400°C and 600°C (from 1.4 to 0.4 mmol/g) is markedly and causes an activity loss. The XRD pattern shows only some loss of crystallinity. Therefore, the loss of BS acidity should be related to the appearance of penta-coordinated $Al^{[V]}$. The model for the explanation of the origin of $Al^{[V]}$ is developed below.

Model-Origin of penta-coordinated aluminum $Al^{[V]}$

Calcination at higher temperature above 400°C causes formation of a huge amount penta-coordinated $Al^{[V]}$ on the expense of tetra-coordinated $Al^{[IV]}$. Whereas only a small portion of

octahedral coordinated extra-framework aluminium $Al^{[VI]}$ (EFAL) is observed in the ^{27}Al MAS NMR spectra (Fig. 22). Generally, the dealumination of zeolite frameworks is connected with the formation of markedly amounts of EFAL, which is missed in the case of clinoptilolite. Therefore, it is concluded that the formed $Al^{[V]}$ is still located in the framework. It is formed by the SI-O-Al bond cleavage due to the thermal decomposition of ammonium ions in the confined space of the lattice pore system. The bond distances and angles of the corresponding Si-O-Al bridges are distorted by the replacement of the NH_4^+ ions by H^+ proton. They are located at the bridging oxygen atoms and cause an elongation of the Al-O bond length in the bridge. Its character becomes silanol-like. The coordination sphere of the partially "de-shielded" aluminium is filled by an OH group or residual water as shown in Scheme 4.

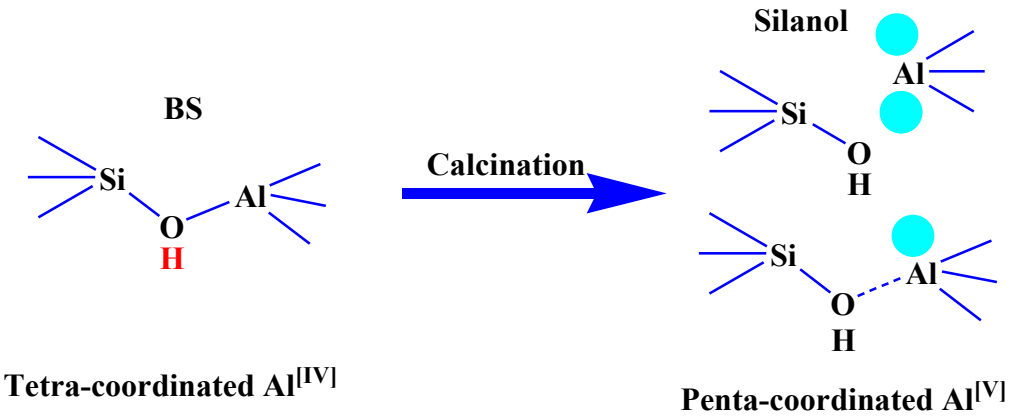

Scheme 4. Systematic illustration of breaking of Al-O bonds in Si-O(H)-Al bridges leaving silanol groups and penta-coordinated aluminum in Si-O(H)-Al bridges. The penta-coordinated $Al^{[V]}$ is still attached to the framework: (top) $Al^{[V]}$ coordinated with 3 framework oxygen atoms and 2 OH/H_2O (top) and bottom) coordinated with 2 framework oxygens, 1 silanol oxygen and 1 OH/H_2O.

A couple of findings support the conclusion that the penta-coordinated aluminum is still attached to the framework:

- XRD crystallinity maintain, slight loss in the framework order; No strong lattice shrinkage due to dealumination. Despite of two or three at 2θ valves which shift markedly by 0.3° (deg.) the observed shift after calcination is in the range which is expected for dehydration of the clinoptilolite lattice. No indication for change of the Si/Al ratio due to markedly dealumination. The high shifts of selected reflections are assigned to Al-O bond cleavage in certain lattice directions.

- The lattice vibration bands are only slightly shifted by increasing the calcination temperature from 400-450 or 500°C. No indication for change in Si/Al ratio or structural damage. The structure sensitive double-ring vibration band in maintained.
- Heating from 400°C to 500°C, where signal intensity of $Al^{[V]}$ at *ca.* 30-40 ppm is strongly increasing, causes a markedly change of the ^{1}H MAS NMR spectrum. A new signal of AlOH species is arising, whereas the BS signal gives rise only to a tailing. Also the intensity of SiOH signal increases. Likely the new AlOH signal at *ca.* 2.3 ppm belongs to the penta-coordinated "framework" aluminum.
- Mostly the microporosity increases and reaches maximum values of 334 m^2/g at 450°C. This is not only due to the cation removal and corresponding pore opening, because acid exchanged samples of similar cation exchange degree show only a specific micropore area of *ca.* 70 m^2/g. It is proposed that the sudden formation of ammonia gas by decomposition of ammonium ions in confined space lead to an internal mechanical (pressure) attack (micro-explosion–popcorn effect) facilitating bond cleavage in lattice oxygen rings and opening of the corresponding micropores. Whereas the mesoporosity, expected to increase with dealumination, is nearly unaffected.

3.1.4 Catalytic activity of calcined ammonium-exchanged CLIN catalysts

The onset acetalization activity of calcined NH_4-CLIN samples at 400°C, 450°C and 500°C by using 100 mg of catalyst are shown in Figure 31 and 32. Markedly differences are observed in the onset activity by increasing the calcination temperature from 400 to 600°C (Fig. 32 and Tab. 14). Highest activity is found with H-CLIN-450°C. It is higher than that of H-CLIN-400°C, although the acidities of both are similar with 0.9 and 1.09 mmol/g, respectively. However, the porosity (micropore volume) of H-CLIN-450°C (0.148 cm^3/g) is markedly higher than that of H-CLIN-400°C (0.06 cm^3/g) showing the important impact of microporosity on activity. The access of active BS in the micropore system is enhanced. With rising temperature to 600°C, the acidity gradually decreases to *ca.* 0.4 mmol/g but the activity decease is much larger (Tab. 13). The activity of H-CLIN-600°C sample is very low compared to H-CLIN-400°C; even the specific surface area and pore volume is somewhat higher than H-CLIN-400°C. An activity drop by 78 % and the acidity decreases by *ca.* 71 % are observed with H-CLIN-600°C. An activity drop by 45 % is observed with H-CLIN-500°C although the acidity decreases only by *ca.* 10%. But the micropore volume decreases by 40 % to 0.09 cm^3/g. A further dramatic loss in activity is observed with heating to 600°C,

which is assigned to pore blocking due to loss of crystallinity and formation of amorphous aluminosilica entities in the pores (XRD, NMR discussion).

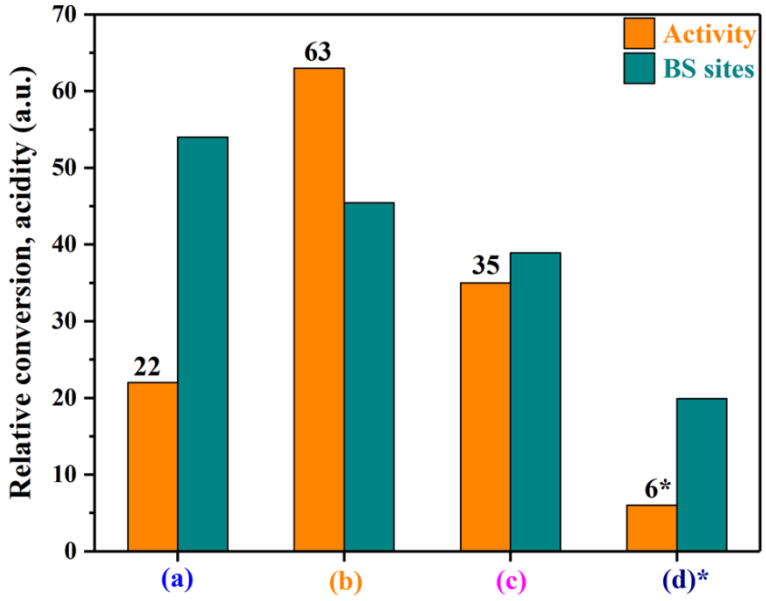

Figure 31. Acetalization of benzaldehyde with butanediol-1,3 over calcined and rehydrated NH_4-CLIN (exchange condition: 0.5 M NH_4NO_3 at 80°C for 1 hour; calcination at 400-600°C, rehydration in humid air at r.t.). **a)** H-CLIN-400°C, **b)** H-CLIN-450°C, **c)** H-CLIN-500°C, **d)** H-CLIN-600°C. H-CLIN means protonic sample, calcined after NH_4^+-exchange at (400-600°C), as catalyst, under reflux. H-CLIN means samples calcined after NH_4^+-exchanged. Reaction conditions, Batch reactor 150 mL, **Catalyst:100 mg** Reactant: 10 g benzaldehyde, 9 g butandiol, Internal Standard: 1 g hexamethyl benzene, Solvent: toluene. Reaction Temperature: *ca*. 113-116°C.*Extrapolated from Tab. 14.

Table 14: Acetalization of benzaldehyde with butanediol-1,3 over calcined and rehydrated NH_4-CLIN (exchange conditions: 0.5 M NH_4NO_3 at 80°C for 1 hour; calcination at 300-600°C, rehydration in humid air at r.t.). H-CLIN means protonic sample, calcined after NH_4^+-exchange at (400-500°C), as catalyst, under reflux. Reaction conditions, Batch reactor 150 mL, **Catalyst:100 mg** Reactant: 10 g benzaldehyde, 9 g butandiol, Internal Standard: 1 g hexamethyl benzene, Solvent: toluene. Reaction Temperature: *ca*. 113-116°C

CLIN catalysts	Acetal formation (%) with reaction time/ (min)					
	30	60	120	180	240	300
H-CLIN-400°C-100mg	22	28	35	42	45	45
H-CLIN-450°C-100mg	63	86	97	99	100	100
H-CLIN-500°C-100mg	35	64	89	94	97	98

The activity of 600°C is much lower as compared to 500°C, corresponding with the substantial increase of $Al^{[V]}$ and decrease of $Al^{[IV]}$. But the very low activity cannot be explained alone by the acidity. The activity compared to acidity is much lower than for H-CLIN-500°C. The markedly low activity of 600°C calcined sample is due to the loss of acidity by transition of $Al^{[V]}$ to $Al^{[IV]}$ and loss in crystallinity (partial amorphization) which leads to a partial pore blockage and low access to the active sites; whereas very small molecules like N_2 and NH_3 can still penetrate the pores (Fig. 32 and 34). These findings show that the catalytic activity of H-CLIN catalysts depends on both, the acidity, i.e. the number of BS, and the (micro) porosity determining the accessibility of BS and mass transfer to and from the catalyst. A structure- porosity-acidity-activity relationship is found with H-CLIN catalysts (Structure property catalysis relationship).

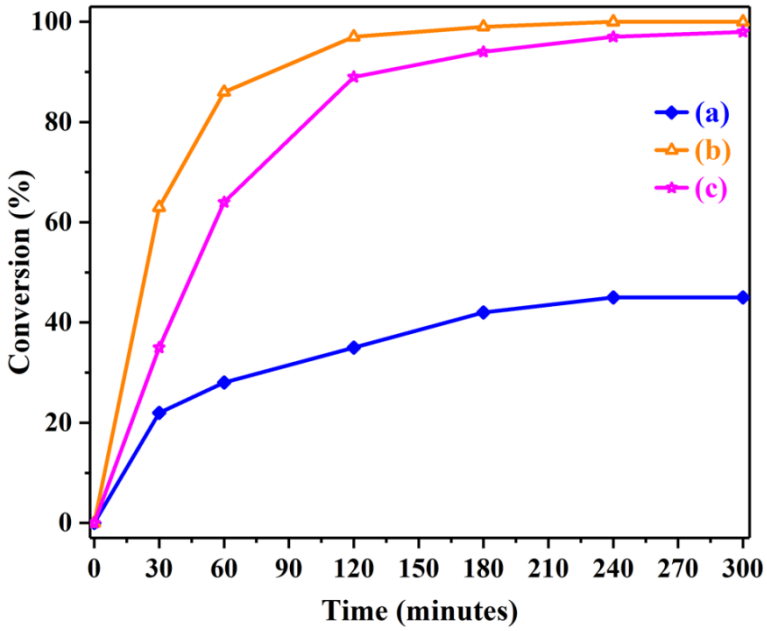

Figure 32. Acetalization of benzaldehyde with butanediol-1,3 over calcined and rehydrated NH_4-CLIN (exchange condition: 0.5 M NH_4NO_3 at 80°C for 1 hour; calcination at 400-500°C, rehydration in humid air at r.t.) as catalyst, under reflux. **a)** H-CLIN-400°C, **b)** H-CLIN-450°C, **c)** H-CLIN-500°C. H-CLIN means protonic sample, calcined after NH_4^+-exchange at (400-500°C). Reaction conditions, Batch reactor 150 mL, **Catalyst:100 mg** Reactant: 10 g benzaldehyde, 9 g butandiol, Internal Standard: 1 g hexamethyl benzene, Solvent: toluene. Reaction Temperature: *ca*. 113-116°C.

Acetalization activity of CLIN and calcined NH_4-CLIN samples using 200mg of catalyst are shown in Figure 33 and acetal formation (%) are compiled in Tab. 15. The increase of the catalyst loading from 100mg to 200 mg leads to a substantial increase of the conversion already at short reaction time of 1 hour. Finally, 90-100 % conversion is achieved showing the high catalytic activity of H-CLIN catalysts and their potential for application in acid catalyzed

reactions. In the natural zeolite clinoptilolite mineral, pores are blocked by extra framework cations i.e. Na^+, K^+, Ca^{2+}, Mg^{2+} ions and absorbed water molecules hindering the active sites. Low activity due to acidity of the starting material is by hydrolysis i.e. during washing process, as some extra framework cations may be replaced with proton (H^+) from water molecules according to following chemical equation.

$$\text{Na,K-CLIN} \quad + \quad H_2O \longrightarrow \quad \text{H-[Na,K-CLIN]}$$

Also some acidity is established in NH_4-CLIN under reaction conditions. Low activity of H-CLIN-600°C is due to pore blockage. Conversion over NH_4-CLIN increases gradually with reaction time; due to ongoing protonation. Whereas in case of starting CLIN and H-CLIN-600°C only an onset activity (conversion) and further slow increase of conversion is observed with prolonged reaction time. The pores are blocked by extra framework cations or amorphous species.

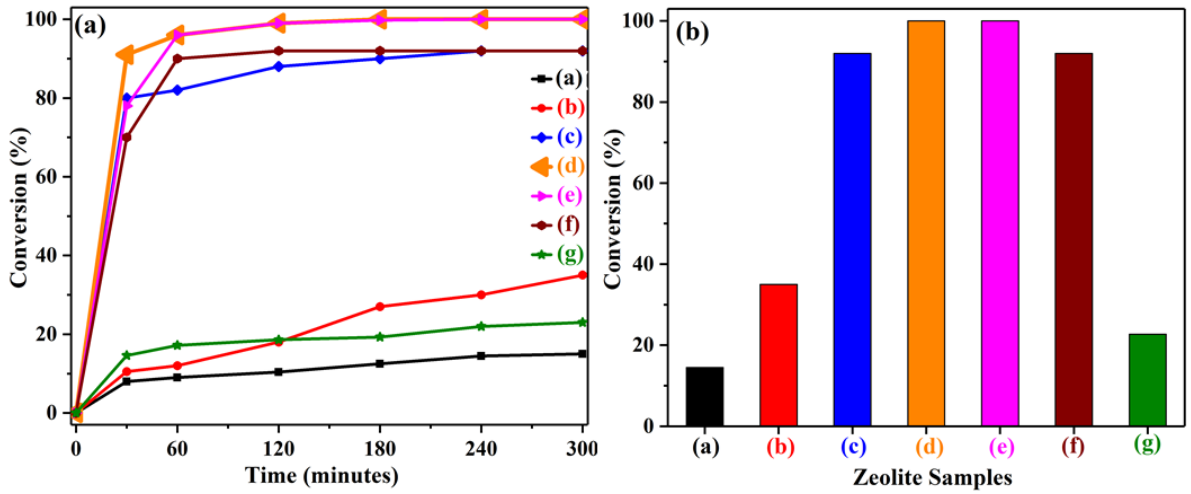

Figure 33. Acetalization of benzaldehyde with butanediol-1,3 over CLIN- starting material and calcined rehydrated NH_4-CLIN (exchange condition: 0.5 M NH_4NO_3 at 80°C for 1 hour; calcination at 300-600°C, rehydration in humid air at r.t.) as catalyst, under reflux. **a)** Starting CLIN, **b)** NH_4-CLIN, **c)** H-CLIN-400°C, **d)** H-CLIN-450°C, **e)** H-CLIN-500°C, **f)** H-CLIN-550°C, **g)** H-CLIN-600°C. H-CLIN means protonic sample, calcined after NH_4^+-exchange at (300-600°C). Reaction conditions, Batch reactor 150mL, **Catalyst:200 mg** Reactant: 10 g benzaldehyde, 9 g butandiol, Internal Standard: 1 g hexamethyl benzene, Solvent: toluene. Reaction Temperature: *ca*. 113-116°C. Figure (a) on left side shows the activity after each 30 minutes of reaction time and Figure (b) on right side shows the total acetalization activity after 5 hours of reaction time.

Calcination of the NH_4-CLIN samples causes dissociation of NH_4^+ ions into NH_3 gas and H^+ ions, responsible for Brønsted acidity and increase in acetalization activity. NH_4^+ ions

dissociation increase with increase in calcination temperature and highest valve of acetal formation obtained for 450°C calcined sample (H-CLIN-450°C), due to maximum decomposition of NH_4^+ ions into NH_3 gas and H^+ ions. Also for this sample highest valve of Strong BS and porosity are obtained, confirming that pores are wide enough and active sites are easily accessible. After calcination at 500°C, relative decrease in acetal formation is observed due to some framework defects and formation of penta-coordinated $Al^{[V]}$, on the expense of tetrahedral framework aluminum $Al^{[IV]}$. After calcination of NH_4-CLIN sample at 600°C maximum conversion to penta-coordinated $Al^{[V]}$ and decrease in acetalization activity are observed. Penta-coordinated $Al^{[V]}$ are not acidic, causing and decrease in acetal formation activity. Some local changes can be seen for calcined NH_4-CLIN samples but the overall structure is maintained by XRD and FTIR. For 600°C calcined sample the peak position shifts to higher 2θ valve in XRD pattern due to breaking of the Al-O bond and silanol groups (SiOH) formation, causing local lattice shrinkage and a shift of the distinct reflections. The action is locally, therefore, only selected reflections are shifted to higher 2θ value (XRD), i.e., lattice plane distance decreases in this area.

Table 15: Acetalization of benzaldehyde with butanediol-1,3 over CLIN- starting material and calcined rehydrated NH_4-CLIN (exchange condition: 0.5 M NH_4NO_3 at 80°C for 1 hour; calcination at 300-600°C, rehydration in humid air at r.t.). H-CLIN means protonic sample, calcined after NH_4^+-exchange at (300-600°C) as catalyst, under reflux. H-CLIN means samples calcined after NH_4^+-exchanged. Reaction conditions, Batch reactor 150 mL, **Catalyst:200mg** Reactant: 10 g benzaldehyde, 9 g butandiol, Internal Standard: 1g hexamethyl benzene, Solvent: toluene. Reaction temperature: *ca*. 113-116°C.

CLIN catalysts	**Acetal formation (%) with reaction time/ (min)**					
	30	**60**	**120**	**180**	**240**	**300**
CLIN	8.5	9	10.4	12.5	14.5	14.5
NH_4-CLIN	10.5	12	18	27	30	35
H-CLIN-300°C	73	78	80	80	82	83
H-CLIN-350°C	75	80	83	85	86	86
H-CLIN-400°C	80	82	88	90	92	92
H-CLIN-450°C	91	96	99	100	100	100
H-CLIN-500°C	78	96	99	99.8	100	100
H-CLIN-550°C	70	90	92	92	92	92
H-CLIN-600°C	14.6	17.2	18.6	19.3	22	23

3.1.5 Summary

- Starting CLIN Si/Al ratio of 5.27 consist of *ca.* 94 % clinoptilolite by ICP-AES analysis. *Ca.* 54 % of extra framework cations are exchanged by NH_4^+ ions and Si/Al ratio increases to 5.5.
- XRD pattern of starting CLIN agrees with the simulated clinoptilolite pattern. For calcined NH_4-CLIN until 600°C, some local changes can be seen but the overall structure is maintained by XRD and FTIR analysis.
- Calcination at 600°C to 800°C, leads a collapse of zeolite framework, background increases markedly and characteristics reflections of clinoptilolite and structure sensitive double-ring vibration band at 607 cm^{-1} disappear due to amorphization.
- CLIN and calcined NH_4-CLIN samples are stable until 600°C by TG/ DSC analysis.
- The ^{29}Si and ^{27}Al MAS NMR spectrum nearly not changes for calcined NH_4-CLIN at 400°C. A relative decrease of the signals Si(nAl), n=1-3 compared to the Si(0Al) signal appears and increase in intensity of extra-framework octahedral aluminum $Al^{[VI]}$ is observed giving rise to a signal around 0 ppm. These changes confirm local framework changes.
- Calcination at 600°C to 800°C, causes maximum conversion to penta-coordinated $Al^{[V]}$ species on the expense of tetrahedral framework aluminum$^{[IV]}$ by ^{27}Al MAS NMR. A broaden, overlapping and not structured ^{29}Si MAS NMR spectrum after high temperature calcination, ranging from -93 to -120 ppm with a maximum located at *ca.* -109 ppm are observed confirming cristobalite formation.
- Maximum BET surface area, micropore area and pore volume valves increases for NH_4-CLIN calcined at 450°C (409 m^2/g, 334 m^2/g, 0.374 cm^3/g). These valves decrease after calcination beyond 450°C due to some framework defects.
- Acidity and acetalization activity valves increases after calcination at 450°C due to maximum decomposition of NH_4^+ ions releasing H^+ ions to produce maximum BS sites.
- For calcined NH_4-CLIN, porosity, acidity and activity are related to the transition of tetra-coordinated aluminium $Al^{[IV]}$ to penta-coordinated aluminium $Al^{[V]}$. Maximum conversion to pent-coordinated $Al^{[V]}$ leads to decrease in porosity, acidity and activity beyond calcination at 450°C.

3.2 Acidic clinoptilolite H-CLIN catalysts prepared by HCl treatment

3.2.1 Material characterization

3.2.1.1 ICP-AES elemental analysis

The ICP-AES elemental analysis results of HCl treated CLIN are shown in Table 16. The major components are silicon and aluminum, as expected for zeolites. Additionally, Ca^{2+}, Mg^{2+}, Na^{+} and K^{+} cations are found, which belong to zeolitic cations needed for the compensation of the negative framework charge introduced by zeolitic aluminum. The amount of positive cation charges (5.8) is nearly equal to the negative charge introduced by framework aluminum (5.88). Therefore, it can be assumed that the detected aluminum is a part of the zeolite framework.

Table 16: ICP-AES chemical analysis data of the elemental composition of H-CLIN catalysts. Starting CLIN and HCl treated CLIN: H-CLIN-0.1 M HCl and H-CLIN-2M HCl for CLIN treated with 0.1 and 2 M HCl at 80°C for 1 h, respectively.

Catalysts	Elemental composition (at. %)							
	Si	Al	Ca	Mg	Na	K	Fe	Ti
CLIN	31.00	5.88	1.00	0.20	0.51	2.90	0.99	0.08
H-CLIN-0.1 M HCl	30.35	5.22	0.04	0.28	0.30	1.73	0.78	0.08
H-CLIN-2 M HCl	29.17	4.48	0.06	0.28	0.35	1.45	0.52	0.08

The overall Si/Al ratio of the starting natural CLIN is *ca.* 5.27. Under the assumption that Si/Al ratio of the CLIN zeolite framework is 5 and all detected aluminum belongs to the framework, the increased Si/Al ratio of 5.27 points to the presence of *ca.* 5 at.-% of the non zeolitic as quartz and cristobalite. This conclusion is confirmed by the XRD pattern. Based on these data the zeolite content is estimated to be *ca.* 95 %. Additionally, also *ca.* 1 % of Fe^{3+} and Ti^{3+} are present. So the final zeolite content of the natural CLIN amounts to *ca.* 94 %. The presence of *ca.* 5 % of non-zeolitic silicon was also taken into account for the estimation of the Si/Al framework ratios of zeolite catalysts obtained after treatment with different concentrated HCl.

Exchange degree of zeolitic cations by protons H^{+} after treatment with 2 M HCl is somewhat higher than with 0.1 M HCl, but the cation exchange capacity CEC and Al content is lower due to dealumination. Two processes compete: the increased HCl concentration enhances the exchange degree of zeolitic cations Me^{z+} by acidic protons H^{+}, but the total amount of acid

sites decreases due to severe dealumination. Remarkably, during the acid treatment a markedly loss of catalyst of *ca.* 11.5-23.75 mass-% is observed (Tab. 29), which decreases the efficiency of this procedure. The chemical analysis shows that K^+ ions located in the center of 8-member ring channel "C" is very hard to remove. Potassium in the O8R ring is coordinated by as many as six oxygen atoms and three additional water molecules. Potassium plays an important role in thermal stability of clinoptilolite. Smaller cations such as Ca^{2+} and Na^+ are too small to keep the channel expanded, whereas K^+ due to its large size keep the structure expanded and prevents the structure from collapsing. Complete removal of K^+ may cause a destruction of the framework.[49]

3.2.1.2 XRD pattern

XRD patterns of HCl treated CLIN are shown in Figure 34. The corresponding crystallite sizes calculated according to the Scherer formula are presented in Table 17. Generally, zeolites are known to be very sensitive to acid treatment and even lower acid concentrations can affect the structure of zeolites.

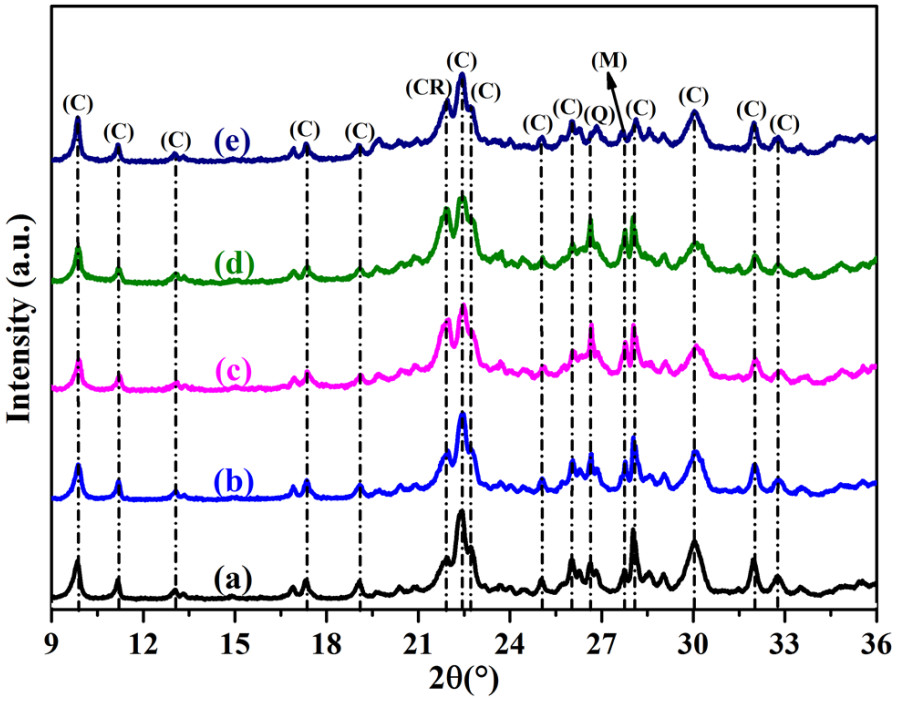

Figure 34. XRD patterns of starting CLIN and rehydrated HCl treated CLIN (exchange condition: 0.1-2 M HCl at 80°C for 1 hour; rehydration in humid air at r.t.). **a)** CLIN, **b)** H-CLIN-0.1 M HCl, **c)** H-CLIN-0.5 M HCl, **d)** H-CLIN-1 M HCl, **e)** H-CLIN-2 M HCl. H-CLIN means protonic sample, after treatment with HCl. "**C**"-clinoptilolite, "**Q**"-α-quartz, "**M**"-mordenite and "**CR**"-cristobalite reflections.

Compared to the starting CLIN treatment with 0.1 M HCl causes only minor changes in the XRD pattern. The background slightly increases. The material is stable under these conditions. Increasing acid concentration to 0.5 and 1 M leads to an increase of the background due to the formation of amorphous phase, e.g. amorphous silicates, and the formation of cristobalite and quartz (reflections at 2θ = 26.61° and 21.95°). The crystallinity of the clinoptilolite framework decreases. The crystallite size decreases from *ca.* 40.16 to 27.7 nm (Tab. 17). In contrast, treatment with 2 M HCl does not affect the crystallite size and hence crystallinity of the zeolite. But the increase in the background points to some amorphization of the starting material, e.g. formation of amorphous silicate due to desilication and dealumination under strong acid treatment. Selected reflections are shifted to higher 2θ values. This conclusion is supported by the former presented chemical analysis data. They show an increase of the Si/Al ratio which is accompanied by a dramatic material loss by dissolution (*ca.* 24 mass-%). Other authors also reported decrease in crystallinity and peak intensities, increase in background and peak broadness by treating clinoptilolite from different origin using different conditions of acid concentrations and temperatures.[55,59,61,62,86]

Table 17: Crystallite size of starting CLIN and HCl treated CLIN (exchange conditions: 0.1-2 M HCl at 80°C for 1 hour; rehydration in humid air at r.t.), and 0.1 M HCl treated and calcined CLIN at 400, 450 and 500°C. H-CLIN means protonic sample, after treatment with HCl.

Name of Sample	Crystallite size (nm)
CLIN	40.16
H-CLIN-0.1M HCl	35.37
H-CLIN-0.5M HCl	30.17
H-CLIN-1M HCl	27.70
H-CLIN-2M HCl	39.45
H-CLIN-0.1M HCl-400°C	30.77
H-CLIN-0.1M HCl-450°C	27.02
H-CLIN-0.1M HCl-500°C	26.03

The XRD patterns of 0.1M HCl treated H-CLIN calcined at 400°C, 450°C and 500°C are shown in Figure 35. The calcination acid treated H-CLIN causes a decline in the crystallinity of the zeolite catalyst as indicated by the decrease of the crystallite size from *ca.* 35.37 to 26.03 nm after thermal treatment of the starting H-CLIN-0.1 M HCl to 500°C (Table 17). The successive increase of the background points to some amorphization of the zeolite framework. Additionally, formation of silica phase cristobalite is observed. Interestingly, a markedly shift

of 2θ value of selected reflections by *ca.* 0.1–0.6° (Tab. 18) to higher value is observed special after heating beyond 400°C. Severe lattice shrinkage occurs after removal of adsorbed water. Hence, the structures of H-CLIN catalysts obtained by HCl treatment are very sensitive to thermal treatment and loose crystallinity.

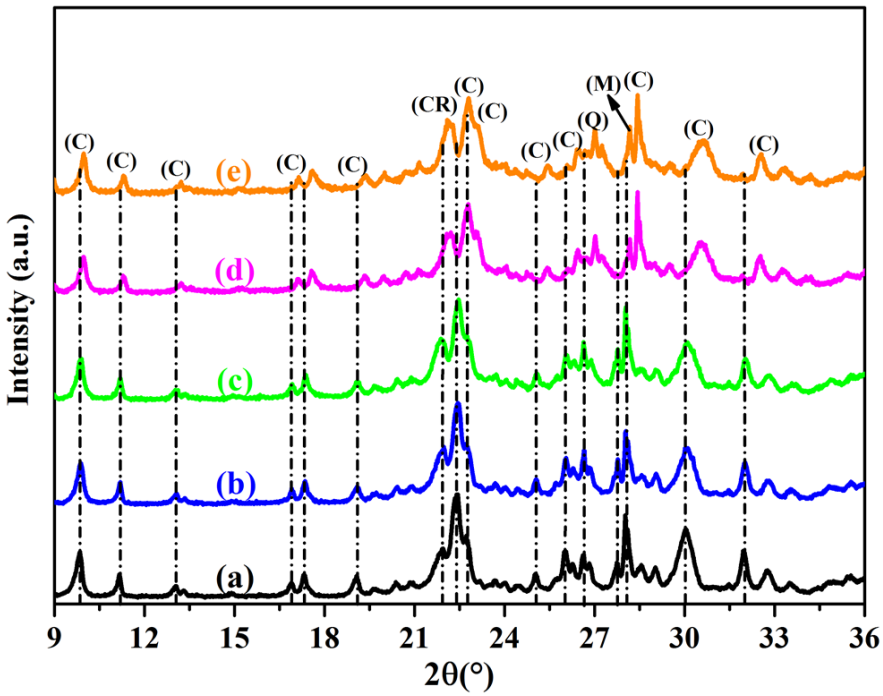

Figure 35. XRD patterns of starting CLIN and rehydrated 0.1 M HCl treated and calcined CLIN (exchange conditions: 0.1 M HCl at 80°C for 1 hour; re-hydration in humid air at r.t. followed by calcination; 400-500°C). **a)** CLIN, **b)** H-CLIN-0.1 M HCl, **c)** H-CLIN-0.1 M HCl-400°C, **d)** H-CLIN-0.1 M HCl-450°C, **e)** H-CLIN-0.1 M HCl-500°C. H-CLIN means protonic sample, after treatment with HCl and calcined at 400°C, 450°C and 500°C. "**C**"-clinoptilolite, "**Q**"-α-quartz, "**M**"-mordenite and "**CR**"-cristobalite reflections.

Table 18: Influence of calcination temperature on 2θ valves shifts for starting CLIN and HCl treated CLIN (exchange conditions: 0.1 M HCl at 80°C for 1 hour; rehydration in humid air at r.t. followed by calcination; 400-500°C). H-CLIN means protonic sample, after treatment with HCl and 400°C, 450°C and 500°C-calcination temperatures.

Catalysts	CLIN and 0.1 M HCl CLIN and calcined samples main peaks 2θ (°) valves										
CLIN	9.85	11.20	13.05	16.95	17.34	19.10	22.44	26.64	28.08	30.06	31.94
H-CLIN-0.1 M HCl	9.87	11.22	13.08	16.98	17.38	19.12	22.47	26.67	28.10	31.18	31.95
H-CLIN-0.1 M HCl-400°C	9.90	11.22	13.08	16.98	17.40	19.12	22.47	26.67	28.10	31.18	31.95
H-CLIN-0.1 M HCl-450°C	9.94	11.28	13.22	17.10	17.56	19.34	22.80	27.03	28.44	31.55	32.52
H-CLIN-0.1 M HCl-500°C	9.97	11.30	13.25	17.15	17.62	19.37	22.82	27.05	28.45	31.65	32.55

3.2.1.3 Fourier-transform infrared spectroscopy (FTIR)

FTIR spectra of HCl treated CLIN are shown in Figure 36. FTIR spectra give information about dealumination and corresponding changes in Si/Al ratio which also may occur with natural zeolite clinoptilolite.[5] The wavenumbers of the different lattice and OH vibrations bands in the spectral range of 400-1800 cm^{-1} are given in Table 19. They are consisting with spectra typically observed with aluminosilicate zeolites showing main absorbance bands at *ca.* 1200-900 cm^{-1}, 800-700 cm^{-1} and at *ca.* 450 cm^{-1}.

These vibration bands are assigned to anti-symmetric at *ca.* 1025 cm^{-1}, symmetric T-O-T at *ca.* 794 cm^{-1}, tetrahedral TO_4 deformation vibrations of aluminosilicate framework at *ca.* 446 cm^{-1} and structural sensitive double ring vibration band at *ca.* 600 cm^{-1}. The presence of the structure sensitive double ring vibration band at *ca.* 610 cm^{-1} confirms the zeolitic nature of the natural material (Tab. 5). The additional absorbance at *ca.*1640 cm^{-1} belongs to deformation bands of the adsorbed water. The maintenance of the double-ring vibration band even after treatment with 2 M HCl confirms the structural stability of the acid treated H-CLIN catalyst. The anti-symmetric T-O-T vibration band shows unusual wavenumber shifts after treatment with different concentrated acid (0.1-2 M HCl). With lower concentrated acid (0.5 M) a shift to higher wavenumber from 1025 to 1044 cm^{-1} is observed. Other authors also reported similar results.[55,56,61,62,65-69]

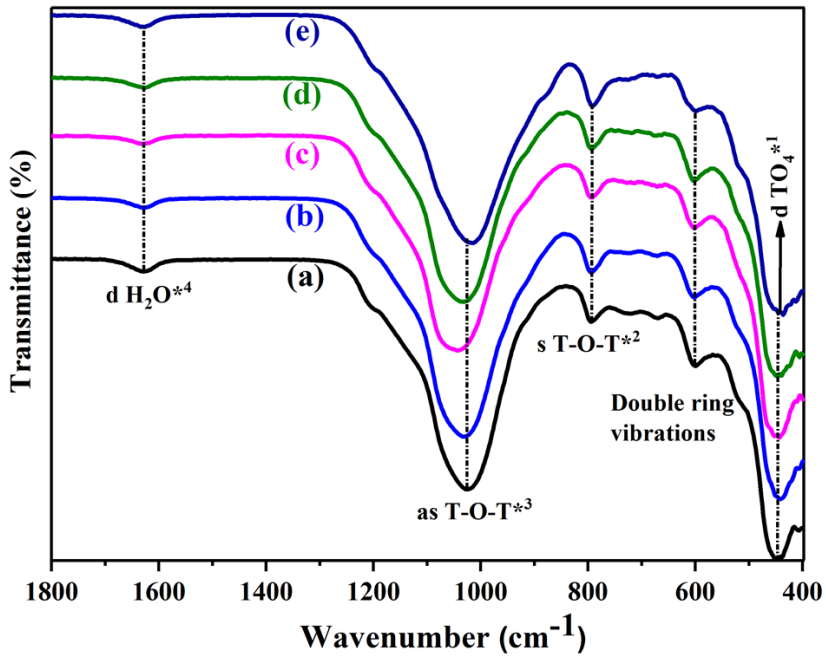

Figure 36. FTIR spectra of starting CLIN and rehydrated HCl treated CLIN (exchange conditions: 0.1-2 M HCl at 80°C for 1 hour; re-hydration in humid air at r.t.). **a)** CLIN, **b)** H-CLIN-0.1 M HCl, **c)** H-CLIN-0.5 M HCl, **d)** H-CLIN-1 M HCl, **e)** H-CLIN-2 M HCl. H-CLIN means protonic sample, after treatment with HCl. **dTO_4*1**- the tetrahedral deformation vibration, **sT-O-T*2**-symmetric T-O-T vibration, **asT-O-T*3**-anti-symmetric stretching T-O-T vibration**,** and **d H_2O*4**-deformation vibrations of adsorbed H_2O.

With higher concentrated HCl (1-2 M) an opposite shift down to 1017 cm^{-1} occurs. Generally, the wavenumbers of the T-O-T vibrations shift with the TOT bond angles and bond lengths. They increase with decreasing T-O distance and growing bond angle and vice versa. I.e., they increase with growing Si/Al ratio. However, opposite effects are observed with different acid treated H-CLIN catalysts which can hardly be explained at this stage. They might indicate the occurrence of complex changes in the local structure (bond angles and distances) due to different cation locations, cation distributions and/or replacement of cations by protons.

Table 19. Position of the main vibration modes in starting CLIN and HCl treated CLIN (exchange conditions: 0.1-2 M HCl at 80°C for 1 hour; rehydration in humid air at r.t.). H-CLIN means protonic sample, after treatment with HCl. **d TO_4*1**-the tetrahedral deformation vibration, **sT-O-T*2**-symmetric T-O-T vibration, and **asT-O-T*3**-anti-symmetric stretching T-O-T vibration.

Catalysts	d TO_4*1	Double ring vibrations	s T-O-T*2	as T-O-T*3
CLIN	446	600	794	1025
H-CLIN-0.1 M HCl	442	602	793	1030
H-CLIN-0.5 M HCl	439	603	792	1044
H-CLIN-1 M HCl	438	601	791	1037
H-CLIN-2 M HCl	437	600	790	1017

For 0.1M HCl treated and calcined H-CLIN the FTIR vibration spectra are shown in Figure 37. They are less sensitive to thermal treatment up to 500°C. A very small increase in anti-symmetric T-O-T vibration band at *ca.*1030 cm^{-1} and a small shift of the structural sensitive double ring vibration band at 600 cm^{-1} to high wavenumber of 608 cm^{-1} is obtained ab. 20). These small changes are due to the dehydration of the zeolite which results in some lattice shrinkage. Dehydration or dehydroxylation occurs also beyond 400°C (Fig. 39).

Table 20: Influence of calcination temperature on FTIR bands for calcined 0.1 M HCl treated CLIN (exchange conditions: 0.1 M HCl at 80°C for 1 hour; rehydration in humid air at r.t. followed by calcination; 400-500°C). H-CLIN means protonic sample, after treatment with HCl calcination at 400°C, 450°C and 500°C.

Samples	d TO_4*[1]	Double ring vibrations	s T-O-T*[2]	as T-O-T*[3]
H-CLIN-0.1 M HCl	442	602	793	1030
H-CLIN-0.1 M HCl-400°C	443	604	793	1030
H-CLIN-0.1 M HCl-450°C	443	606	793	1031
H-CLIN-0.1 M HCl-500°C	442	608	791	1032

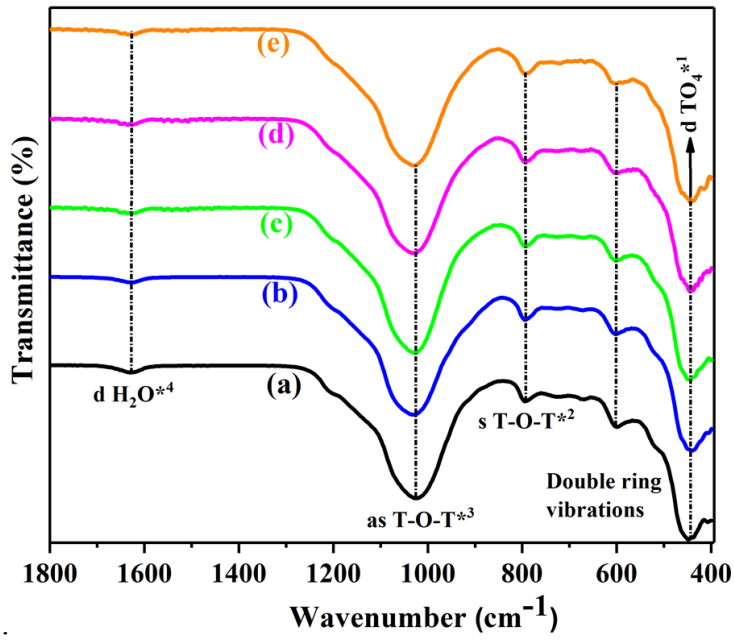

Figure 37. FTIR spectra of starting CLIN and HCl treated CLIN (exchange conditions: 0.1 M HCl at 80°C for 1 hour; re-hydration in humid air at r.t., calcination; 400-500°C). **a)** CLIN, **b)** H-CLIN-0.1 M HCl, **c)** H-CLIN-0.1 M HCl-400°C, **d)** H-CLIN-0.1 M HCl-450°C, **e)** H-CLIN-0.1 M HCl-500°C. H-CLIN means protonic sample, after treatment with HCl. **d TO_4*[1]**-the tetrahedral deformation vibration, **s T-O-T*[2]**-symmetric T-O-T vibration, **as T-O-T*[3]**-anti-symmetric stretching T-O-T vibration**,** and **d H_2O*[4]**-deformation vibrations of adsorbed H_2O.

3.2.1.4 Thermal Analysis (TG-DSC)

TG/DSC curves of re-hydrated HCl treated (0.1-2 M) CLIN are shown in Figure 38. Two main broad, but well-defined, weight loss steps are observed with 0.1-2 M HCl treated CLIN between r.t. and 300°C and between 310 and 650°C. They are assigned desorption of loosely bound water and medium strong bound water in the cage. The second weight loss is assigned to desorption of strong bound cationic water, as well as tightly fixed water confined in cages or windows. Both losses are strongly endothermic as typical water desorption. The DSC curves show that the maximum temperatures of the weight losses are *ca.* 25-180°C with a peak maximum at 140°C due to loss of loosely bond water, a shoulder between *ca.* 180-430°C due to desorption of cationic or medium strong bound water, and a peak at c*a.* 430-700°C with a peak maximum at 480°C due to loss of tightly bond water and de-hydroxylation. The shoulder at *ca.* 60°C is characteristic of loosely bound external water. Specially, 0.5 M HCl treated CLIN show endothermal peaks *ca.* 200-300°C with peak maxima at 250°C due to medium strong bound water in the cage. For 2 M HCl treated CLIN the endothermal peaks *ca.* 200-300°C with peak maxima at 250°C and shoulder at *ca.* 60°C is characteristic of loosely bound external water disappear due framework defects and *ca.* 24 % weight loss during treatment with 2 M HCl for 1hour. The overall appearance of the TG and DSC curves are maintained also after treatment with 2M HCl.

An increase in weight loss can be seen with increasing acid concentration. The increase in the total water content of *ca.* 12.37 %, after treatment with 2 M HCl can be explained by the increase of the accessible pore volume due to the loss of extra framework cations and zeolitic surface by acid treatment. Increase of HCl concentration causes a decrease of the total amount of adsorbed water. This could be an indication for some crystallinity loss, pore blockage or other changes affecting the water adsorption capacity. The weight losses of loosely, cationic and tightly bound water show a similar behavior with rising calcination temperature. The total weight loss is in line with former results observed with clinoptilolite minerals from different origins.[67,70-74] The observed total weight loss and weight losses at low, medium and high temperature are summarized in Table 21. The total weight loss, mostly due to water desorption, is similar (9-12 wt.-%) for all samples confirming the stability of the zeolite structure until treatment with 2 M HCl. No structure transition signal is observed in the DSC curve. Usually it is narrow and exothermic. The increased total weight loss observed with H-CLIN-2 M HCl is assigned to an increased dehydroxylation of the framework or increased (dehydroxylated) amorphous silica included in part in the cages of the structure. It causes an

enhanced adsorption of loosely bound water. Strongly bound water and dehydroxylation occurs beyond 400°C.

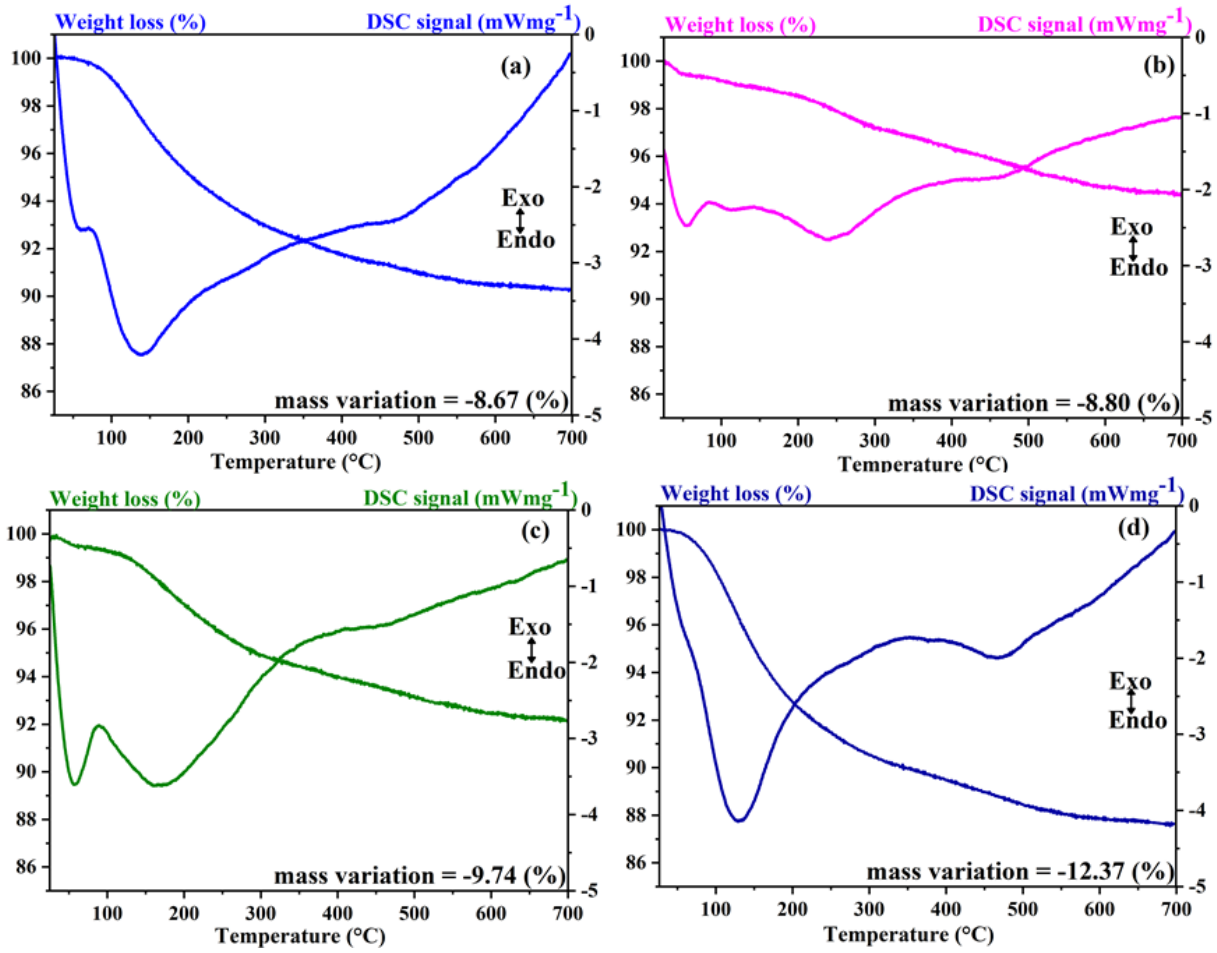

Figure 38. TG/DSC curves of rehydrated HCl treated CLIN (exchange conditions: 0.1-2 M HCl at 80°C for 1 hour; rehydration in humid air at r.t.). **a)** H-CLIN-0.1 M HCl, **b)** H-CLIN-0.5 M HCl, **c)** H-CLIN-1 M HCl, **d)** H-CLIN-2 M HCl. H-CLIN means protonic sample, after treatment with HCl. TG/DSC for samples were recorded during heating up to 700°C at 10°C/mint.

Table 21: TG/DSC weight losses (%) at each dehydration stage for rehydrated CLIN and of HCl treated CLIN (exchange conditions: 0.1-2 M HCl at 80°C for 1 hour, re-hydration in humid air at r.t.).

Catalysts	Total weight loss (%)	Loosely bond water	Cationic bonded water	Tightly bound zeolite water*
		25-180°C	180-430°C	430-700°C
CLIN	9.20	3.41	3.70	2.09
H-CLIN-0.1 M HCl	8.67	3.10	3.41	2.16
H-CLIN-0.5 M HCl	8.80	3.25	3.50	2.05
H-CLIN-1 M HCl	9.74	3.70	3.70	2.34
H-CLIN-2 M HCl	12.37	4.94	3.85	3.58

*dehydroxylation and strongly bound water e.g. in small cages

3.2.1.5 Framework local structure analysis by ^{29}Si, ^{27}Al and ^{1}H MAS NMR

^{29}Si MAS NMR spectra of HCl treated CLIN

Zeolites as clinoptilolite consist of 3-dimensional frameworks of 4-fold connected (Si, Al)O_4-tetrahedral, connected via Si-O-Si and Si-O-Al aluminosiloxane bridges. Al-O-Al connections are forbidden according to the Löwenstein and five different aluminum environments exist for the tetrahedral silicon denoted Si(nAl), with n=0-4 (Fig. 19). Where, n corresponds to the number of nearest next neighbored aluminum atoms in the second coordination sphere of silicon atoms. They give rise to appearance of selective characteristic signals in the ^{29}Si MAS NMR spectra of zeolites appearing at different chemical shifts (Tab. 8). The ^{29}Si MAS NMR spectra of HCl treated CLIN are shown in Figure 39. The ^{29}Si MAS NMR spectra of HCl treated CLIN consist of three overlapping resonances located at *ca*. -100, -107 and -113 ppm which are assigned to Si(2Al), Si(1Al) and Si(0Al) units respectively. The low field tailing of the spectrum *ca.* -97 ppm might indicate the presence of some Si(3Al) unit. The occurrence of stable Si(2Al) units, which do not disappear with acid treatment, points to the presence of isolated stable bridged Si-O(H)-Al-O-Si-O-Al-O(H)-Si Brønsted acidic units in the protonated H-CLIN (medium silica-rich). Similar changes were observed other authors.[49,61,75-82,90]

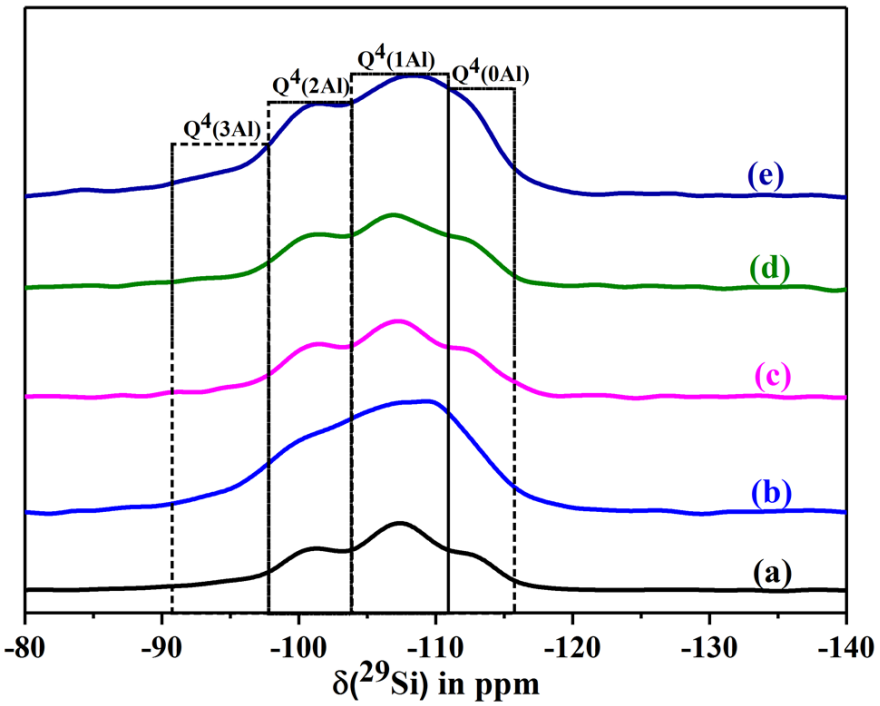

Figure 39. ^{29}Si MAS NMR spectra of dehydrated HCl treated (0.1–2 M) CLIN at 80°C for 1 hour. **a)** CLIN, **b)** H-CLIN-0.1 M HCl, **c)** H-CLIN-0.5 M HCl, **d)** H-CLIN-1 M HCl, **e)** H-CLIN–2 M HCl. All samples are activated at 400°C for 1 hour, heating rate of 5°C/min.

The acid treatment leads to the appearance of a new signal at *ca.* -109 ppm, which is assigned to cristobalite. Additionally, a broadening of the signals (loss of structure) is observed which is typically observed with amorphous silicates. These changes are most pronounced with the samples treated with 0.1 M and 2M HCl. These conclusions are supported by the XRD pattern (Fig. 35) of the corresponding samples. They show formation of cristobalite and a partial amorphization (increased background) after acid treatment. But the main part of the zeolite structure is maintained. Similar findings are observed after calcination at 400-500°C.

^{29}Si MAS NMR spectra of 0.1 M HCl treated and calcined CLIN at 400°C, 450°C and 500°C are shown in Figure 40. Again the increased signal intensity at *ca.* -109 ppm and the broadening of the signals points to the formation of cristobalite and some amorphous materials by partial destruction of the framework. This is confirmed by the XRD although the main part of the zeolite framework is still maintained even at high temperature. These results are in line with XRD and FTIR analysis (Fig. 36).

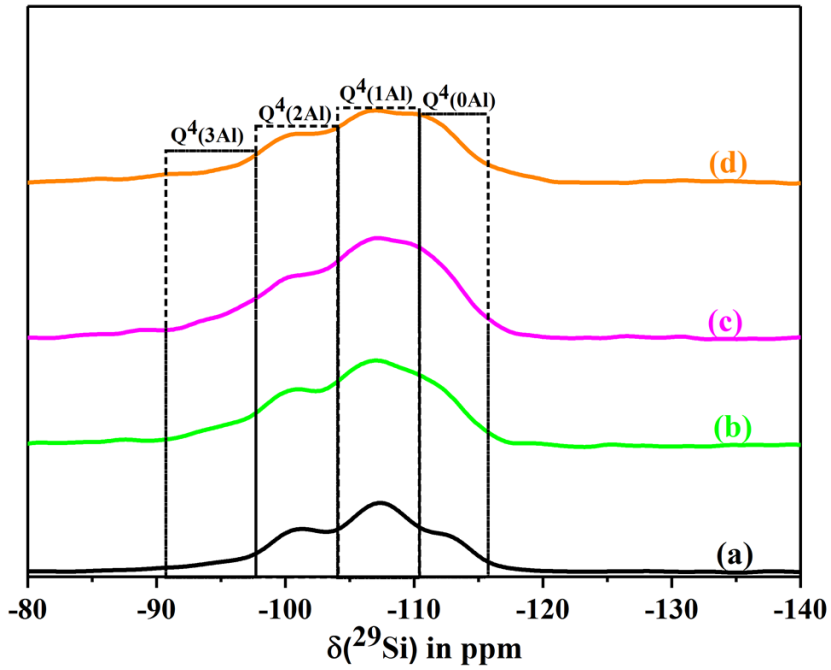

Figure 40. ^{29}Si spectra of starting CLIN and calcined 0.1M HCl treated (at 80°C for 1 hour) CLIN. **a)** CLIN, **b)** H-CLIN-0.1 M HCl, **c)** H-CLIN-0.1 M HCl-400°C, **d)** H-CLIN-0.1 M HCl-450°C, **e)** H-CLIN-0.1 M HCl-500°C.

^{27}Al MAS NMR spectra of HCl treated CLIN samples

The ^{27}Al MAS NMR spectra of HCl treated (0.1-2 M) CLIN catalysts 0.1 M are shown in Figure 41**.** Starting cationic clinoptilolite shows one signal at *ca*. 55 ppm with a pronounced shoulder at *ca.* 59 ppm belonging to tetrahedral coordinated framework aluminum $Al^{[IV]}$. The

treatment with different concentrated HCl causes only minor changes. The signal of tetrahedral aluminum is maintained. But the signal is broadened and in some cases the shoulder at *ca.* 59 ppm is less resolved. This might indicate some framework distortion. Change in the Si/Al ratio and T-O-T bond distances and angles leads to shifts of the positions of the NMR signals. This assumption is plausible because the acid treatment leads to partial dissolution of the zeolite. This is accompanied by some dealumination of the remaining framework as evidenced by the increase of the Si/Al ratio from *ca.* 5 to 6.17 (Tab. 16). A mass loss of up to *ca.* 24 % was observed. The observed broadening is in line with the decreased crystallite size, i.e. crystallinity of acid treated samples (Tab. 17). The 2 M HCl treat H-CLIN makes an exception. It shows still a well resolved shoulder at 59 ppm. Its crystallite size is close to that of the starting CLIN. It is concluded that the dissolution (2 M HCl solution at 80°C) of a part of zeolite framework, which is accompanied with an increase of the Si/Al ratio in the remaining zeolite, is connected with a re-crystallization (healing process) under the hydrothermal conditions.[59] The released framework aluminum is dissolved by the acid. Only a very weak signal of EFAL at *ca.* +10 to -10 ppm is observed with acid treated samples. Also penta-coordinated aluminum giving rise to a signal at *ca.* 30-40 ppm is not observed.[61,75,76,83,84]

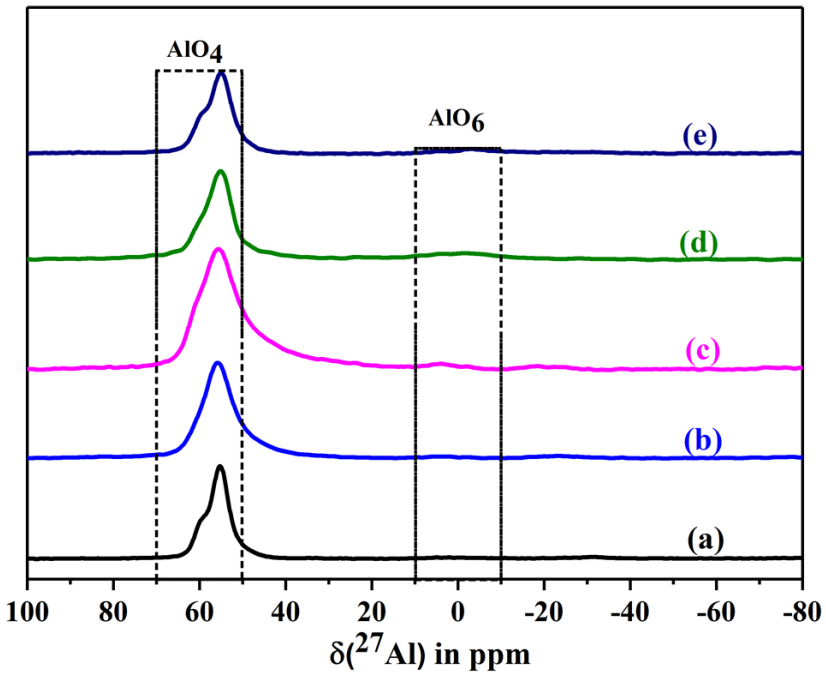

Figure 41. ^{27}Al MAS NMR spectra of dehydrated HCl treated (0.1–2 M) CLIN at 80°C for 1 hour. **a)** CLIN, **b)** H-CLIN-0.1 M HCl, **c)** H-CLIN-0.5 M HCl, **d)** H-CLIN-1 M HCl, **e)** H-CLIN–2 M HCl. All samples are activated at 400°C for 1 hour, heating rate of 5°C/min.

^{27}Al MAS NMR spectra of 0.1M HCl treated and calcined CLIN at 400°C, 450°C and 500°C are shown in Figure 42. In contrast to NH_4-CLIN, the calcination beyond 400°C does not cause a transition of tetrahedral framework aluminum $Al^{[IV]}$ to penta-coordinated aluminum $Al^{[V]}$ one. The H-CLIN is stable against thermal dealumination. EFAL signals are not detected.

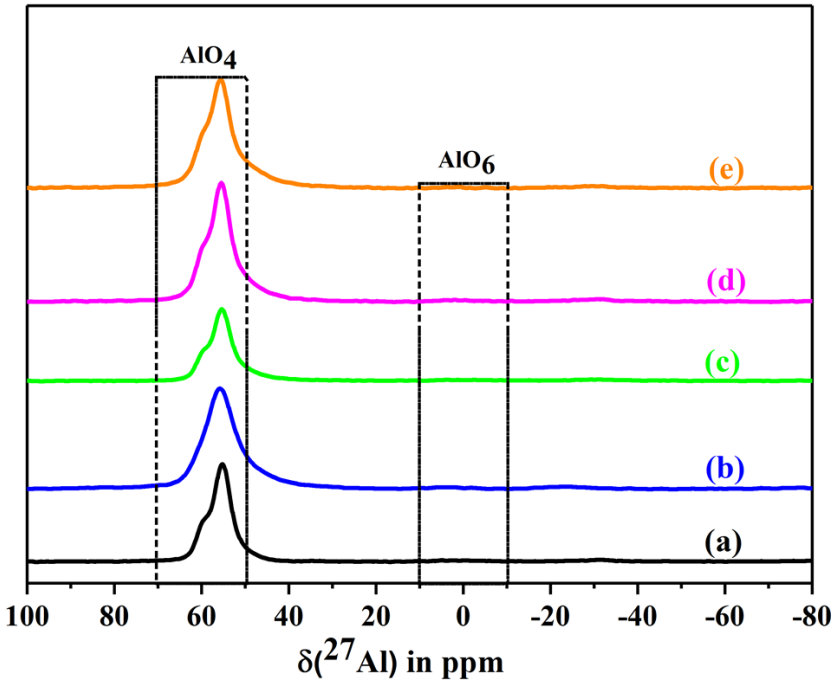

Figure 42. ^{27}Al spectra of starting CLIN and calcined 0.1M HCl treated (at 80°C for 1 hour) CLIN samples. **a)** CLIN, **b)** H-CLIN-0.1 M HCl, **c)** H-CLIN-0.1 M HCl-400°C, **d)** H-CLIN-0.1 M HCl-450°C, **e)**.H-CLIN-0.1 M HCl-500°C.

^{1}H MAS NMR spectra of HCl treated CLIN samples

The ^{1}H MAS NMR spectra of HCl treated CLIN samples are shown in Figure 43. The chemical shifts of protons located on different sites in zeolite frameworks are given in Table 10. In case of the 0.1 M HCl treated CLIN a broad signal arises ranging from *ca*. 8 to 2 ppm showing two maxima. The broad should with maximum at *ca.* 4.3 ppm is assigned to acidic bridging OH groups. Brønsted sites in small channels and cavities give rise to signals at *ca.* 5.5 ppm. This is in line with the clinoptilolite structure containing small cages and oxgen-8-rings (O8R-Fig. 11). The broad dominating maximum at *ca.* 2.45 ppm is assigned to AlOH species. Additionally a well-resolved weak signal at *ca*. 0.5 ppm is observed which belongs to cationic MeOH groups. The tailing intensity between at *ca.* 6-7 ppm which is assigned to distributed Brønsted acid sites (Tab. 10). For CLIN treated with 0.5 and 1 M HCl the intensity of Brønsted sites appearing between 4 and 6 ppm decreases compared the intensity at *ca.*

2.45 ppm. This finding is in line with the TPD data shown below (Tab. 24 and 25). It cannot be exclude that the intense signal at *ca.* 2.45 ppm originates also from Brønsted acid sites, because nearly no EFAL could be detected in the ^{27}Al MAS NMR spectra. MeOH signal at *ca.* 0 ppm are due to OH groups attached to remaining extra framework metal cations.

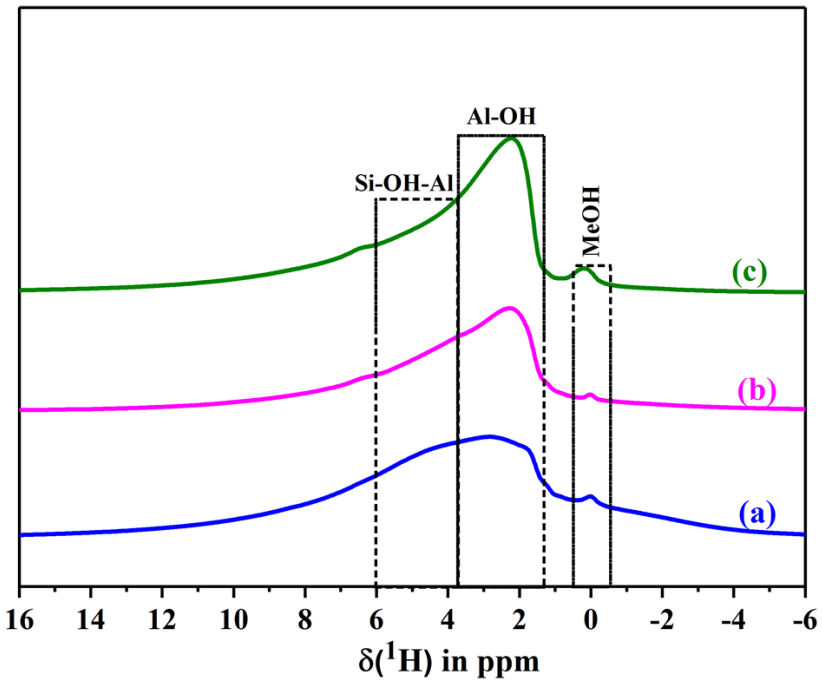

Figure 43. ^{1}H MAS NMR spectra of dehydrated HCl treated (0.1–1 M) CLIN at 80°C for 1 hour. **a)** H-CLIN-0.1 M HCl, **b)** H-CLIN-0.5 M HCl, **c)** H-CLIN-1M HCl. All samples were activated at 400°C for 1hour, heating rate of 5°C/min.

3.2.2 Textural characterization

3.2.2.1 Scanning electron microscopy (SEM)

SEM images of the HCl treated CLIN are shown at different magnification Figure 44. After treatment with acid in aqueous solution of HCl at 80°C for 1 h, i.e. under hydrothermal conditions, the big size agglomerate of starting CLIN in now divided and distributed. However, it is highly probable that acid treatment may result in the partial dissolution and elimination of amorphous binder material initially present between the zeolite crystals. Accordingly, it is concluded that the voids observable between the zeolite crystals (Fig. 45) are mainly due to the extraction of such material and loss of zeolitic material due to acid attack on surface of zeolite. This porosity is not detected by the nitrogen adsorption measurements, because the pores are too large.

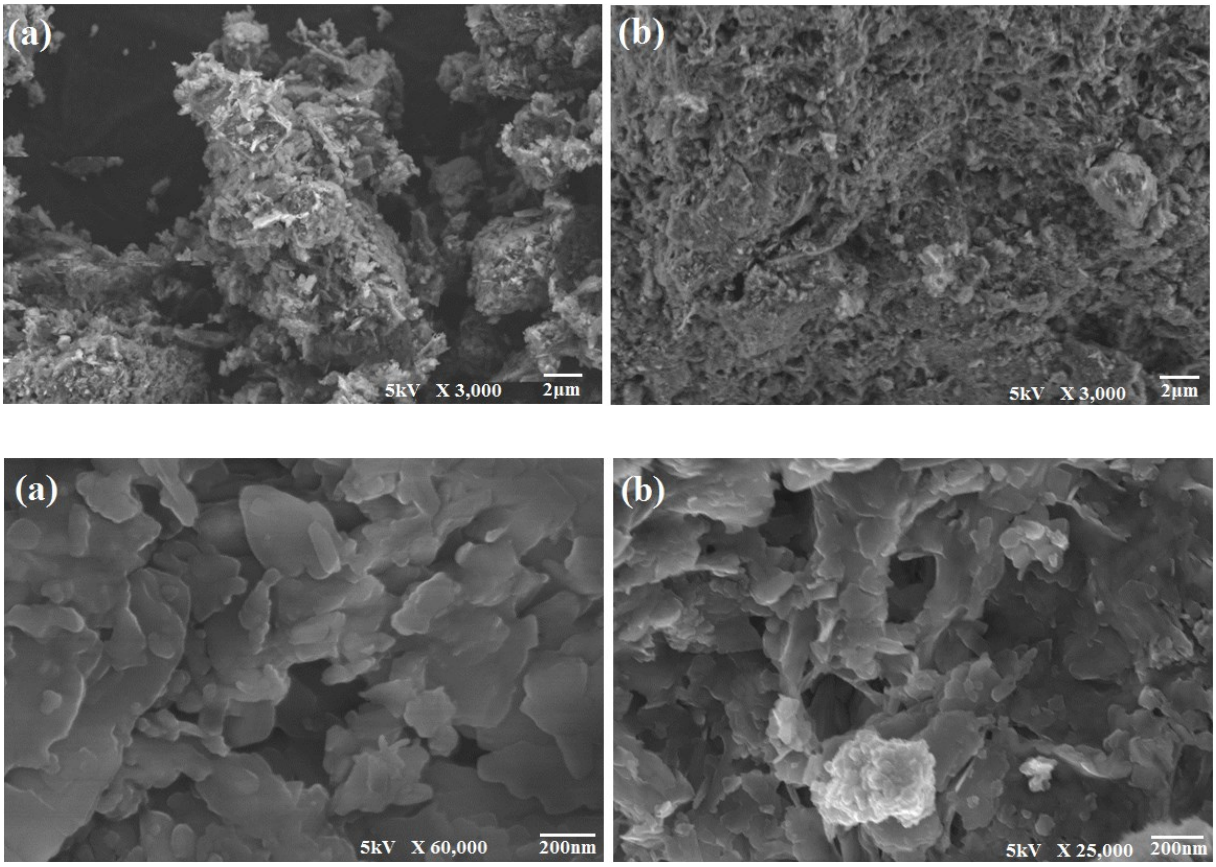

Figure 44. SEM images of 0.1 M and 2 M HCl treated CLIN samples. **a)** H-CLIN-0.1 M HCl, **b)** H-CLIN-2 M HCl

3.2.2.2 Nitrogen adsorption-desorption

N_2-adsorption-desorption isotherms of HCl treated CLIN samples are shown in Figure 45 and the specific surface areas and pore volumes are summarized in Table 22. All clinoptilolite catalysts show the same type IV isotherm according to IUPAC classification. They show a steep nitrogen uptake at very low relative pressure (of p/p_0 <0.01) and a less steep increase up to of p/p_0 =0.05 due to the adsorption in small and larger zeolitic micropores. It is followed by slow increase of the adsorption isotherm with growing relative pressure until of p/p_0 of ca. 0.8 due to adsorption in adsorption in mesopores or multilayer adsorption. Beyond this value adsorption of nitrogen in textural larger meso, nano or macropores located in between the crystals starts. Acid treatment causes an increase in the specific surface area (BET) by 44 to 59 % compared to the starting CLIN. The specific micropore area increases by 67 to 77 % (Tab. 22).

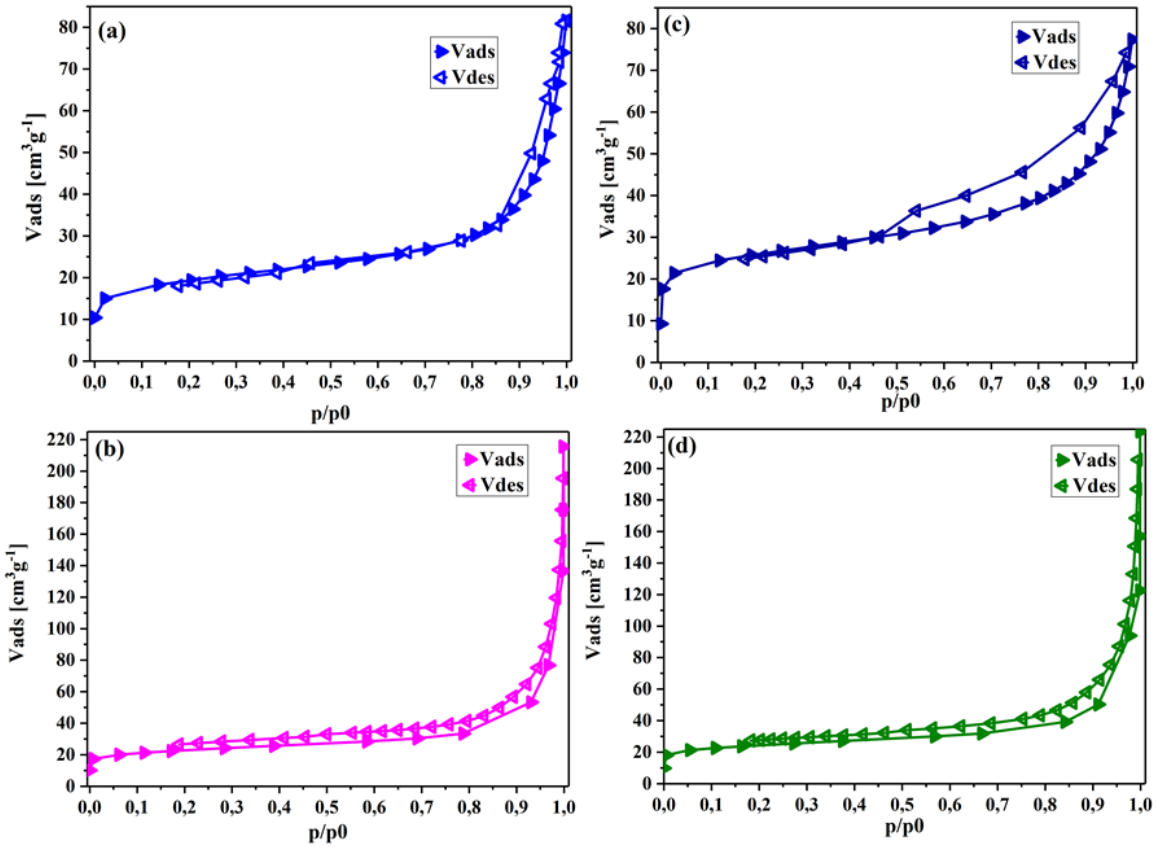

Figure 45. N_2-adsorption desorption isotherm of rehydrated HCl treated CLIN (exchange condition: 0.1-2M HCl at 80°C for 1 hour; rehydration in humid air at r.t.). **a)** H-CLIN-0.1 M HCl, **b)** H-CLIN-0.5 M HCl, **c)** H-CLIN-2 M HCl, **d)** H-CLIN-1 M HCl. H-CLIN means protonic sample, after treatment with HCl. Samples were dried by heating at 300°C for 2 h at 3 K/min and pumping under the reduced pressure and measurement was carried out at 77 K (-196 °C).

The removal of the cations and the loss of adsorbed zeolite water results in an opening of the pores. The micropore system becomes available for adsorbed molecules and results an increase of the nitrogen uptake at very low relative pressure. It reaches maximum after treatment with 2 M HCl. High acid concentration causes severe framework defects and amorphization, shrinkage of pore volumes and high weight loss of *ca.* 24 %. These results are in agreements with XRD and FTIR results for acid treated samples. Other authors have also reported similar results by treating clinoptilolite from different origin using different conditions of acid concentrations and temperatures.[69,70,62,63]

Table 22: Structural parameters calculated from adsorption–desorption isotherms of nitrogen for HCl treated CLIN (exchange conditions: 0.1-2 M HCl at 80°C for 1 hour; rehydration in humid air at r.t.). H-CLIN means protonic sample, after treatment with HCl. Samples are dried by heating at 300°C for 2 h at 3 K/min and pumping under the reduced pressure and measurement carried out at 77 K (-196 °C).

Catalysts	SSA (m^2g^{-1})[a]	Micropore area (m^2g^{-1})	Mesopore area (m^2g^{-1})[b]	Pore volume (cm^3g^{-1})[c]	Micropore vol. (cm^3g^{-1})[b]	Mesopore vol. (cm^3g^{-1})	Nanopore vol. (cm^3g^{-1})
CLIN	44.3	15.79	28.51	0.12	0.018	0.017	0.085
H-CLIN-0.1M HCl	78.5	48	30.5	0.13	0.03	0.016	0.084
H-CLIN-0.5M HCl	90.406	55.207	35.199	0.14	0.035	0.018	0.087
H-CLIN -1M HCl	95.685	56.895	38.79	0.15	0.037	0.021	0.092
H-CLIN -2M HCl	107.33	70.31	37.02	0.12	0.034	0.026	0.06

[a]Specific surface area BET, [b]t-Method, [c]Gurvich at $p/p^0 = 1$

The effect of HCl (0.1-2 M) treatment on micropore, mesopore and nanopore volumes are shown in Figure 46.

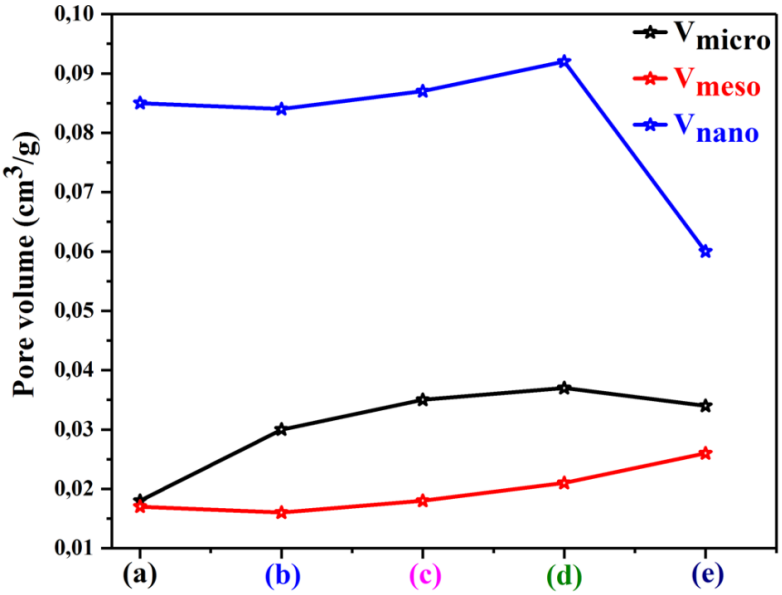

Figure 46. Micropore, mesopore and nanopore volumes of starting CLIN and rehydrated HCl treated CLIN (exchange conditions: 0.1-2 M HCl at 80°C for 1 hour; rehydration in humid air at r.t.). **a)** H-CLIN-0.1 M HCl, **b)** H-CLIN-0.5 M HCl, **c)** H-CLIN-1 M HCl, **d)** H-CLIN-2 M HCl. H-CLIN means protonic sample, after treatment with HCl. Samples are dried by heating at 300°C for 2 h at 3 K/min and pumping under the reduced pressure and measurement was carried out at 77 K (-196°C).

N_2-ads/des isotherms of 0.1M HCl treated CLIN calcined at 400,450 and 500°C are shown in Figure 47. A decrease in specific surface areas of micro and mesopores occurs with increasing

calcination temperature (Tab. 23). Additionally, a hysteresis loop appears in the nitrogen adsorption and desorption isotherms.

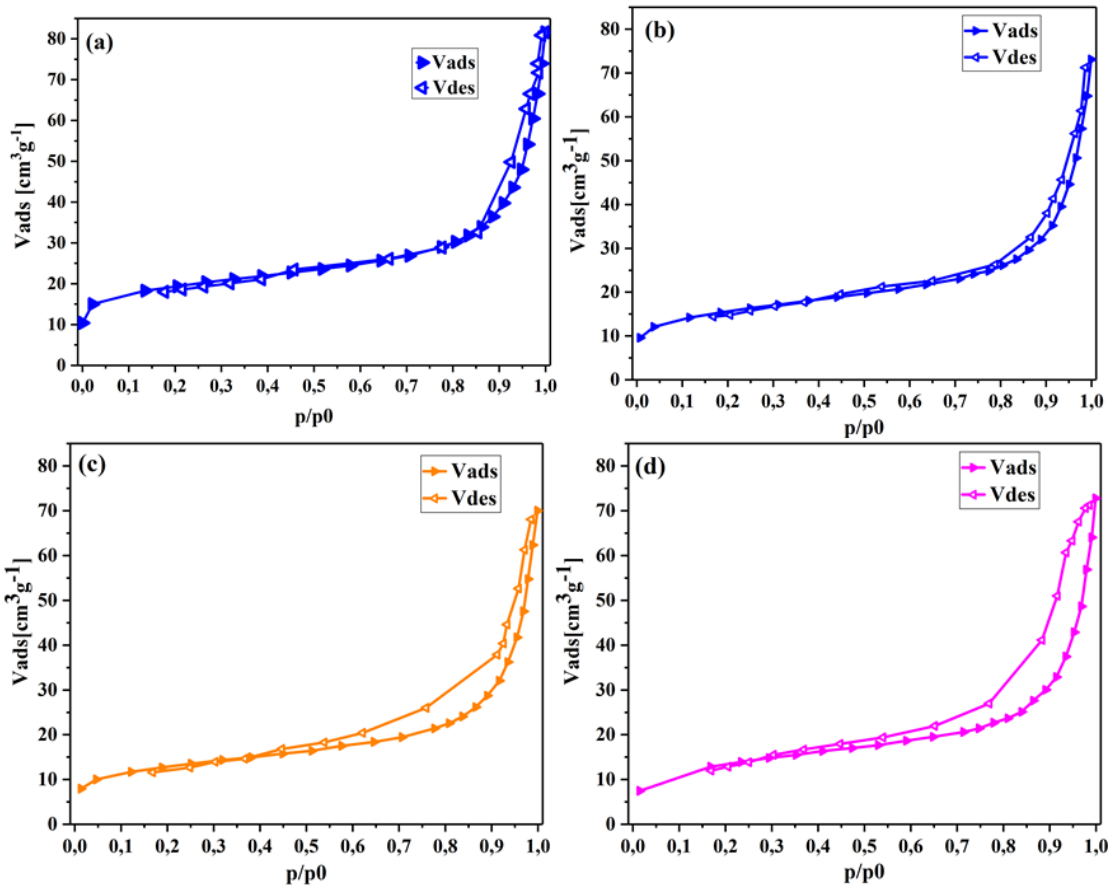

Figure 47. N_2-adsorption desorption isotherm of rehydrated 0.1 M HCl treated and calcined CLIN (exchange conditions: 0.1 M HCl at 80°C for 1 hour; rehydration in humid air at r.t.) and calcined at 400°C, 450°C and 500°C. **a)** H-CLIN-0.1 M HCl, **b)** H-CLIN-0.1 M HCl-400°C, **c)** H-CLIN-0.1 M HCl-450°C, **d)** H-CLIN-0.1 M HCl-500°C. Samples were dried by heating at 300°C for 2 h at 3 K/min and pumping under the reduced pressure and measurement was carried out at 77 K (-196°C).

Table 23: Structural parameters calculated from adsorption–desorption isotherms of nitrogen for 0.1 M HCl treated CLIN (exchange condition: 0.1 M HCl at 80°C for 1 hour; rehydration in humid air at r.t.) and calcined at 400°C, 450°C and 500°C. Samples are dried by heating at 300°C for 2 h at 3 K/min and pumping under the reduced pressure and measurement was carried out at 77 K (-196°C).

Catalysts	SSA (m^2g^{-1})[a]	Micropore area (m^2g^{-1})	Mesopore area (m^2g^{-1})[b]	Pore volume (cm^3g^{-1})[c]	Micropore vol. (cm^3g^{-1})[b]	Mesopore vol. (cm^3g^{-1})	Nanopore vol. (cm^3g^{-1})
CLIN	44.3	15.79	28.51	0.12	0.018	0.017	0.085
H-CLIN-0.1 M HCl	78.5	48	30.5	0.13	0.03	0.016	0.084
H-CLIN-0.1 M HCl-400°C	61.86	31.62	30.24	0.11	0.024	0.016	0.07
H-CLIN-0.1 M HCl-450°C	49.25	22.21	27.04	0.11	0.019	0.015	0.076
H-CLIN-0.1 M HCl-500°C	47.48	21.36	26.12	0.11	0.02	0.016	0.074

[a]Specific surface area BET, [b]t-Method, [c]Gurvich at $p/p^0 = 1$

The effect of the calcination temperature on the micropore, mesopore and nanopore volumes of 0.1 M HCl treated CLIN are shown in Figure 48. The acid treatment followed by high temperature calcination results does nearly not affect the porosity of the catalysts material.

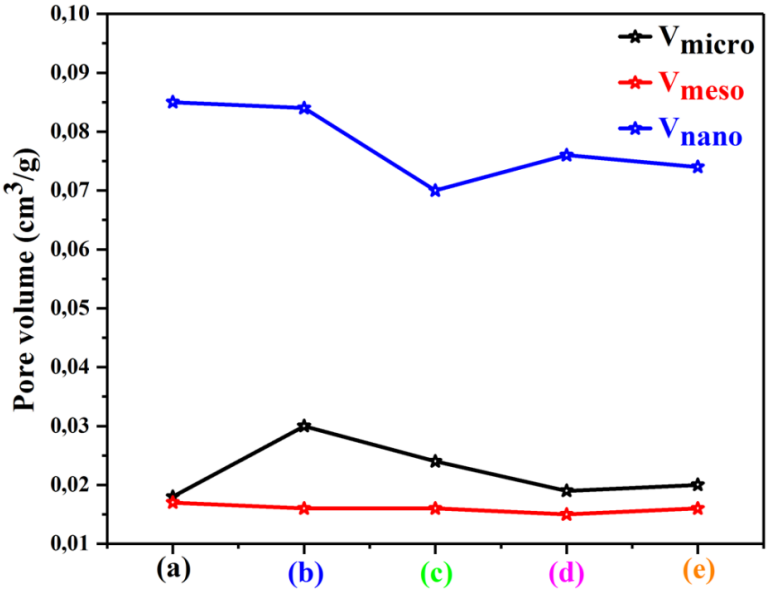

Figure 48. Micropore, mesopore and nanopore volumes of starting CLIN and 0.1 M HCl treated and calcined CLIN (exchange condition: 0.1 HCl at 80°C for 1 hour; rehydration in humid air at r.t.) and calcined at 400°C, 450°C and 500°C. **a)** CLIN, **b)** H-CLIN-0.1 M HCl, **c)** H-CLIN-0.1 M HCl-400°C, **d)** H-CLIN-0.1 M HCl-450°C, **e)** H-CLIN-0.1 M HCl-500°C. Sample are dried by heating at 300°C for 2 h at 3 K/min and pumping under the reduced pressure and measurement was carried out at 77 K (-196°C).

3.2.3 Acidity (TPD) of HCl treated CLIN catalyst

NH_3-TPD profiles of HCl treated CLIN are shown in Figure 49. The desorption profile is structured into low, medium and high temperature peaks which can be related to weak, medium, strong and very strong bound ammonium ions. The low temperature peak (shoulder) shoulder below 300°C and the peak at *ca.* 330°C is assigned to weak and medium strong BS. The high temperature peaks (HTP) between 400°C to 600°C, with maxima at *ca*. 450°C and 520°C can be related to strong and very strong BS, respectively. The distributions of weak, medium, strong and very strong Lewis sites (LS) and Brønsted acid sites (BS) are shown in Table 24 and 25. Highest content of BS sites, i.e. 0.764mmol/g, is obtained after treatment with 0.1 M HCl (H-CLIN-0.1 M HCl). With increase in acid concentration the BS and LS sites conc. Decreases (Tab. 24 and 25).

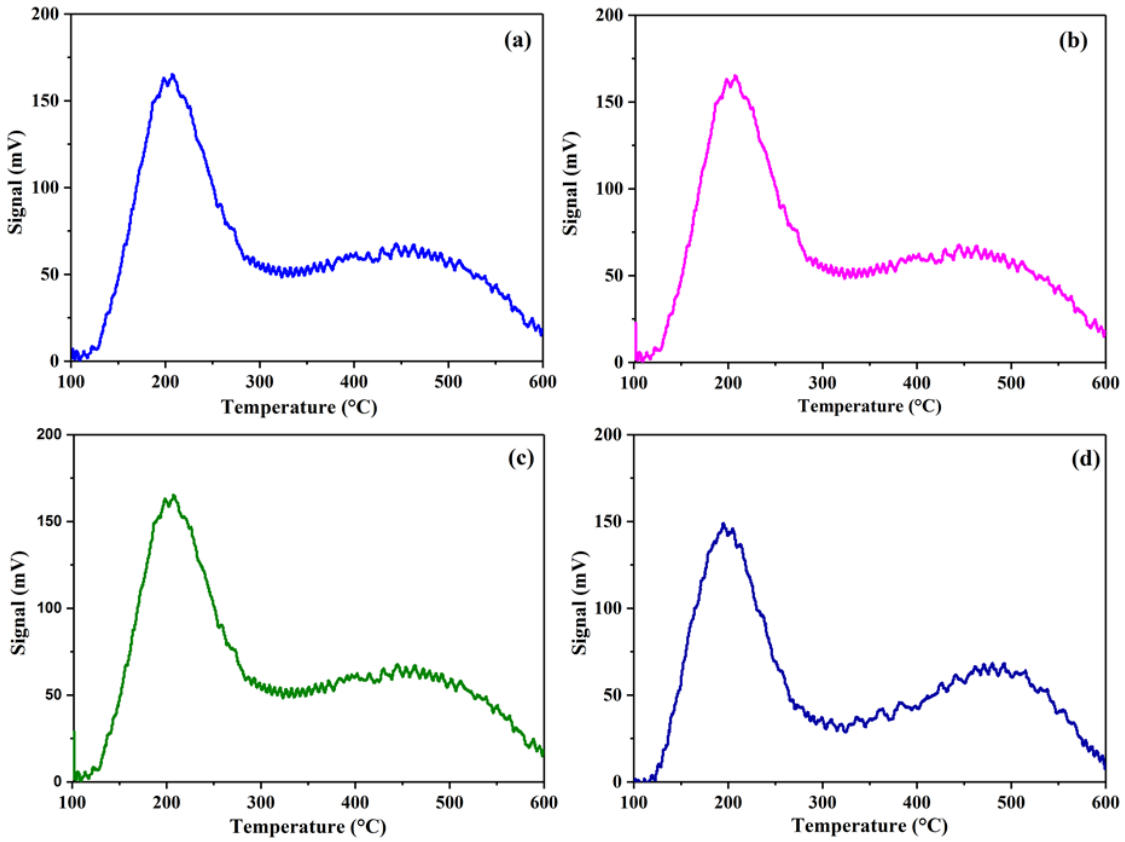

Figure 49. Temperature programmed desorption profiles of rehydrated HCl treated CLIN (exchange condition: 0.1-2 M HCl at 80°C for 1 hour; rehydration in humid air at r.t.). **a)** H-CLIN-0.1 M HCl, **b)** H-CLIN-0.5 M HCl, **c)** H-CLIN-1 M HCl, **d)** H-CLIN-2 M HCl. H-CLIN means protonic sample, after treatment with HCl. Pretreatment of samples at 180°C, NH_3 gas loading at 100°C and desorption analysis at 600°C.

Table 24: Concentration of BS sites (mmol/g) and distribution of medium, strong and very strong BS acidic sites for rehydrated HCl treated CLIN (exchange conditions: 0.1-2 M HCl at 80°C for 1 hour; rehydration in humid air at r.t.). And rehydrated 0.1 M HCl treated and calcined at 400°C, 450°C and 500°C. Pretreatment of samples at 180°C, NH_3 gas loading at 100°C and desorption analysis at 600°C.

Catalysts	Medium BS* sites	Strong and very strong BS sites	Total BS Sites (mmol/g)
	300-400°C	400-600°C	300-600°C
H-CLIN-0.1 M HCl	0.217	0.55	0.767
H-CLIN-0.5 M HCl	0.147	0.444	0.591
H-CLIN-1 M HCl	0.156	0.484	0.64
H-CLIN-2 M HCl	0.122	0.51	0.632
H-CLIN-0.1M HCl-400°C	0.175	0.42	0.585
H-CLIN-0.1M HCl-450°C	0.152	0.367	0.515
H-CLIN-0.1M HCl-500°C	0.118	0.28	0.398

Table 25: Concentration of BS sites (mmol/g) and distribution of weak LS, medium and strong BS acidic sites for rehydrated HCl treated CLIN (exchange conditions: 0.1-2 M HCl at 80°C for 1 hour; rehydration in humid air at r.t.). And rehydrated 0.1 M HCl treated and calcined at 400°C, 450°C and 500°C. Pretreatment of samples at 180°C, NH_3 gas loading at 100°C and desorption analysis at 600°C.

Catalysts	Total BS sites	Weak LS** sites	Weak LS & BS sites	Total adsorbed
	300-600°C	100-230°C	230-300°C	NH_3 (mmol/g)
H-CLIN-0.1 M HCl	0.767	0.275	0.168	1.21
H-CLIN-0.5 M HCl	0.591	0.249	0.10	0.94
H-CLIN-1 M HCl	0.64	0.248	0.13	1.01
H-CLIN-2 M HCl	0.632	0.228	0.097	0.957
H-CLIN-0.1 M HCl-400°C	0.585	0.217	0.124	0.926
H-CLIN-0.1 M HCl-450°C	0.515	0.23	0.118	0.863
H-CLIN-0.1 M HCl-500°C	0.398	0.20	0.102	0.70

For 0.1M HCl treated and calcined CLIN, a markedly decrease of the Lewis and Brønsted acidity is observed too after calcination at 400, 450 and 500°C, respectively (Fig. 50, Tab. 24 and 25).

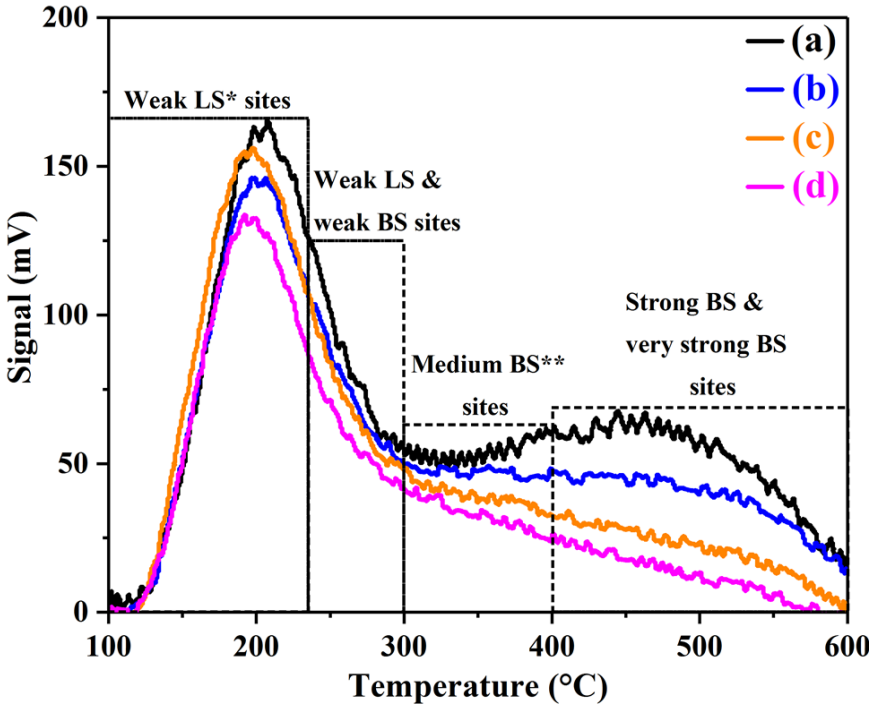

Figure 50. Temperature programmed desorption profiles of calcined 0.1 M HCl treated CLIN at 400°C, 450°C and 500°C. **a)** H-CLIN-0.1 M HCl, **b)** H-CLIN-0.1 M HCl-400°C, **c)** H-CLIN-0.1 M HCl-450°C, **d)** H-CLIN-0.1 M HCl-500°C. Pretreatment of samples at 180°C, NH_3 gas loading at 100°C and desorption analysis at 600°C.

The decrease in the BS acidity amounts to *ca*. 20 % in case of acid treated catalysts. This decrease is nearly directly related to the expected loss of BS site due to the increase of the Si/Al ration from ca. 5 to 6.17. The loss in the BS acidity after calcination is much higher due to additional partial amorphization. The latter decreases the zeolite content of the catalyst. It amounts to *ca.* 24 % after heating to 400°C and *ca.* 50 % after heating to 500°C. It is concluded that the thermal stability of BS sites is lower with H-CLIN catalysts obtained by acid treatment compared to H-CLIN obtained via ammonium ion exchange and thermal activation. These observations are in close agreement with observed markedly decrease in the specific surface area of these catalysts. They are also confirmed by the XRD results which show loss in crystallinity (increased background, peak broadening, decreasing crystallite size) and a markedly shift of 2θ by 0.1-0.6° to higher angle after heating from 400 to 500°C (Fig. 36 and Tab. 18). Severe changes in the zeolite framework are induced (probably increased disorder).

3.2.4 Catalytic activity of HCl treated CLIN catalyst

The onset acetalization activity of fresh prepared and not thermally activated HCl treated CLIN by using 100 mg of catalyst are shown in Figure 51 and 52.

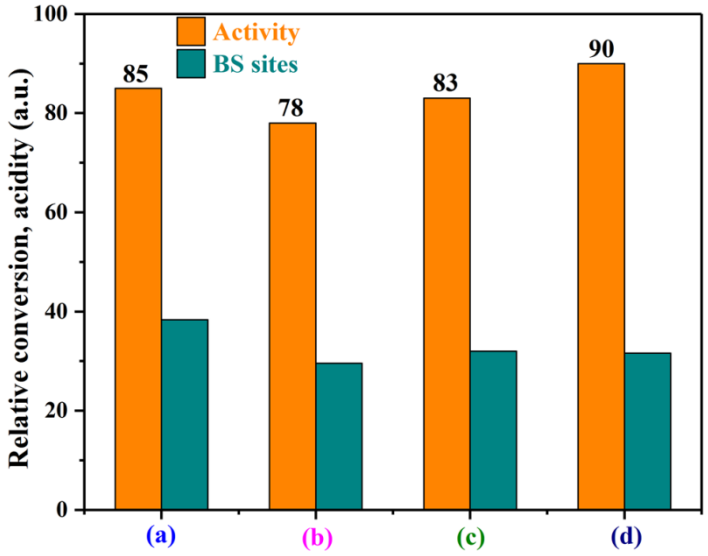

Figure 51. Acetalization of benzaldehyde with butanediol-1,3 over starting CLIN rehydrated HCl treated CLIN (exchange condition: 0.1-2 M HCl at 80°C for 1 hour; re-hydration in humid air at r.t.). **a)**H-CLIN-0.1 M HCl, **b)** H-CLIN-0.5 M HCl, **c)** H-CLIN-1 M HCl, **d)** H-CLIN-2 M HCl. H-CLIN means protonic sample, after treatment with HCl. Reaction conditions, Batch reactor 150 mL, **Catalyst:100 mg** Reactant:10 g benzaldehyde, 9 g butandiol, Internal Standard: 1 g hexamethyl benzene, Solvent: toluene. Reaction Temperature: *ca*. 113-116°C.

The acetal formation (%) during the course of reaction is given in Table 26. Highest acetal formation after 30 min of reaction of *ca.* 85 % is found with non-activated 2 M and 0.1 M HCl treated CLIN; even they contain only medium concentrations of BS of 0.55 and 0.51 mmol/g respectively (Fig. 52).

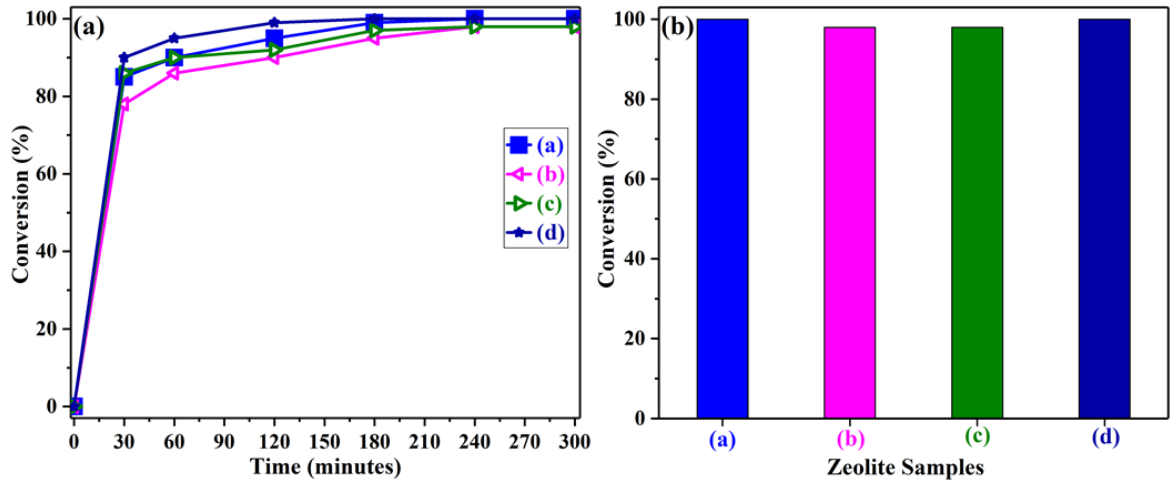

Figure 52. Acetalization of benzaldehyde with butanediol-1,3 over rehydrated HCl treated CLIN (exchange conditions: 0.1-2 M HCl at 80°C for 1 hour; re-hydration in humid air at r.t.). **a)** H-CLIN-0.1 M HCl, **b)** H-CLIN-0.5 M HCl, **c)** H-CLIN-1 M HCl, **d)** H-CLIN-2 M HCl. H-CLIN means protonic sample, after treatment with HCl. Reaction conditions, Batch reactor 150mL, **Catalyst:100 mg**, Reactant: 10 g benzaldehyde, 9 g butandiol, Internal Standard: 1 g hexamethyl benzene, Solvent: toluene. Reaction Temperature: *ca*. 113-116°C. Figure **(a)** on left side shows the activity after each 30 minutes of reaction time and Figure **(b)** on right side shows the total acetalization activity after 5 hours of reaction time.

Table 26: Acetalization formation (%) over re-hydrated calcined NH_4-CLIN catalyst (exchange condition: 0.5 M NH_4NO_3 and 0.1-2 M HCl at 80°C for 1 hour, rehydration in humid air at r.t. under reflux) as well as over 0.1 M HCl treated CLIN calcined at 400, 450 and 500°C. Reaction conditions: batch reactor 150mL, **catalyst:100 mg,** reactant: 10 g benzaldehyde, 9 g 1,3-butandiol, internal standard: 1 g hexamethyl benzene, solvent: toluene, reaction temperature: *ca*. 113-116°C.

Catalysts	Acetal formation (%) with reaction time/ (min)					
	30	**60**	**120**	**180**	**240**	**300**
H-CLIN-400°-100 mg	22	28	35	42	45	45
H-CLIN-450°C-100 mg	63	86	97	99	100	100
H-CLIN-500°C-100 mg	35	64	89	94	97	98
H-CLIN-0.1 M HCl-400°C-100 mg	35	38	40	41	41	41
H-CLIN-0.1 M HCl-450°C-100 mg	29	31	33.5	35	35	35
H-CLIN-0.1 M HCl-500°C-100 mg	22	24	28	30	30	30

Table 27: Acetalization of benzaldehyde with butandiol-1,3 over CLIN-starting material and rehydrated HCl treated H-CLIN catalyst (exchange condition: 0.1-2 M HCl at 80°C for 1 hour, rehydration in humid air at r.t. under reflux) as well as over 0.1 M HCl treated CLIN calcined at 400, 450 and 500°C. Reaction conditions: batch reactor 150 mL, **catalyst:200(100) mg,** reactant: 10 g benzaldehyde, 9 g 1,3-butandiol, internal standard: 1 g hexamethyl benzene, solvent: toluene, reaction temperature: *ca*. 113-116°C.

Catalysts	Acetal formation (%) with reaction time/ (min)					
	30	**60**	**120**	**180**	**240**	**300**
CLIN	8.5	9	10.4	12.5	14.5	14.5
H-CLIN-0.1 M HCl	94	99	99	100	100	100
H-CLIN-0.5 M HCl	80	90	93	99	100	100
H-CLIN-1 M HCl	88	92	97	100	100	100
H-CLIN-2 M HCl	98	99	100	100	100	100
H-CLIN-0.1 M HCl-100 mg	85	90	95	99	100	100
H-CLIN-0.5 M HCl-100 mg	78	86	90	95	98	98
H-CLIN-1 M HCl-100 mg	83	88	92	97	98	98
H-CLIN-2 M HCl-100 mg	90	95	99	100	100	100
H-CLIN-0.1 M HCl-400°C-200 mg	70	76	80	82	82	82
H-CLIN-0.1 M HCl-450°C-200 mg	58	62	67	70	70	70
H-CLIN-0.1 M HCl-500°C-200 mg	45	48	56	60	60	60

Acetal formation over 0.1 M HCl treated CLIN calcined at high temperature of 400°C to 500°C is shown in Figure 53. The data are summarized in in Table 26. The activity decreases by 52 % after heating to 500°C after 1 h of reaction. Activation of acid treated CLIN at 400°C causes a tremendous decrease in the acetal formation by *ca*. 60 % (Tab. 26 and 27). But the acidity decreases only by *ca.* 24 % Therefore, the high activity of fresh prepared catalysts is assigned to remaining supported HCl (after washing), which is removed after thermal treatment at 400°C. The activity of HCl treated catalysts is lower than that obtained via ammonium ion exchange. Heating from 400°C to 500°C leads to an activity loss ca. 37 %. These losses are directly related to the acidity decreases which amounts to ca. 48 % and 32 %, respectively (Table 25). After 3 hours the loss in activity (in terms of acetal formation) is still 40 %. These findings are in line with increase in background, peak broadness and shift of 2θ to higher valve in the range of 0.1-0.6° by XRD (Fig. 36 and Tab. 18) as well as a visible shift in structural sensitive double ring vibration band at 600 cm^{-1} to high wavenumber (cm^{-1}) value of 608 cm^{-1} by FTIR (Tab. 20).

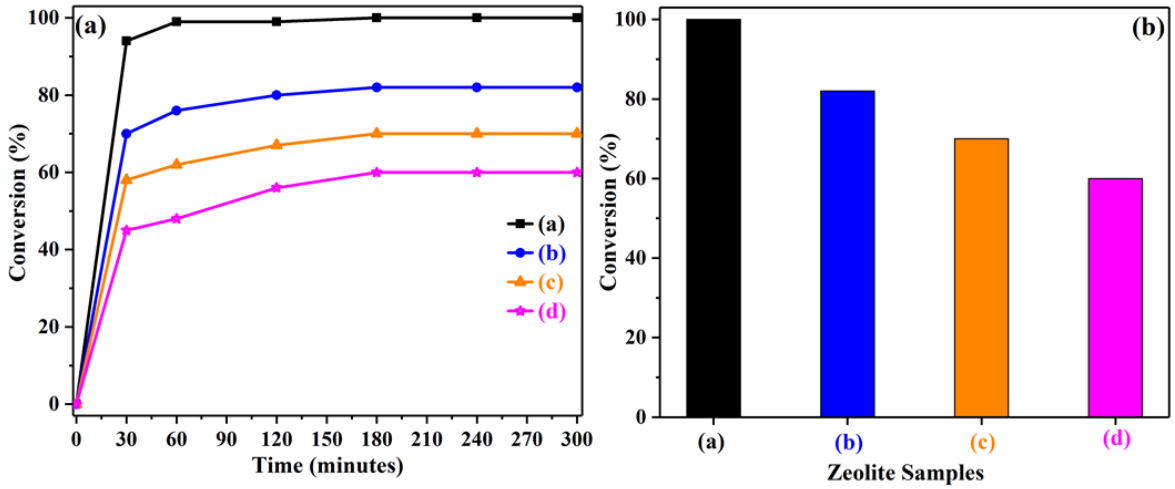

Figure 53. Influence of thermal pre-treatment on the course of acetalization of benzaldehyde with butanediol-1,3 over re-hydrated 0.1 M HCl treated CLIN catalyst (exchange condition: 0.1 M HCl at 80°C for 1 hour; rehydration in humid air at r.t.) and calcined at 400°C, 450°C and 500°C, as catalyst, under reflux. Figure **56 a**, on left side shows the course of acetalization activity after each 30 minutes of reaction time and Figure **56 b**, on right side shows the total acetalization activity after 5 hours of reaction time. **a)** H-CLIN-0.1 M HCl, **b)** H-CLIN-0.1 M HCl-400°C, **c)** H-CLIN-0.1 M HCl-450°C, **d)** H-CLIN-0.1 M HCl-500°C. Reaction conditions: batch reactor 150 mL, **catalyst:200 mg,** reactant: 10 g benzaldehyde, 9 g 1,3-butandiol, internal standard: 1 g hexamethyl benzene, solvent: toluene, reaction temperature: *ca*. 113-116°C.

3.2.5 Summary

- Starting CLIN Si/Al ratio of 5.27 consist of *ca.* 94 % clinoptilolite by ICP-AES analysis. More than 50 % of extra framework cations are exchanged by H^+ ions from acid and Si/Al ratio increases to 6.17.
- Increase in Si/Al ratio confirms increase in acidic character and framework local changes.
- XRD pattern of starting CLIN agrees with the simulated clinoptilolite pattern. Background increases and peak broadness increases with acid concentration, due to decrease in crystallinity and amorphization can be observed.
- For acid treated and calcined CLIN at high temperature visible shift of peaks to higher 2θ valves are observed.
- From ^{27}Al MAS NMR no clear and visible transition to penta-coordinated $Al^{[V]}$ at the expense of tetra coordinated framework aluminum $Al^{[IV]}$ can be seen for HCl treated and calcined CLIN.
- Porosity increases with increase in acid concentration. With 2 M HCl the pore volume decreases due to framework defects also visible by FTIR spectra and XRD pattern.

- For acid treated CLIN the increased activity as compared to acidity are due to the remaining supported acid after washing.
- For calcined acid treated CLIN at high temperature; porosity, acidity and activity decreases with increase in calcination temperature. The markedly decrease are due to framework defects, decrease in crystallinity, amorphization and loss of active sites also visible by XRD pattern.

4 Final conclusions

New natural zeolite catalysts (H-CLIN) are obtained via mild/soft treatment conditions of ammonium ions exchange (0.5 M NH_4NO_3, 80°C and 1 hour) followed by calcination (300-600°C) and direct treatment with HCl (0.1-2 M, 80°C and 1 hour).

Maximum decomposition of NH_4^+-ions occur at 450°C. For ammonium exchange CLIN calcined at 450°C (H-CLIN-450°C), highest valve of porosity, acidity and acetal formation activity are obtained. Transition of tetrahedral framework $Al^{[IV]}$ to penta-coordinated $Al^{[V]}$ and relative decrease in porosity, acidity (BS sites) and acetal formation activity are observed beyond calcination at 450°C. After calcination at 600°C, a markedly dramatic decrease in acetal formation activity, acidity and maximum conversion to penta-coordinated $Al^{[V]}$ at the expense of tetrahedral framework $Al^{[IV]}$ are observed.

For acid treated CLIN, porosity, acidity (BS sites) and acetal formation activity increases with increase in acid concentration. Relatively small increase in porosity and high weight loss of *ca.* 24 % compared to calcined NH_4-CLIN are observed. Porosity, acidity and activity of acid treated CLIN decreases after calcination at high temperature (400-500°C).

These findings show that the catalytic activity of H-CLIN catalysts depends on both,

- The acidity; i.e. the number of BS sites,

And,

- The (micro) porosity determining the accessibility of BS and mass transfer to and from the catalyst.

A Synthesis-Structure-Porosity-Acidity-Activity Relationship is found with H-CLIN catalysts (Structure Property Catalysis Relationship).

5 Appendix

5.1 Specifications of used Chemicals

Table 28: Chemical reagents used; names, CAS no and origin

Chemical names	CAS no	Origin
Hexamethyl benzene	87-85-4	HMB, Acros Organics, 98%
1,3-butanediol	Made in Germany (49064)	VEB Laborchemie Apolda
Benzaldehyde	100-52-7	Sigma-Aldrich, 99%
Toluene	108-88-3	Sigma-Aldrich, 99.8%
Ammonium nitrate	6484-52-2	Sigma-Aldrich, extra pure.
Hydrochloric acid (HCl)	7647-01-0	Sigma-Aldrich, 35-38%

5.2 Preparation of acidic form of catalyst

Natural zeolite Clinoptilolite sample "clinofit® Si PREMIUM", is in powder form, green gray in colour of VITARING®-biomed systems GmbH Germany. The powders were grinded uniformly by mortar and pestles for getting uniform particle size. Clinoptilolite [$Ca(Na,K)_4(Al_6Si_{30}O_{72})\ 20H_2O$], designated as "CLIN" is converted into H-form via ammonium exchange followed by calcinations and direct Hydrochloric acid treatment.

5.2.1 Route 1: NH_4^+ ions exchange followed by calcination

Starting clinoptilolite (CLIN) was transferred into ammonium form by suspending 4 grams of CLIN in 100 mL of 0.5 M solution of NH_4NO_3 (I g zeolite:25 mL NH_4NO_3 solution) by continuous stirring at 300 rpm 1 h at 80°C in 250 mL beaker (LABSOLUTE). Heidolph MR 3001 K stirrer was used for stirring. After ammonium ion exchange, the samples were separated by filtration, washed with freshly distilled water 3 times, dried in air, kept in oven at 80°C for overnight and the dried ammonium exchanged sample obtained was named as NH_4-CLIN. 2 gram of NH_4-CLIN sample in 50 mL porcelain crucible from Ajax Scientific was subjected to calcination in Nabertherm furnace under airflow at different temperatures (300–600°C). It is assumed that during NH_4^+ exchange followed by calcination, different reactions are taking place in many steps. In the start during exchange process, the native cations are exchanged by NH_4^+ ions. In the next calcination process step, the NH_4^+-ions dissociate into H^+ and NH_3 gas. The H^+ ions replace the positions of native cations and NH_3 gas evolved (Scheme 5).

Table 29: Starting CLIN treated with 0.5 M NH_4NO_3 (80°C, 1 hour), and calcined (300-600°C). 4 grams of sample added to form 100 mL of solution (1 g: 25 mL).

Catalysts	Treatment
CLIN	Starting clinoptilolite
NH_4-CLIN	Ammonium exchanged clinoptilolite
H-CLIN-300°C	NH_4-CLIN calcined at 300°C
H-CLIN-350°C, H-CLIN-400°C, H-CLIN-450°C, H-CLIN-500°C, H-CLIN-550°C and H-CLIN-600°C, are NH_4-CLIN calcined at 350°C, 400°C, 450°C, 500°C, 550°C and 600°C respectively.	

$$\text{Ca(Na,K)-CLIN} + NH_4NO_3 \xrightarrow{80°C,\ 1hr} (NH_4^+,K)\text{-CLIN}$$

$$(NH_4^+,K)\text{-CLIN} \xrightarrow[300\text{-}600°C]{\text{Calcination}} \text{H-CLIN}$$

The shallow bed furnace was operated at a heating rate of 5°C/min and kept at the final temperature for 1 hour. These temperatures were chosen, because the structure of zeolites is sensitive to high temperature especially in the presence of water vapors. Ammoniun ion (NH_4^+) replaces the Na^+ ions present as extra framework cations. Potassium ions (K^+) located in channel C is very hard to remove and stay inside the zeolite channels. NH_4^+-ions decomposes to NH_3 gas leaving behind H+ ions, compensating the negative charge of the framework. Weight losses of 8-10 % are observed for NH_4^+ exchanged and calcined samples.

5.2.2 Route 2: Treatment with hydrochloric acid

HCl solutions of 0.1 M, 0.5 M, 1 M and 2 M were prepared in 1 L flat bottom volumetric glass flask. 4 grams of CLIN was suspended in 100 mL of HCl solution in 250 mL beaker (LABSOLUTE), mounted on a heated Heidolph MR 3001 K magnetic stirrer. During the experiment, the solution was continuously stirred at 300 rpm and the temperature was maintained at 80°C for 1 hour. After ion exchange was completed, solids particles were filtered and rinsed with distilled water several times until to remove all the traces of entertained acid, dried in air and kept in oven at 80°C overnight. Weight losses (%) of sample after treatment are noted. Samples details with weight loss (%) are given in Table 29.

$$\text{(Na,K)-CLIN} + HCl \xrightarrow[80°C,1h]{0.1\text{-}2M} \text{H-CLIN}$$

Table 30: Starting CLIN treated with 0.1-2 M HCl (80°C, 1 hour), samples names with weight loss (%). 4 grams of the CLIN sample was suspended in 100 mL of aqueous acid (1 g: 25 mL).

Catalysts	Treatment details	Weight after treatment (g)	Weight loss (%)*
CLIN	Starting clinoptilolite	4	-
H-CLIN-0.1 M HCl	Clinoptilolite treated with 0.1 M HCl	3.54	11.5
H-CLIN-0.5 M HCl	Clinoptilolite treated with 0.5 M HCl	3.35	16.25
H-CLIN–1 M HCl	Clinoptilolite treated with 1 M HCl	3.23	19.25
H-CLIN–2 M HCl	Clinoptilolite treated with 2 M HCl	3.05	23.75

**Ca.* 5% of weight loss is due to the weight decrease by exchange of heavy metal cations by protons.

It is believed that with these modifications the extra-framework cations are replaced with H^+ to compensate the negative charge of Al^{3+} (Scheme 5).

The conversion of a natural clinoptilolite to hydrogen form (H-form) by ammonium exchange followed by calcination and direct treatment with hydrochloric acid (HCl) has a great influence on the effective acidity and surface area of clinoptilolite, both parameters increased after the treatment.

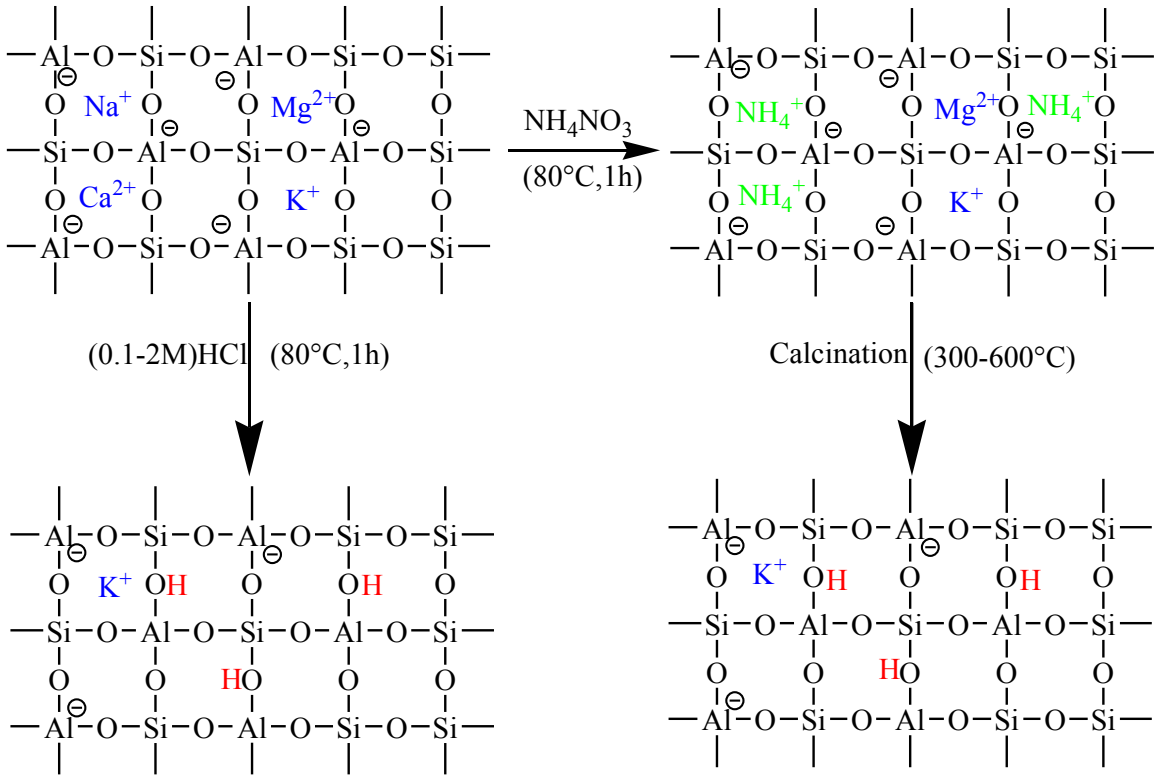

Scheme 5. Schematic representation of the mechanism of NH_4^+ ions exchange followed by calcination (300-600°C) steps and H^+ ions exchange by acid in the framework of zeolites.

5.3 Characterization methods

5.3.1 ICP-Atomic Emission Spectroscopy (ICP-AES)

Inductively coupled plasma atomic emission spectroscopy (ICP-AES) was used for the detection of major, minor and some trace elements in starting CLIN, ammonium exchanged and calcined CLIN and HCl trearted CLIN. It is a type of emission spectroscopy, inductively coupled plasma (ICP) is used to produce excited atoms from a sample. These emit electromagnetic radiation at wavelengths characteristic of a particular element. A spectrometer separates and resolves these lines and measures their strength. The intensity of this emission is indicative of the concentration of the element within the sample. Varian 715-ES (ICP Optical Emission Spectrometer) was used for analysis of samples. Plasma energy is given to an analysis sample from outside; the component elements (atoms) are excited. When the excited atoms return to low energy position, emission rays (spectrum rays) are released and the emission rays that correspond to the photon wavelength are measured. The element type is determined based on the position of the photon rays, and the content of each element is determined based on the ray's intensity.

5.3.2 X-ray diffraction (XRD)

X-ray diffraction (XRD) is a rapid analytical technique primarily used for phase identification of a crystalline material and can provide information on unit cell dimensions. The analyzed material is finely ground, homogenized, and average bulk composition is determined. X-ray wavelength are similar to the distance between atoms, X-ray Diffraction (XRD) techniques uses the same principal to elucidate the crystalline nature of materials. Light scattering in a periodic way with a long-range order produces constructive interference at specific angles and scattering occur. The scattering of X-rays from atoms produce a diffraction pattern that contains information about the atomic arrangement in crystal. Zeolite samples in fine powder and rehydrated form were characterized by X-Ray diffraction powder patterns in the 2θ range from 5 to 80°, using mono chromatized Cu-Kα radiation with STOE STADI P transmissions and reflections diffractometer of linear PSD. The program suite of WinXPOW (Stoe & Cie GmbH) with the assistance of the powder diffraction file PDF2, from the International Centre of Diffraction Data (ICDD), was used to determine the phase composition. The crystallite size of particles was estimated from XRD line broadening analysis by using the Scherrer equation:

$$D = K \times \lambda / \beta.\cos\theta$$

Where

- D is the average crystallite size,
- K is Scherer constant (0.89),
- θ is the diffraction angle (Bragg angle) of the studied phase (2θ/2), and
- β is peak width at half height(2θ).

5.3.3 Differential Scanning Calorimetry (DSC) and Thermogravimetric Analysis (TGA)

Thermal analysis was performed on a Setaram TGA Labsys 1600 DSC under Ar gas at a heating rate of 10°C/min. The weight losses were evaluated on the derivation of the thermogravimetry (TG) curve. All data were obtained by using the 2000 Setsoft software. Sample (28-30 mg) was put in a 0.1 cm^3 alumina (Al_2O_3) crucible.

5.3.4 Fourier Transform Infrared spectroscopy (FTIR)

FTIR spectroscopy is a vibrational spectroscopy that records absorptions of IR light by chemical bonds in all molecules incl. polymers. Since different bonds absorb IR light at characteristic but different wavelengths FTIR spectroscopy is often referred to as fingerprint spectroscopy. As a consequence pure compounds have characteristic and unique FTIR spectra. In principle, all states of matter, gas-liquid-solid, can be analyzed. Since light transmittance through a sample is necessary (IR light should read the detector) very thin film material or a sample finely dispersed in a non-absorbing matrix normally needs to be prepared. FTIR spectra were measured with a smart orbit ATR (Attenuated Total Reflection) Nicollet 380 FTIR spectrometer from Bruker Alpha in total reflection mode. The samples were traced in the range of 4000-400 cm^{-1} and the band intensities were expressed in transmittance (%). Resolution power was 4 cm^{-1} and no. of scans were 64.

5.3.5 ^{1}H MAS NMR, ^{27}Al MAS NMR and ^{29}Si MAS NMR (solid state NMR)

Bruker AVANCE-600 spectrometer was used for ^{27}Al MAS NMR and ^{1}H MAS NMR measurements, and Bruker DMX-400 spectrometer for ^{29}Si MAS NMR measurements. About 15 mg of sample was packed in 2.5 mm rotor (^{1}H MAS NMR), 130 mg in 4 mm ZrO_2 rotor (^{27}Al MAS NMR) and ~ 300 mg in 7 mm rotor (^{29}Si MAS NMR). ^{1}H MAS NMR measurement was performed using Bruker AVANCE-600 spectrometer with MAS spinning speed of 12.5 kHz with a pulse length of 3.5 μs, recycle time of 2 s, accumulation number of 32 using adamantine (1.78 ppm) as external reference. ^{27}Al MAS NMR measurement was

performed using Bruker AVANCE-600 spectrometer with MAS spinning speed of 12.5 kHz with a pulse length of 3.5 µs, recycle time of 2 sec, accumulation number of 64 using Yttrium aluminum garnet (AlO_6 peak 0.6 ppm) as external reference. ^{29}Si MAS NMR measurement was performed using Bruker DMX-400 spectrometer with MAS spinning speed of 6.5 kHz with a pulse length of 7.5 µs, recycle time of 3–1800 sec, accumulation number of 192 using Kaolinite (upfield peak, -91.5 ppm) as external reference (Tab. 30).

Table 31: MAS NMR Spectrometer Specifications and conditions used for measurements of MAS NMR spectra

	^{1}H MAS NMR	**^{27}Al MAS NMR**	**^{29}Si MAS NMR**
Field strength (Wide bore magnet)	14.7	14.7	9.4
Spectrometer	AVANCE-600	AVANCE-600	DMX-400
MAS rotor diameter (mm)	4	4	7
MAS spinning speed (kHz)	12.5	12.5	6
Pulse length (µs)	3.5	3.75 (optimized for strong quadrupolar interaction)	7.5
Recycle delay (s)	2	2	300
Accumulation number	32	64	32
Secondary field standard	Adamantane, 1.78 ppm	Yttrium aluminum garnet, AlO_6 peak, 0.6 pmm	Kaolinite, upfield peak,−91.5 ppm

Sample activation procedure for MAS NMR measurements

1 gram of sample in 50 mL porcelain crucible from Ajax Scientific, were subjected to activation in Nabertherm furnace under air flow at 400°C with a heating rate of 5°C/min. Sample was kept at 400°C for one hour. The heated sample was transferred to schlenk tube with outer joint and glass stop cock under vacuum and kept in desiccator having a strong drying agent. The same procedure was used for all samples. Rotors were filled inside the glove box. Experimental conditions shown in Table 31 were used for sample analysis.

5.3.6 Scanning electron microscope (SEM)

Samples were analyzed by a field emission scanning electron microscope (SEM, MERLIN® VP Compact, Company Zeiss, Oberkochen) equipped with an energy dispersive X-ray (EDX) detector (XFlash 6130, Company Bruker, Berlin). Representative areas of the samples were analyzed and mapped for elemental distribution on basis of the EDX-spectra data by

QUANTAX ESPRIT Microanalysis software (version 2.0). Samples were mounted on aluminum SEM-carrier (Company: Agar Scientific) with sticky Leit-Tabs (Company: PLANO GmbH). Samples are either measured uncoated or coated under vacuum (co. PLANO, Wetzlar) or coated with carbon under vacuum (EM SCD 500, Co. Leica, Bensheim). SEM-images were taken from the selected regions.

5.3.7 N_2 adsorption-desorption measurement

The N_2 sorption analysis was performed on Thermo Sorptomatic 1990 instrument. Activation of samples was performed under reduced pressure with heating at 300°C at 3 K/min for 2 hours. Nitrogen adsorption measurements were carried out at 77 K (-196 °C). The specific surface area (SSA) values were calculated by the BET (Brunauer-Emmett-Teller) equation in the interval $0.05 \leq p/p^o \leq 0.3$. The pore size distributions were calculated by using the BJH (Barrett-Joyner-Halenda) model applied to the desorption branch from p/p^o 0.3-0.95. Sample weight (280-300 mg) was used.

5.3.8 Acidity by NH_3-TPD

Surface acidity was measured by temperature programmed desorption (TPD) of NH_3 in a Thermo Scientific TPDRO 1100 series device. The TPD profile of the ammonium exchanged clinoptilolite allows to differentiate between different types of acid sites on basis of the temperature of ammonia desorption.

Procedure

Thermo Scientific TPDRO, 1100 series was used to measure NH_3-TPD. In a quartz reactor 100 mg of the samples were pretreated in a stream of He (20 ccm/min) at 180°C for 1 hour, cooled to 100°C under flushing He. Samples were saturated under flow of 10.03 % ammonia/helium gas (20 ccm/min) at 100°C for 30 minutes. Physiosorbed Ammonia was removed at 100°C with flushing He. Ammonia consumption was monitored by a TCD detector at 10°C/min from 100°C-600°C under a flow of He (20 ccm/min).

5.3.9 Catalytic Activity by Acetalization reaction

For checking the activity of the catalyst prepared acetalization reaction of 1,3-butandiol with benzaldehyde, using toluene as solvent and HMB as internal standard was selected. Acetalization reaction is easy to handle, take place in liquid medium at ordinary atmospheric pressure and at reflux temperature of *ca.* 115°C.

Procedure

In 3 necks round bottom flask (500 mL) with Dean-Stark apparatus (for water removal), reflux condenser, and a thermometer, 80 mL of toluene was taken. 10.6 g of benzaldehyde was added under automatic thermoregulator controlled stirring at 300 rpm and heating to 40^{o}C in 5 minutes, followed by abrupt addition of 1 g of HMB. Reaction mixture was continuously stirred and heated to reflux condition (115^{o}C) in controlled duration of 15 minutes. 9 g of 1,3-butandiol was added to the reaction mixture with 10 mL toluene washings. The thermal acetalization starts abruptly which is monitored with separating of 2 mL aliquot within 1 minute of the reaction mixture. 100-200 mg of catalyst was added to the reaction mixture with 10 mL toluene washings. Catalytic acetalization is recorded from this point. 2 mL of samples were taken after specific time interval of 1, 30, 60, 120, 180, 240, 300 minutes and analyzed with GC and NMR.

Actalization Reaction

Activity of the catalyst prepared was monitored by reaction of benzaldehyde and 1,3-butandiol using toluene as solvent and HMB as internal standard to form bezaldehyde propylene glycol acetal (Acetal). Acetalization reaction is easy to handle, take place in liquid medium at ordinary atmospheric pressure and at reflux temperature of 115°C.

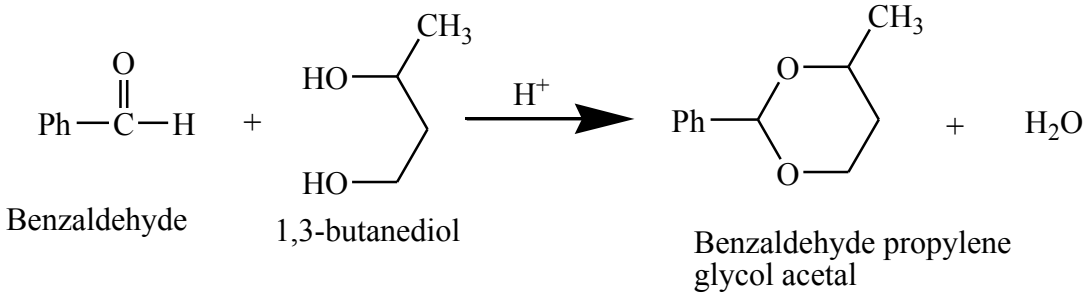

Figure 54. Formation of acetal from benzaldehyde and 1,3-butanediol

Analysis of product

The product formed during acetalization reaction was analyzed by

- **Liquid phase Proton (^{1}H) NMR**

AVANCE-300 (BRUKER) was used for NMR measurement. Sample was filled in 5 ml diameter of glass tube using D-chloroform as internal standard. By integration method, amount of reactant (benzaldehyde) consumed and product (acetal) formed calculated (%), using the intensity of the ^{1}H NMR signals of the acetal located at *ca.* 5-6 ppm and of benzaldehyde at *ca.*9-10 ppm.

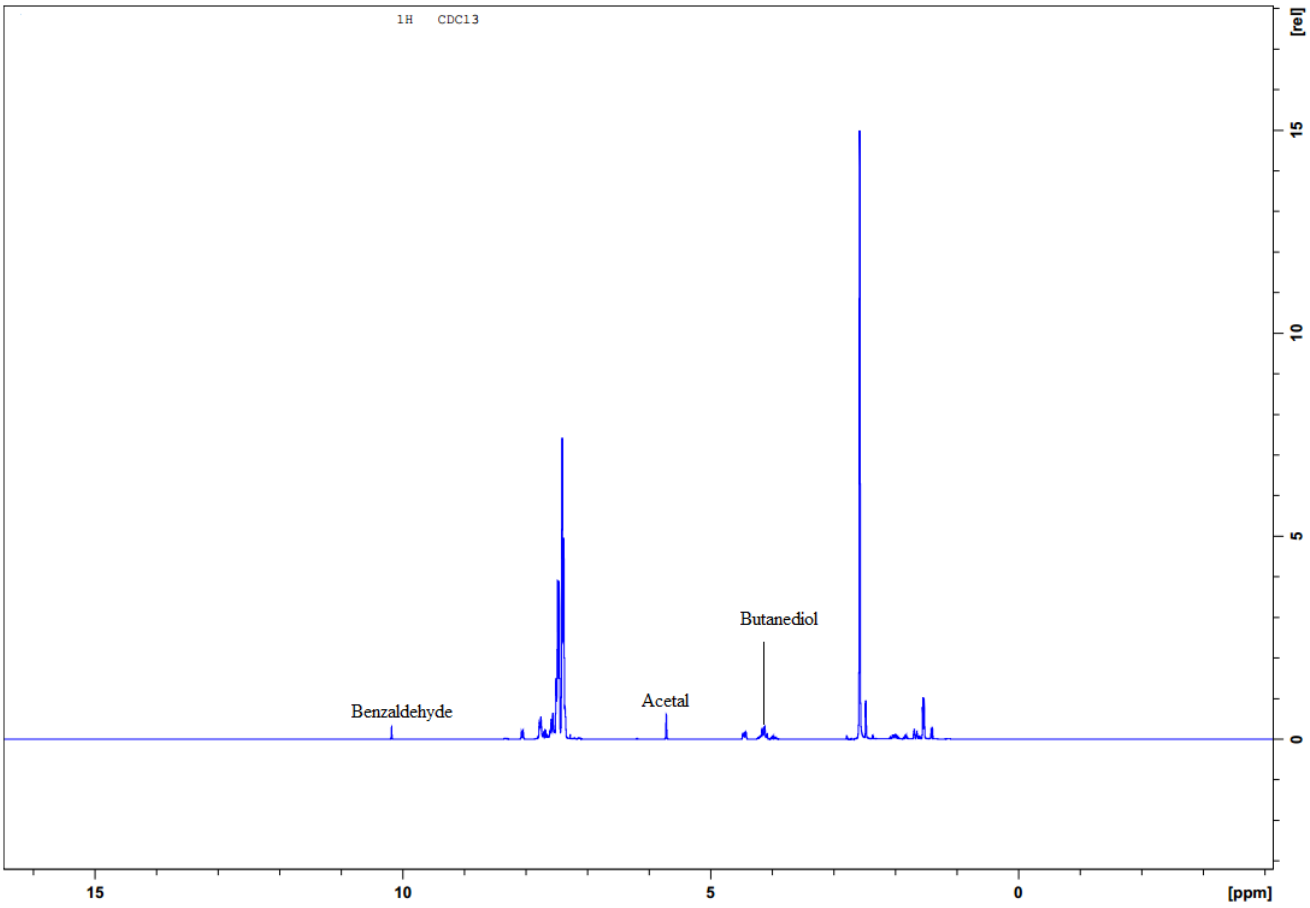

- **By GC analysis**

GC measurements were performed by GC-system 7890 A from Agilent Technologies. Column : 30 m HP-5 (Agilent Technologies) and Argon (1mL/min) was used as carrier gas. The following oven programme was used during analysis: 50°C; 8°C/min to 260°C; 5 min; 8°C/min to 280°C; 5 min; 8°C/min to 300°C. Under these conditions the GC signals of the solvent toluene, the benzaldehde and the acetal appear at retention times (minutes).

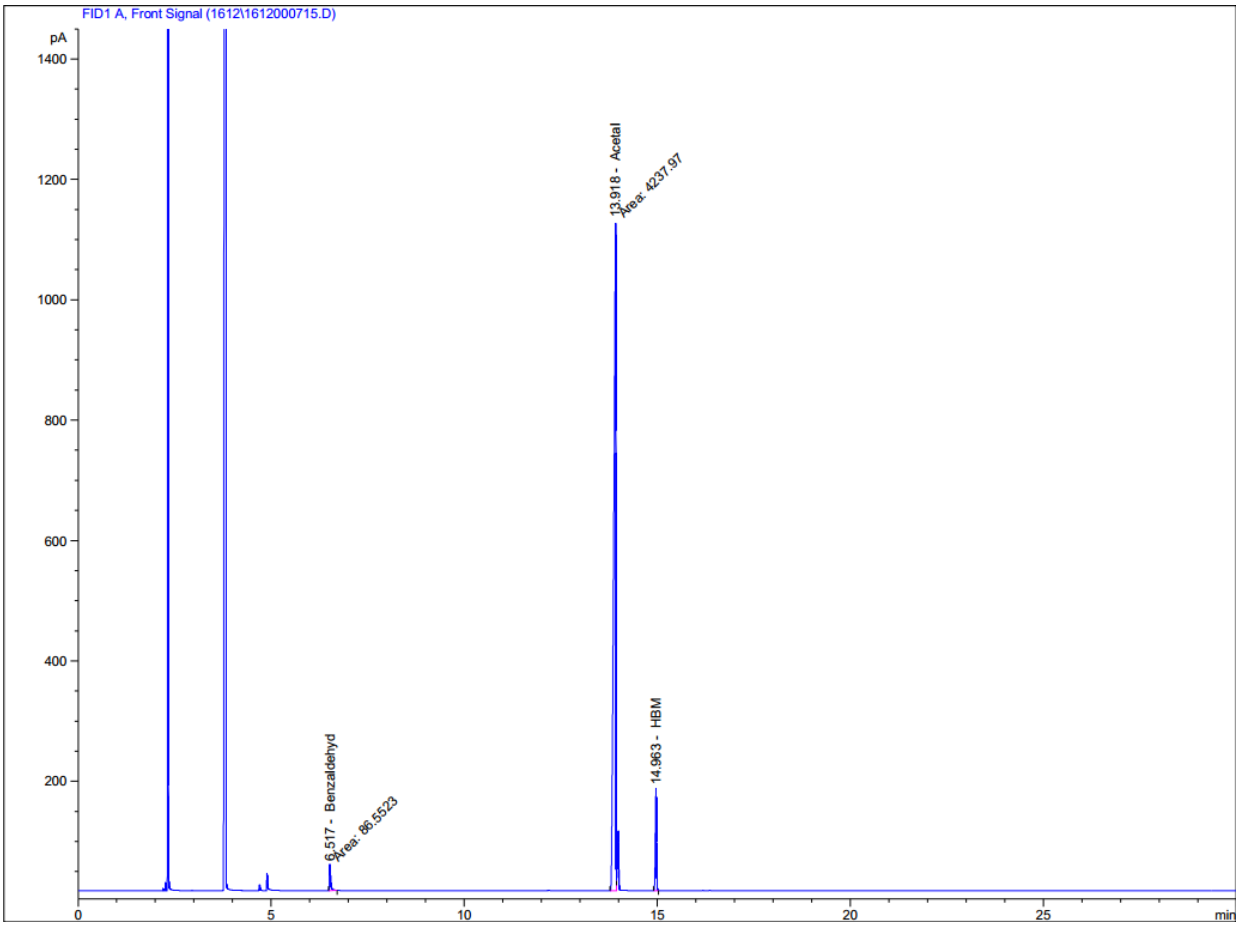

Table 32: Clinoptilolite Literature Review-State of Art

Source /region	Conditions	Characterization						Testing		Year	Ref.
		XRD	BET(m^2/g)	FTIR	^{27}Al	^{29}Si	DSC	TPD	Catalysis/ Adsorptin		
Mount Hector, California (85-95% pure)	10 g/150 mL of 0.25, 0.5, 1, 2, 5, 10, 15 and 30 N HCl for 4 h at 100°C. All samples outgased at 350°C for 15 h for BET.	Yes	CLIN=30,1 N=360 2 N=380,15 N=250 30 N=90	No	No	No	No	No	Adsorption of H_2O, CH_3OH, C_2H_5OH, C_6H_6, and iso-C_5H_{12}	1964	[59]
Castilla (Cuba) 85% pure	S_1=CLIN+1 M NH_4Cl & S_2=CLIN+5 M HCl at reflux for 5 h dried at 120°C,calcined at 400°C for 3 h. S_3= CLIN+700°C+0.25 M HCl, dried at 120°C. [CEC=2.7 Eq/g] CLIN=1.1, S_1=2.10 S_2=1 and S_3= 0.25 mmol/g		CLIN=51, S_1=256, 0.082 pore vol (p.v) S_2=200, 0.162p.v S_3=120,0.192p.v	Yes	No	No	No	Yes	ethanol dehydration o-xylene isomerization and CLIN and S_1=177 Å S_2=114 Å crystal size	1994	[55]
Bigadic (Turkey) 87% pure	23 g CLIN/0.5 N NaCl, filtered & dried. **(a)**Na-CLIN+1N NH_4Cl (2-fold), dried and calcined at 300°C(NH1), 400°C(NH2), 500°C(NH), 600°C (NH3). **(b)**NH_4-CLIN+0.1 N HCl (NHA), **(c)**0.1 N HCl+350°C(DH1), **d)**0.2 N HCl+350°C (DH2), **(e)**1 N HCl+350°C(DH3) (b), (c), (d) and (e) at 80°C for 3h.	Yes	NH1=NH2=36 m^2/g, NH=220 m^2/g, 0.58 nm NH3=50 m^2/g, NHA=260 m^2/g, 0.6 nm,	No	Yes	No	No	No	Adsorption of gases DH1=220 m^2/g, 0.6 nm ,DH3=315 m^2/g, 0.6 nm	2002	[56]
Tosoh chemical, Si/Al = 6	K-CLIN +1 M NH_4NO_3 2 times refluxing overnight and calcined at 600°C for 6 h. H-CLIN-600°C =1.36 mmol/g	Yes	BET and micropore volume=214 and 0.07					yes	Methanol conversion to Dimethyl-ether	2008	[60]
Caimanes,Moa (Cuba) , 87% pure	1 g NZ/10ml of I M NH4Cl at 100°C for 40 h (8-fold), dried at 60°Covernight=NH_4Z. NH_4Z +400°C for 16h = HZ. 1 g HZ/10 ml+0.6 M HCl at100°C for 2 h, Washed 3 times in ultrasonic bath with 0.05 M HCl(1 g/25 ml) for each 15 min at 70°C, dried overnight at 60°C=HZD1, HZ + 3 times treatment=HZD3. HZ +5 times treatment=HZD5	Yes	NZ=20, HZ=248, HZD1=259, HZD3=291, HZD5=305	Yes	Yes	Yes	Yes	No	gas adsorption and separation processes	2010	[61]
Sokyrnytsya (Ukraine),70-75%	15 g NZ/250 ml of 2 M HCl solution, kept for 24 h filtered, dried at room tempterature.		NZ = 13.4, H-CLIN-2M =78.3	No	No	No	Yes	No	gas adsorption	2010	[70]

Manisa–Demirci and Sivas–Yavu Turkey	NZ (Y&D)+0.5 M NH_4NO_3 (2-fold) at 80°C, dried at 120°C=[Y1 and D1], NH_4NZ +600°C for 2 h= [Y3 and D3], NH_4NZ+1 M HCl for 30 min,+600°C for 2 h=[Y5 and D5]	Yes	73.6, 89.4, 93.8, 52.3, 57.6 and 79.1 m^2/g respectively.	Yes	No	No	No	Valve not given	Adsorption	2012	[63]
Aftar Tehran (Iran).	CLIN-air dried and CLIN +2 M HCl, CLIN - 2 M HCl=177.6, 0.0626 cm^3/g pore vol	Yes	CLIN=84.45 and 0.054 cm^3/g pore volume	Yes	No	No	Yes	No	Adsorption	2013	[67]
Lyulinskii ,68 % pure.	1 g NZ/100 mL of 4 M HCl at 25°C with stirring for 4 h.	No	CLIN=7.9 and 0.002, CLIN-4 M HCl=92.2, 0.031 micropore	Yes	No	No	No	No	Adsorption	2014	[69]
Kucin, Slovakia, 83 % pure.	**(a)**1 g NZ/15 mL (0.05-11.5 M) HCl for 4 h at 95-97°C, dried at 80°C. **(b)**NZ+10 % NH_4NO_3 (3-fold) at 80°C for 4 h, calcined at 300°C(6 h), 400°C (4 h), and 500°C (4 h) to get H-CLIN. NZ=0.474, 300°C=0.738, 0.05=0.507, 0.1=0.5, 0.25=0.3 mmol/g respectively.	Yes	NZ=33.5, 300°C=62.6, 400°C=130.6, 500°C=143.4, 0.05 M=44.1, 0.1 M=59.1, 0.25 M=98.1, 1 M=143.3, 2 M=164.7, 5 M=80.9, 8 M=79.1, 11.5 M=90 m^2/g	Yes	Yes	No	No	Yes	α-pinene conversion	2015	[91]

6 References

[1] M. Moshoeshoe, M. S. Nadiye-tabbiruka, V. Obuseng, *Am. J. Mater. Sci.* **2017**, *7*, 196–221.

[2] C. Li, H. Zhong, S. Wang, J. Xue, Z. Zhang, *Colloids Surfaces A Physicochem. Eng. Asp.* **2015**, *470*, 258–267.

[3] R. C. Deka, *Indian J. Chem. Technol.* **1998**, *5*, 109–123.

[4] B. Jha, D. N. Singh, *Adv. Struct. Mater.* **2016**, *78*, 5–31.

[5] B. Jha, D. N. Singh, *J. Mater. Educ.* **2011**, *33*, 65–132.

[6] M. W. Ackley, S. U. Rege, H. Saxena, *Microporous Mesoporous Mater.* **2003**, *61*, 25–42.

[7] Ž. Sekulić, B. Kolonja, M. Kragović, B. Ivošević, S. Mihajlović, *Gospod. Surowcami Miner.* **2014**, *30*, 5–16.

[8] J. Huang, Y. Jiang, V. R. R. Marthala, B. Thomas, E. Romanova, M. Hunger, *J. Phys. Chem. C* **2008**, *112*, 3811–3818.

[9] E. Polat, M. Karaca, H. Demir, a N. Onus, *J. Fruit Ornam. Plant Reserarch* **2004**, *12*, 183–189.

[10] F. A. Mumpton, *Proc. Natl. Acad. Sci.* **1999**, *96*, 3463–3470.

[11] W. P. Phyu, *Tech. Rep. (No. 1017/1/2004)* **2004**, 1–23.

[12] D. Mravec, J. M. a J. Ling, *Chem Pap.* **1987**, *41*, 335–341.

[13] B. M. Weckhuysen, J. Yu, *Chem. Soc. Rev.* **2015**, *44*, 7022–7024.

[14] C. J. Harpel, P. R. Kyle, N. W. Dunbar, *J. Volcanol. Geotherm. Res.* **2008**, *177*, 549–568.

[15] C. J. Rhodes, *Sci. Prog.* **2010**, *93*, 1–63.

[16] C. J. Rhodes, *R. Soc. Chem.* **2007**, *103*, 287–325.

[17] D. S. Coombs, A. Alberti, T. Armbruster, G. Artioli, C. Colella, E. Galli, J. D. Grice, F.

Liebau, E. H. Nickel, E. Passaglia, et al., *Can. Mineral.* **1997**, *35*, 1571–1606.

[18] H. Cheng, M. Reinhard, *Environ. Sci. Technol.* **2006**, *40*, 7694–7701.

[19] P. A. Wright, M. Lozinska, *Structural Chemistry and Properties of Zeolites*, **2011**.

[20] B. Jha, D. N. Singh, *J. Mater. Educ.* **2011**, *33*, 65–132.

[21] L. B. McCusker, F. Liebau, G. Engelhardt, *Pure Appl. Chem.* **2001**, *73*, 381–394.

[22] R. F. Lobo, M. Tsapatsis, C. C. Freyhardt, S. Khodabandeh, P. Wagner, C. Y. Chen, K. J. Balkus, S. I. Zones, M. E. Davis, *J. Am. Chem. Soc.* **1997**, *119*, 8474–8484.

[23] S. M. Auerbach, K. A. Carrado, P. K. Dutta, *Zeolite Science and Technology*, **2003**.

[24] C. Sangeetha, P. Baskar, *Agric. Rev.* **2016**, *37*, 101–108.

[25] M. E. Davis, *Ind. Eng. Chem. Res.* **1991**, *30*, 1675–1683.

[26] A. M. Beale, F. Gao, I. Lezcano-Gonzalez, C. H. F. Peden, J. Szanyi, *Chem. Soc. Rev.* **2015**, *44*, 7371–7405.

[27] L. E. Bento Ribeiro, G. P. De Alcântara, M. G. Andrade, F. Fruett, *Sensors & Transducers* **2015**, *193*, 80–85.

[28] S. Sircar, A. Myers, *Gas Separation by Zeolites*, **2003**.

[29] B. S. Sekhon, M. K. Sangha, *Resonance* **2004**, *9*, 35–45.

[30] N. Rakovitsky, I. Brook, J. Van Rijn, M. Ryskin, Z. Mkhweli, H. Etkin, S. Nir, *Appl. Clay Sci.* **2016**, *132–133*, 267–272.

[31] V. K. Gupta, H. Sadegh, M. Yari, R. Shahryari Ghoshekandi, B. Maazinejad, M. Chahardori, *Glob. J. Environ. Sci. Manag.* **2015**, *1*, 149–158.

[32] A. A. Zorpas, V. Inglezakis, M. Loizidou, H. Grigoropoulou, *J. Colloid Interface Sci.* **2002**, *250*, 1–4.

[33] Y. Taamneh, S. Sharadqah, *Appl. Water Sci.* **2017**, *7*, 2021–2028.

[34] D. Barthomeuf, *Catal. Rev. - Sci. Eng.* **1996**, *38*, 521–612.

[35] B. Yilmaz, U. Müller, *Top. Catal.* **2009**, *52*, 888–895.

[36] J. Weitkamp, *Solid State Ionics* **1998**, *131*, 175–188.

[37] D. Mravec, J. Hudec, I. Janotka, *Chem. Pap.* **2005**, *59*, 62–69.

[38] A. Kareem, S. Chand, I. M. Mishra, *J. Sci. Ind. Res. (India).* **2001**, *60*, 319–327.

[39] S. M. Csicsery, *Pure Appl. Chem.* **1986**, *58*, 841–856.

[40] C. Song, J. M. Garcés, Y. Sugi, *Am. Chem. Soc.* **2000**, 1–16.

[41] X. Querol, A. Alastuey, A. López-Soler, F. Plana, J. M. Andrés, R. Juan, P. Ferrer, C. R. Ruiz, *Environ. Sci. Technol.* **1997**, *31*, 2527–2533.

[42] A. Simon-Masseron, J. P. Marques, J. M. Lopes, F. R. Ribeiro, I. Gener, M. Guisnet, *Appl. Catal. A Gen.* **2007**, *316*, 75–82.

[43] S. Wang, Y. Peng, *Chem. Eng. J.* **2010**, *156*, 11–24.

[44] M. a. Hernández, L. Corona, a. I. González, F. Rojas, V. H. Lara, F. Silva, *Ind. Eng. Chem. Res.* **2005**, *44*, 2908–2916.

[45] A. Arcoya, J. A. González, G. Llabre, X. L. Seoane, N. Travieso, *Microporous Mater.* **1996**, *7*, 1–13.

[46] A. Langella, M. Pansini, G. Cerri, P. Cappelletti, M. De'Gennaro, *Clays Clay Miner.* **2003**, *51*, 625–633.

[47] T. C. Keller, J. Arras, S. Wershofen, J. Pérez-Ramírez, *ACS Catal.* **2015**, *5*, 734–743.

[48] J. Stolz, P. Yang, T. Armbruster, *Microporous Mesoporous Mater.* **2000**, *37*, 233–242.

[49] K. Koyama, Y. Takéuchi, *J. Crystallogr.* **1977**, *145*, 216–239.

[50] M. A. Hernández, F. Rojas, V. H. Lara, *J. Porous Mater.* **2000**, *7*, 443–454.

[51] N. W. Ockwig, R. T. Cygan, M. A. Hartl, L. L. Daemen, T. M. Nenoff, *J. Phys. Chem.* **2008**, *10*, 800–807.

[52] T. V. O. James Philip Brassell, L. F. Petrik, in *Zeolites - Useful Miner.*, **2016**, pp. 3–23.

[53] T. Armbruster, M. E. Gunter, *Rev. Mineral. Geochemistry* **2001**, *45*, 1–67.

[54] R. Szostak, *Handbook of Molecular Sieves*, Van Nostrand Reinhold, **1992**.

[55] X. L. S. A. Arcoya, J. A. Gonzalez, N. Travieso, *Clay Miner.* **1994**, *29*, 123–131.

[56] H. Kurama, A. Zimmer, W. Reschetilowski, *Chem. Eng. Technol.* **2002**, *25*, 301–305.

[57] A. D. P. A. S. Shadrikov, in *Mod. Technol. ZEOLITE TUFF USAGE Ind.*, **2014**, pp. 162–167.

[58] P. Kowalczyk, M. Sprynskyy, A. P. Terzyk, M. Lebedynets, J. Namieśnik, B. Buszewski, *J. Colloid Interface Sci.* **2006**, *297*, 77–85.

[59] R. M. Barrer, M. B. Makki, *Can. J. Chem.* **1964**, *42*, 1481–1487.

[60] S. C. Baek, Y. J. Lee, K. W. Jun, S. B. Hong, *Energy and Fuels* **2009**, *23*, 593–598.

[61] Y. Garcia-Basabe, I. Rodriguez-Iznaga, L. C. De Menorval, P. Llewellyn, G. Maurin, D. W. Lewis, R. Binions, M. Autie, A. R. Ruiz-Salvador, *Microporous Mesoporous Mater.* **2010**, *135*, 187–196.

[62] M. R.-M. J. Anna Dziedzicka, Bogdan Sulikowski, *Catal. Today* **2015**, *259*, 50–58.

[63] A. Ates, C. Hardacre, *J. Colloid Interface Sci.* **2012**, *372*, 130–140.

[64] W. Lutz, *Adv. Mater. Sci. Eng.* **2014**, *2014*, 1–20.

[65] G. Rodríguez-Fuentes, a. R. Ruiz-Salvador, M. Mir, O. Picazo, G. Quintana, M. Delgado, *Microporous Mesoporous Mater.* **1998**, *20*, 269–281.

[66] F. Cakicioglu-Ozkan, S. Ulku, *Microporous Mesoporous Mater.* **2005**, *77*, 47–53.

[67] N. Mansouri, N. Rikhtegar, H. A. Panahi, F. Atabi, B. K. Shahraki, *Environ. Prot. Eng.* **2013**, *39*, 139–152.

[68] E. P. Favvas, C. G. Tsanaktsidis, A. A. Sapalidis, G. T. Tzilantonis, S. K. Papageorgiou, A. C. Mitropoulos, *Microporous Mesoporous Mater.* **2016**, *225*, 385–391.

[69] D. L. Kotova, S. Y. Vasilyeva, T. A. Krysanova, F. Roessner, E. V. Borodina, D. T.

Long, *Nanotechnologies Russ.* **2014**, *9*, 474–479.

[70] M. Sprynskyy, R. Golembiewski, G. Trykowski, B. Buszewski, *J. Phys. Chem. Solids* **2010**, *71*, 1269–1277.

[71] K. Stocker, M. Ellersdorfer, M. Lehner, J. G. Raith, *Berg- Huettenmaenn. Monatsh.* **2017**, *162*, 142–147.

[72] B. E. Alver, M. Sakizci, E. Yörükoğullari, *J. Therm. Anal. Calorim.* **2010**, *100*, 19–26.

[73] E. Yörükoğullar, G. Yilmaz, S. Dikmen, *J. Therm. Anal. Calorim.* **2010**, *100*, 925–928.

[74] O. Korkuna, R. Leboda, J. Skubiszewska-Zięba, T. Vrublevs'ka, V. M. Gun'ko, J. Ryczkowski, *Microporous Mesoporous Mater.* **2006**, *87*, 243–254.

[75] G. Engelhardt and D. Michel, *High Resolution Solid State NMR of Silicates and Zeolites*, Wiley VCH Verlag GmbH & Co. KGaA, **1988**.

[76] A. Rivera, T. Farías, L. C. De Ménorval, M. Autié-Pérez, A. Lam, *J. Phys. Chem. C* **2013**, *117*, 4079–4088.

[77] F. Chávez-Rivas, G. Rodríguez-Fuentes, G. Berlier, I. Rodríguez-Iznaga, V. Petranovskii, R. Zamorano-Ulloa, S. Coluccia, *Microporous Mesoporous Mater.* **2013**, *167*, 76–81.

[78] L. Tichagwa, H. Pasch, E. D. Dikio, *S. Afr. J. Chem.* **2015**, *68*, 143–152.

[79] S. Ramdas, J. Klinowski, *Nature* **1984**, *308*, 521–523.

[80] C. A. Fyfe, Y. Feng, H. Grondey, G. T. Kokotailo, H. Gies, *Chem. Rev.* **1991**, *91*, 1525–1543.

[81] E. Lippmaa, M. Magi, A. Samoson, G. Engelhard, A. R. Grimmer, *J. Am. Chem. Soc.* **1980**, *102*, 4889–4893.

[82] E. Lippmaa, M. Mági, A. Samoson, M. Tarmak, G. Engelhardt, *J. Am. Chem. Soc.* **1981**, *103*, 4992–4996.

[83] B. H. Wouters, T. H. Chen, P. J. Grobet, *J. Am. Chem. Soc.* **1998**, *120*, 11419–11425.

[84] H.-M. Kao, C. P. Grey, *J. Phys. Chem.* **1996**, *100*, 5105–5117.

[85] M. Hunger, *Solid State Nucl. Magn. Reson.* **1996**, *6*, 1–29.

[86] N. Ghasemian, C. Falamaki, M. Kalbasi, M. Khosravi, *Chem. Eng. J.* **2014**, *252*, 112–119.

[87] K. A. Tarach, J. Tekla, W. Makowski, U. Filek, K. Mlekodaj, V. Girman, M. Choi, K. Góra-Marek, *Catal. Sci. Technol.* **2016**, *6*, 3568–3584.

[88] M. Rutkowska, L. Chmielarz, M. Jabłońska, C. J. Van Oers, P. Cool, *J. Porous Mater.* **2014**, *21*, 91–98.

[89] L. H. Ong, M. Dömök, R. Olindo, A. C. Van Veen, J. A. Lercher, *Microporous Mesoporous Mater.* **2012**, *164*, 9–20.

[90] M. Mägi, E. Lippmaa, A. Samoson, G. Engelhardt, A. R. Grimmer, *J. Phys. Chem.* **1984**, *88*, 1518–1522.

[91] M. R.-M. Anna Dziedzicka, Bogdan Sulikowski, *Catal. Today* **2015**, *259*, 50–58.

[92] G. E. Kowalczyk, Quantitative Determination Of Crystalline Silica Utilizing Solid State Silicon-29NMR, Lehigh University, **1992**.

Curriculum Vitae

Personal Data :

Name :	Riaz Muhammad
Nationality :	Pakistan
Date of birth :	03.01.1982
Email :	**riaz.muhammad@uni-rostock.de**
	e2chemist.rk@gmail.com
Languages :	English, Urdu, Pashto and basic German.

Academics :

2002-2004	**M.Sc Analytical Chemistry (Peshawar University, Pakistan)**
Title of Thesis :	***Catalytic Liquefaction of Iso-Butylene Isoprene Rubber into valuable Hydrocarbons***
Thesis Theme.	The main purpose was transforming waste Tube Rubber into valuable Hydrocarbons. The physical and chemical tests of the study indicate that the oil obtained is a mixture of kerosene, diesel and light oil and could be used for fuel purposes.
2009-2010	**M.Ed Education (Peshawar University, Pakistan)**
05.2015 – 07.2018	**Ph.D Chemistry (Universität Rostock, Germany)**
Ph.D Research topic:	***Green Natural Zeolite Catalyst - Preparation, Characterization and Acid Catalytic Performance***
Ph.D Theme.	The main purpose is the modification of natural zeolite Clinoptilolite to more acidic and porous catalyst. Aim of study was conversion of heavy oil feed stock into simple valuable hydrocarbons, polyethylene and tube rubber conversion into useful fuel oils and determination of acidic sites and porosity of modified natural zeolites.